KoG

SCIENTIFIC - PROFESSIONAL JOURNAL
OF CROATIAN SOCIETY FOR GEOMETRY AND GRAPHICS

No. 21. (2017)
ISSN 1331-1611

ISSN 1331-1611
9 771331 161005

Official publication of the Croatian Society for Geometry and Graphics publishes scientific and professional papers from the fields of geometry, applied geometry and computer graphics.

Founder and Publisher

Croatian Society for Geometry and Graphics

Design

Miroslav Ambruš-Kiš

Layout

Sonja Gorjanc, Ema Jurkin

Cover Illustration

Jelena Beban-Brkić, photography

Print

SAND d.o.o., Zagreb

URL address

http://www.hdgg.hr/kog
http://hrcak.srce.hr

Edition

150

Published annually

Guide for authors
Please, see the last page

KoG is reviewed, cover to cover, by Mathematical Reviews (MathSciNet).

This issue has been financially supported by the Foundation of the Croatian Academy of Sciences and Arts and the Ministry of Science and Education.

INSTRUCTIONS FOR AUTHORS

SCOPE. "KoG" publishes scientific and professional papers from the fields of geometry, applied geometry and computer graphics.

SUBMISSION. Scientific papers submitted to this journal should be written in English, professional papers should be written in Croatian or English. The papers have not been published or submitted for publication elsewhere.
The manuscript should be sent in PDF format via e-mail to the editor:

Ema Jurkin
ema.jurkin@rgn.hr

The first page should contain the article title, author and coauthor names, affiliation, a short abstract in English, a list of keywords and the Mathematical subject classification.

UPON ACCEPTANCE. After the manuscript has been accepted for publication authors are requested to send its LaTex file via e-mail to the address:

ema.jurkin@rgn.hr

Figures should be titled by the figure number that match to the figure number in the text of the paper.

The corresponding author and coauthors will receive hard copies of the issue free of charge.

UPUTE ZA AUTORE

PODRUČJE. "KoG" objavljuje znanstvene i stručne radove iz područja geometrije, primijenjene geometrije i računalne grafike.

UPUTSTVA ZA PREDAJU RADA. Znanstveni radovi trebaju biti napisani na engleskom jeziku, a stručni na hrvatskom ili engleskom. Rad ne smije biti objavljen niti predan na recenziju u drugim časopisima.
Rukopis se šalje u PDF formatu elektronskom poštom na adresu urednice:

Ema Jurkin
ema.jurkin@rgn.hr

Prva stranica treba sadržavati naslov rada, imena autora i koautora, podatke o autoru i koautorima, sažetak na hrvatskom i engleskom, ključne riječi i MSC broj.

PO PRIHVAĆANJU RADA. Tekst prihvaćenog rada autor dostavlja elektronskom poštom kao LaTeX datoteku. Slike trebaju imati nazive koji odgovaraju rednom broju slike u tekstu članka. Adresa:

ema.jurkin@rgn.hr

Svaki autor i koautor dobiva po jedan primjerak časopisa.

ISSN 1331–1611

No. 21
Zagreb, 2017

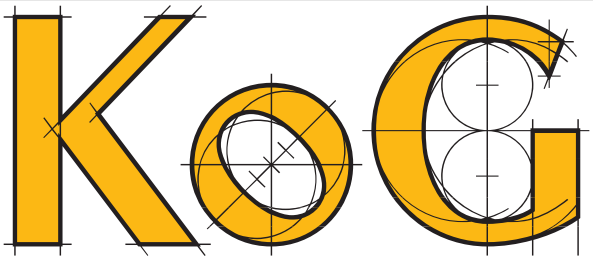

SCIENTIFIC AND PROFESSIONAL JOURNAL OF
CROATIAN SOCIETY FOR GEOMETRY AND GRAPHICS

CONTENTS

ORIGINAL SCIENTIFIC PAPERS

PROFESSIONAL PAPERS

ISSN 1331–1611

KoG

BROJ 21
Zagreb, 2017

ZNANSTVENO-STRUČNI ČASOPIS
HRVATSKOG DRUŠTVA ZA GEOMETRIJU I GRAFIKU

SADRŽAJ

ORIGINALNI ZNANSTVENI RADOVI

STRUČNI RADOVI

Original scientific paper
Accepted 13. 1. 2017.

ZDENKA KOLAR–BEGOVIĆ

An Affine Regular Icosahedron Inscribed in an Affine Regular Octahedron in a GS-Quasigroup

An Affine Regular Icosahedron Inscribed in an Affine Regular Octahedron in a GS-Quasigroup

ABSTRACT

A golden section quasigroup or shortly a GS–quasigroup is an idempotent quasigroup which satisfies the identities $a(ab\cdot c)\cdot c=b, a\cdot(a\cdot bc)c=b$. The concept of a GS–quasigroup was introduced by VOLENEC. A number of geometric concepts can be introduced in a general GS–quasigroup by means of the binary quasigroup operation. In this paper, it is proved that for any affine regular octahedron there is an affine regular icosahedron which is inscribed in the given affine regular octahedron. This is proved by means of the identities and relations which are valid in a general GS–quasigrup. The geometrical presentation in the GS–quasigroup $\mathbb{C}(\frac{1}{2}(1+\sqrt{5}))$ suggests how a geometrical consequence may be derived from the statements proven in a purely algebraic manner.

Key words: GS–quasigroup, GS–trapezoid, affine regular icosahedron, affine regular octahedron

MSC2010: 20N05

Afino pravilan ikozaedar upisan u afino pravilan oktaedar u GS-kvazigrupi

SAŽETAK

Kvazigrupa zlatnog reza ili kraće GS–kvazigrupa idempotentna je kvazigrupa u kojoj vrijede identiteti $a(ab\cdot c)\cdot c=b, a\cdot(a\cdot bc)c=b$. Pojam GS–kvazigrupe uveo je VOLENEC. Razni geometrijski pojmovi mogu biti uvedeni u GS–kvazigrupi pomoću binarne operacije te kvazigrupe. Korištenjem relacija i identiteta u općoj GS-kvazigrupi u ovom je radu pokazano da se svakom afino pravilnom oktaedru može upisati afino pravilan ikozaedar. Geometrijski prikaz u kvazigrupi $\mathbb{C}(\frac{1}{2}(1+\sqrt{5}))$ pokazuje kako geometrijske tvrdnje mogu biti posljedica potpuno algebarskih razmatranja.

Ključne riječi: GS–kvasigrupa, GS–trapezoid, afino pravilan ikozaedar, afino pravilan oktaedar

1 Introduction

The concept of a GS–quasigroup was introduced by Volenec in [1].
A quasigroup $(Q,\cdot)$, which satisfies the identity of idempotency

$$aa=a \tag{1}$$

and the (mutually equivalent) identities

$$a(ab\cdot c)\cdot c=b, \tag{2}$$

$$a\cdot(a\cdot bc)c=b, \tag{2}'$$

is called a golden section quasigroup or shortly a GS–quasigroup.

It can be proved that the considered GS–quasigroup $(Q,\cdot)$ satisfies the identitites of mediality, elasticity, left and right distributivity, i.e., the identities

$$ab\cdot cd=ac\cdot bd, \tag{3}$$

$$a\cdot ba=ab\cdot a, \tag{4}$$

$$a\cdot bc=ab\cdot ac, \tag{5}$$

$$ab\cdot c=ac\cdot bc. \tag{5}'$$

are valid. Some other identities, e.g.

$$a(ab\cdot b)=b, \tag{6}$$

$$(b\cdot ba)a=b, \tag{6}'$$

are also valid in a general GS–quasigroup.

Let us mention the best known example of a GS–quasigroup. Let $\mathbb{C}$ be the set of points of the Euclidean plane. For any two different points a, b we define $ab = c$ if the point b divides the pair a, c in the ratio of the golden section. In [1], it is proved that $(\mathbb{C}, \cdot)$ is a GS–quasigroup. This quasigroup is denoted by $\mathbb{C}(\frac{1}{2}(1+\sqrt{5}))$ because we have $c = \frac{1}{2}(1+\sqrt{5})$ if $a = 0$ and $b = 1$. As this quasigroup has a nice geometrical interpretation, we shall use this quasigroup for the purpose of illustrating the identities and relationships holding in a general GS–quasigroup.
From now on, let $(Q, \cdot)$ be any GS–quasigroup. The elements of the set Q are said to be points.
Some geometric concepts, such as parallelograms, GS–trapezoids, affine regular pentagons, an affine regular icosahedron and an affine regular octahedron, can be introduced by means of the given binary quasigroup operation (see [1], [2], [3], [4]).
The points a, b, c, d are said to be the vertices of a parallelogram and we write $Par(a, b, c, d)$ if the identity

$$a \cdot b(ca \cdot a) = d \tag{7}$$

holds. In [1], some properties of the quaternary relation Par on the set Q are proved. It is proved that the structure (Q, Par) is a parallelogram space, i.e., that the following three properties hold:

(P1) For any three points a, b, c, there exists one and only one point d such that there holds $Par(a, b, c, d)$.

(P2) From $Par(a, b, c, d)$ there follows $Par(e, f, g, h)$, where (e, f, g, h) is any cyclic permutation of (a, b, c, d) or (d, c, b, a).

(P3) From $Par(a, b, c, d)$ and $Par(c, d, e, f)$ there follows $Par(a, b, f, e)$.

In [1], the following statement is proved.

Lemma 1 *From Par(a,b,d,e) and Par(b,c,e,f) there follows Par(c,d,f,a).*

We shall say that b is the midpoint of the pair of points a, c and write $M(a, b, c)$ if $Par(a, b, c, b)$.
In [2], the concept of a GS–trapezoid is defined. The points a, b, c, d successively are said to be the vertices of the golden section trapezoid and it is denoted by $GST(a, b, c, d)$ if the identity

$$a \cdot ab = d \cdot dc \tag{8}$$

holds.
In [2], it is proved that any two of the five statements

$$GST(a, b, c, d), GST(b, c, d, e), GST(c, d, e, a),$$
$$GST(d, e, a, b), GST(e, a, b, c) \tag{9}$$

imply the remaining statement.
In [3], the concept of an affine regular pentagon is defined. The points a, b, c, d, e successively are said to be the vertices of the affine regular pentagon and it is denoted by $ARP(a, b, c, d, e)$ if any two (and then all five) of the five statements (9) are valid.

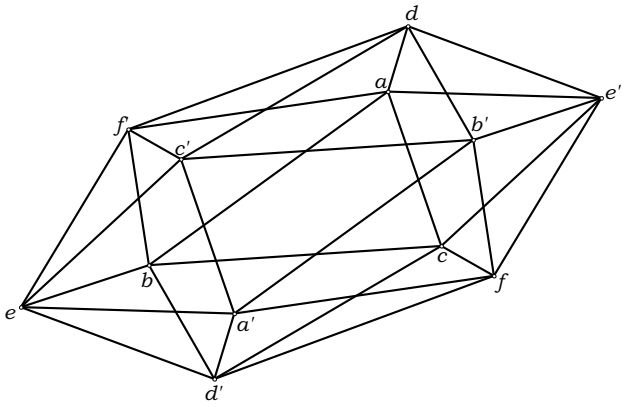

Figure 1: *Affine regular icosahedron in* $\mathbb{C}(\frac{1}{2}(1+\sqrt{5}))$

In [4], the concepts of an affine regular icosahedron and an affine regular octahedron in a general GS–quasigroup are introduced.
We shall say that the points $a, b, c, d, e, f, a', b', c', d', e', f'$ are the vertices of an affine regular icosahedron (Figure 1) and write $ARI(a, b, c, d, e, f, a', b', c', d', e', f')$ if the following twelve statements are valid

$$ARP(b, c, f, a', e), \quad ARP(c, a, d, b', f),$$
$$ARP(a, b, e, c', d), \quad ARP(b', c', f', a, e'),$$
$$ARP(c', a', d', b, f'), \quad ARP(a', b', e', c, d'),$$
$$ARP(b, c, e', d, f'), \quad ARP(c, a, f', e, d'),$$
$$ARP(a, b, d', f, e'), \quad ARP(b', c', e, d', f),$$
$$ARP(c', a', f, e', d), \quad ARP(a', b', d, f', e).$$

The points a, b, c, a', b', c' are the vertices of an affine regular octahedron with the center o if the statements $M(a, o, a')$, $M(b, o, b')$, $M(c, o, c')$ are valid (Figure 2).

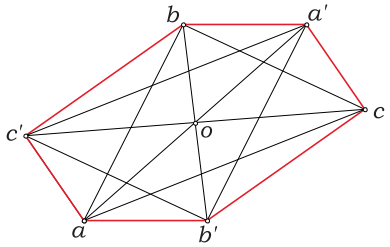

Figure 2: *Affine regular octahedron in* $\mathbb{C}(\frac{1}{2}(1+\sqrt{5}))$

The vertices of an affine regular octahedron are the vertices of three parallelograms. We have the statement.

Lemma 2 *From $M(c,o,c')$ and $M(b,o,b')$ there follows $Par(b',c',b,c)$.*

Proof. The statements $M(c,o,c')$ and $M(b,o,b')$ are equivalent to $Par(c,o,c',o)$ and $Par(b,o,b',o)$, from where, according to (P2), we get $Par(o,b',o,b)$, whence by Lemma 1 we obtain $Par(b',c',b,c)$. □

In [4], it is proved that for any regular octahedron there is a regular icosahedron which is circumscribed to the given affine regular octahedron. Now, we shall prove that for any affine regular octahedron there is a regular icosahedron which is inscribed in the given affine regular octahedron. So, we have the following statement.

Theorem 1 *If a,b,c,a',b',c' are the vertices of an affine regular octahedron, then $ARI(a_b,b_c,c_a,a'_{b'},b'_{c'},c'_{a'},a_{b'},b'_c,c_{a'},a'_b,b_{c'},c'_a)$, where $a_b = ab\cdot b$, $b_c = bc\cdot c$, ... , $c'_{a'} = c'a'\cdot a'$, (Figure 3).*

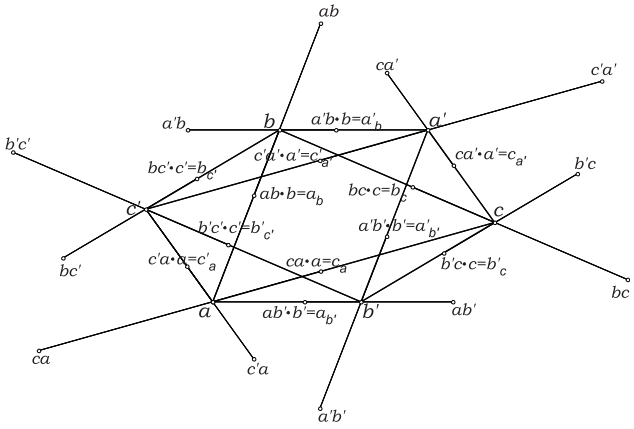

Figure 3.

Proof. It is enough to prove the statement $ARP(a_b,c_a,a_{b'},b'_{c'},b_{c'})$. According to (9), it is sufficient to prove that the statements $GST(a_b,c_a,a_{b'},b'_{c'})$ and $GST(a_{b'},c_a,a_b,b_{c'})$ are valid. In fact, it is enough to prove only the first one because the second statement follows from the first one by substitution $b \leftrightarrow b'$. According to the definition of a GS–trapezoid, because of (8), for the proof of the first statement we have to prove

$$a_b \cdot a_b c_a = b'_{c'} \cdot b'_{c'} a_{b'}.$$

We obtain

$$\begin{aligned} a_b \cdot a_b c_a &= (ab\cdot b)\cdot(ab\cdot b)(ca\cdot a) \\ &\overset{(3)}{=} (ab)(ab\cdot b)\cdot b(ca\cdot a) \\ &\overset{(5)}{=} (a\cdot ab)b\cdot b(ca\cdot a) \overset{(6')}{=} a\cdot b(ca\cdot a), \end{aligned}$$

from where, owing to (7), we get that the point $a_b \cdot a_b c_a$ is the fourth vertex of the parallelogram with the vertices a,b,c, i.e., $Par(a,b,c,a_b\cdot a_b c_a)$. We can get $Par(b',c',a,b'_{c'}\cdot b'_{c'}a_{b'})$ in the same way. It is necessary to prove that the fourth vertices of these two parallelograms are coincident, i.e., the statement $Par(a,b,c,x)$ implies the statement $Par(b',c',a,x)$. However, because the points b',c',b,c are the vertices of the octahedron, according to Lemma 2, $Par(b',c',b,c)$ holds, which, together with $Par(b,c,x,a)$ and by P3, gives $Par(b',c',a,x)$. □

In this case, we shall say that an affine regular icosahedron is *inscribed* in the given affine regular octahedron (*Figure 4).*

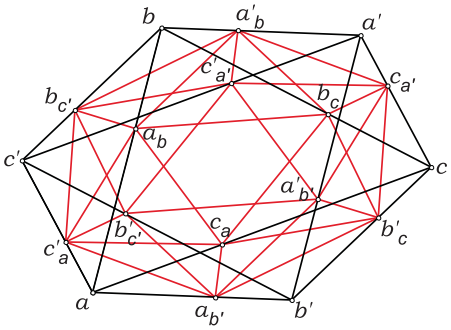

Figure 4.

References

[1] V. VOLENEC, *GS*–quasigroups, *Čas. pěst. mat.* **115** (1990), 307–318.

[2] V. VOLENEC, Z. KOLAR–BEGOVIĆ, *GS*–trapezoids in *GS*–quasigroups, *Math. Commun.* **7** (2002), 143–158.

[3] V. VOLENEC, Z. KOLAR–BEGOVIĆ, Affine regular pentagons in *GS*–quasigroups, *Quasigroups Related Systems* **12** (2004), 103–112.

[4] V. VOLENEC, Z. KOLAR–BEGOVIĆ, R. KOLAR–ŠUPER, Affine regular icosahedron circumscribed around the affine regular octahedron in GS–quasigroup, *Comment. Math. Univ. Carolin.* **53** (2012), 501–507.

Zdenka Kolar–Begović
orcid.org/0000-0001-8710-8628
e-mail: zkolar@mathos.hr

Department of Mathematics, University of Osijek
Gajev trg 6, HR-31 000 Osijek, Croatia

Original scientific paper
Accepted 17. 7. 2017.

HARUN BARIŞ ÇOLAKOĞLU

Trigonometric Functions in the m-plane

Trigonometric Functions in the m-plane

ABSTRACT

In this paper, we define the trigonometric functions in the plane with the m-metric. And then we give two properties about these trigonometric functions, one of which states the area formula for a triangle in the m-plane in terms of the m-metric.

Key words: Taxicab metric, Chinese checker metric, alpha metric, m-metric, m-trigonometry

MSC2010: 51K05, 51K99

Trigonometrijske funkcije u m-ravnini

SAŽETAK

U članku definiramo trigonometrijske funkcije u ravnini s m-metrikom. Zatim pokazujemo dva svojstva ovih trigonometrijskih funkcija gdje jedno od njih daje formulu površine trokuta u m-ravnini s primjenom m-metrike.

Ključne riječi: Taxicab metrika, metrika kineskog šaha, alfa metrika, m-metrika, m-trigonometrija

1 Introduction

The *taxicab metric* was given in a family of metrics of the real plane by Minkowski [16]. And the taxicab geometry introduced by Menger [15], and developed by Krause [14]. Later, Chen [7] developed the *Chinese checker metric*, and Tian [19] gave a family of metrics, α-metric for $\alpha \in [0,\pi/4]$, which includes the taxicab and Chinese checker metrics as special cases, and Çolakoğlu [8] extended the α -metric for $\alpha \in [0,\pi/2)$. Afterwards, Bayar, Ekmekçi and Akça [5] presented a generalization of α-metric: the *generalized absolute value metric*. Finally, Çolakoğlu and Kaya [10] gave a generalization for all these metrics: m-metric (or m-generalized absolute value metric). During the recent years, trigonometry on the plane geometries based on these metrics have been studied. See [1], [2], [3], [4], [5], [6], [12], [17] and [18] for some of studies. In this paper, we study on trigonometry in the plane with the generalized m-metric. First, we give definitions of trigonometric functions for the m-metric, which also generalize the definitions given before, and then give two properties about these trigonometric functions, one of which states a formula to calculate the area of any triangle in the m-plane, being an alternative to the one given in [13]. This study also provides a facility for further subjects as cosine theorem, norm and inner-product in terms of the m-metric.

Let $P_1=(x_1,y_1)$ and $P_2=(x_2,y_2)$ be two points in $\mathbb{R}^2$. For each real numbers a and b, such that $a \geq b \geq 0 \neq a$, the function $d_m : \mathbb{R}^2 \times \mathbb{R}^2 \to [0,\infty)$ defined by

$$d_m(P_1,P_2) = (a\Delta_{AB} + b\delta_{AB}) \diagup \sqrt{1+m^2} \tag{1}$$

where

$$\Delta_{AB} = \max\{|(x_1-x_2)+m(y_1-y_2)|, |m(x_1-x_2)-(y_1-y_2)|\}$$

and

$$\delta_{AB} = \min\{|(x_1-x_2)+m(y_1-y_2)|, |m(x_1-x_2)-(y_1-y_2)|\},$$

is called the *m- distance function* in $\mathbb{R}^2$, and the real number $d_m(P_1,P_2)$ is called the *m-distance* between points P_1 and P_2.

Cartesian coordinate plane endowed with the m-metric forms a metric space, $\mathbb{R}^2_m$ or $(\mathbb{R}^2,d_m)$, and it is constructed by simply replacing the well-known Euclidean distance function

$$d_E(P_1,P_2) = ((x_1-x_2)^2+(y_1-y_2)^2)^{1/2} \tag{2}$$

by the m-distance function d_m in $\mathbb{R}^2$ (see [10]). In all that follows, we use $a' = a \diagup \sqrt{1+m^2}$ and $b' = b \diagup \sqrt{1+m^2}$ to shorten phrases.

2 Trigonometric Functions

We know that if $P=(x,y)$ is a point on the Euclidean unit circle, then $x=\cos\theta$ and $y=\sin\theta$, where θ is the angle with the positive x-axis as the initial side and the radial line passing through the point P as the terminal side. One can determine the standard definitions of the trigonometric functions using the unit m-circle in $\mathbb{R}^2_m$, in the same way one determines their Euclidean analogues. The unit m-circle (see Figure 1) is the set of points (x,y), which satisfies the equation

$$a'\max\{|x+my|,|mx-y|\}+b'\min\{|x+my|,|mx-y|\}=1. \tag{3}$$

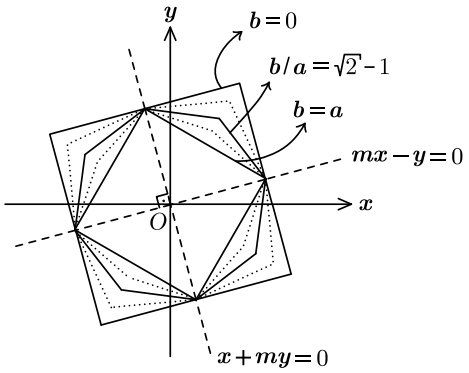

Figure 1: *Graph of unit m-circles*

So, for the point $P=(x,y)$ on the m-unit circle, let us determine *sine* and *cosine* functions in $\mathbb{R}^2_m$ as $x=\cos_m\theta$ and $y=\sin_m\theta$, where θ is the angle with the positive x-axis as the initial side and the radial line passing through the point P as the terminal side. Clearly, *tangent* and *cotangent* functions do not depend on the metric, since the slope of the radial line passing through the point (x,y) does not change. Thus, we have

$$\tan_m\theta=\frac{\sin_m\theta}{\cos_m\theta}=\tan\theta \quad\text{and}\quad \cot_m\theta=\frac{\cos_m\theta}{\sin_m\theta}=\cot\theta.$$

Obviously, the equation of the line joining (x,y) and $(0,0)$ is $y=(\tan\theta)x$. Solving the system

$$\begin{cases} y=(\tan\theta)x \\ a'\max\{|x+my|,|mx-y|\}+b'\min\{|x+my|,|mx-y|\}=1 \end{cases}$$

one gets *sine* and *cosine* functions in $\mathbb{R}^2_m$:

$$\cos_m\theta=\frac{\cos\theta}{a'\max\{X,Y\}+b'\min\{X,Y\}}, \tag{4}$$

$$\sin_m\theta=\frac{\sin\theta}{a'\max\{X,Y\}+b'\min\{X,Y\}}, \tag{5}$$

where $X=|\cos\theta+m\sin\theta|$, $Y=|m\cos\theta-\sin\theta|$.

We can also determine *secant* and *cosecant* functions as in Euclidean plane: $\csc_m\theta=\frac{1}{\sin_m\theta}$ and $\sec_m\theta=\frac{1}{\cos_m\theta}$. For some values of a, b and m, graphs of $y=\sin_m x$ and $y=\cos_m x$ are given in Figure 2, Figure 3, Figure 4 and Figure 5, for $-2\pi<x<2\pi$.

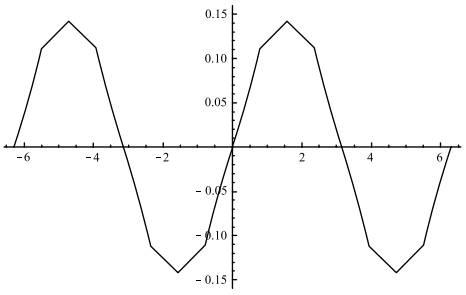

Figure 2: *Graph of* $y=\sin_m x$ *for* $a=7$, $b=2$ *and* $m=0$

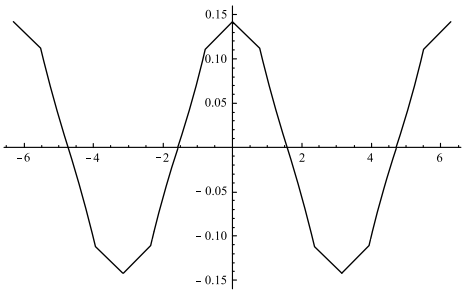

Figure 3: *Graph of* $y=\cos_m x$ *for* $a=7$, $b=2$ *and* $m=0$

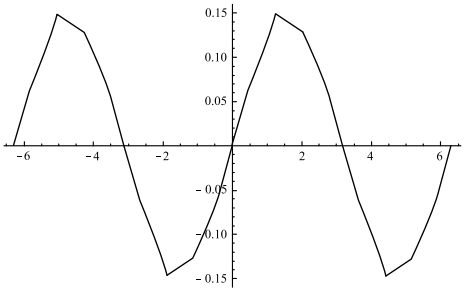

Figure 4: *Graph of* $y=\sin_m x$ *for* $a=7$, $b=2$ *and* $m=\frac{1}{2}$

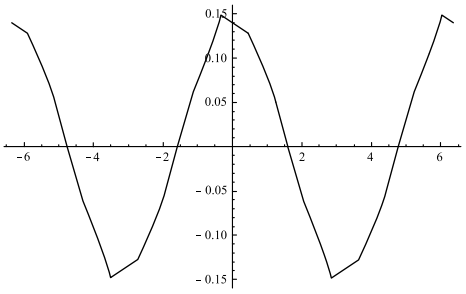

Figure 5: *Graph of* $y=\cos_m x$ *for* $a=7$, $b=2$ *and* $m=\frac{1}{2}$

In $\mathbb{R}^2_m$, the trigonometric identities differ from their Euclidean analogues in most cases. Some of the identities of these functions are like their Euclidean counterparts:

$$\cos_m(\frac{\pi}{2}+\theta) = -\sin_m\theta, \quad \sin_m(\frac{\pi}{2}+\theta) = \cos_m\theta$$
$$\cos_m(\frac{3\pi}{2}+\theta) = \sin_m\theta, \quad \sin_m(\frac{3\pi}{2}+\theta) = -\cos_m\theta$$
$$\cos_m(\pi+\theta) = -\cos_m\theta, \quad \sin_m(\pi+\theta) = -\sin_m\theta$$
$$\cos_m(2\pi+\theta) = \cos_m\theta, \quad \sin_m(2\pi+\theta) = \sin_m\theta.$$

It is well known that the Pythagorean identity is the relation between sine and cosine functions: $\sin^2\theta+\cos^2\theta = 1$. In terms of the generalized m-metric, we get the following equation

$$\begin{aligned} &a'\max\{|\cos_m\theta + m\sin_m\theta|, |m\cos_m\theta - \sin_m\theta|\} \\ &\quad +b'\min\{|\cos_m\theta + m\sin_m\theta|, |m\cos_m\theta - \sin_m\theta|\} = 1. \end{aligned} \tag{6}$$

One can also get the following equations easily:

$$\begin{aligned} &a'\max\{|1+m\tan\theta|, |m-\tan\theta|\} \\ &\quad +b'\min\{|1+m\tan\theta|, |m-\tan\theta|\} = |\sec_m\theta| \\ &a'\max\{|\cot\theta+m|, |m\cot\theta-1|\} \\ &\quad +b'\min\{|\cot\theta+m|, |m\cot\theta-1|\} = |\csc_m\theta|. \end{aligned} \tag{7}$$

Using the sum and difference formulas for tangent function one gets also the following equations:

$$\tan_m(u\mp v) = \frac{\tan_m u \mp \tan_m v}{1 \pm \tan_m u \tan_m v} \tag{8}$$
$$\cot_m(u\mp v) = \frac{1 \pm \cot_m u \cot_m v}{\cot_m u \mp \cot_m v}$$

$$\sin_m(u\mp v) = \sin_m u\cos_m v \mp \sin_m v\cos_m u \tag{9}$$
$$\cos_m(u\mp v) = \cos_m u\cos_m v \pm \sin_m u\sin_m v.$$

3 Trigonometric Functions with Reference Angle

Unlike the Euclidean case, there is a non-uniform increment in the arc length as the angle θ is incremented by a fix amount, in $\mathbb{R}^2_m$. So, it is necessary to develop the trigonometric functions for any angle θ using the reference angle α of θ (see [18]).

Definition 1 *Let θ be an angle with the reference angle α which is the angle between θ and the positive direction of the x-axis in m -unit circle. Then the cosine and sine functions of the angle θ with the reference angle α,* $\mathrm{mcos}\,\theta$ *and* $\mathrm{msin}\,\theta$*, are defined by*

$$\mathrm{mcos}\,\theta = \cos_m(\alpha+\theta)\cos_m\alpha + \sin_m(\alpha+\theta)\sin_m\alpha \tag{10}$$

$$\mathrm{msin}\,\theta = \sin_m(\alpha+\theta)\cos_m\alpha - \cos_m(\alpha+\theta)\sin_m\alpha. \tag{11}$$

In this definition, the angles of α and $(\alpha+\theta)$ are in standard position. So, the values of $\cos_m(\alpha+\theta)$, $\sin_m(\alpha+\theta)$, $\cos_m\alpha$ and $\sin_m\alpha$ are calculated by using equations (4) and (5). If $\alpha = 0$, then

$$\mathrm{m}\cos\theta = \frac{\cos_m\theta}{a'\max\{1,|m|\}+b'\min\{1,|m|\}} \tag{12}$$

$$\mathrm{m}\sin\theta = \frac{\sin_m\theta}{a'\max\{1,|m|\}+b'\min\{1,|m|\}}. \tag{13}$$

The general definitions of other trigonometric functions for the angles which are not in standard position can be given similarly: $\mathrm{mtan}\,\theta = \frac{\mathrm{m}\sin\theta}{\mathrm{m}\cos\theta} = \tan\theta$, $\mathrm{mcot}\,\theta = \frac{\mathrm{m}\cos\theta}{\mathrm{m}\sin\theta} = \cot\theta$, $\mathrm{mcsc}\,\theta = \frac{1}{\mathrm{m}\sin\theta}$ and $\mathrm{msec}\,\theta = \frac{1}{\mathrm{m}\cos\theta}$. Consequently, the general definitions of trigonometric functions can be given by defining angles with the reference angle in plane with the generalized m-metric.

It is well-known that all rotations and translations preserve the Euclidean distance. In $\mathbb{R}^2_m$, all translations and the rotations of the angle $\theta \in \{\frac{\pi}{2}, \pi, \frac{3\pi}{2}, 2\pi\}$ when $b/a \neq \sqrt{2}-1$ and also the rotations of the angle $\theta \in \{\frac{\pi}{4}, \frac{3\pi}{4}, \frac{5\pi}{4}, \frac{7\pi}{4}\}$ when $b/a = \sqrt{2}-1$ preserve m-distance (see [10]). The change of the length of a line segment by a rotation can be given by the following theorem:

Theorem 1 *Let any two points be A and B in $\mathbb{R}^2_m$, and let the line segment AB be not parallel to the x-axis and the angle α between the line segment AB and the positive direction of x-axis. If $A'B'$ is the image of AB under the rotation with the angle θ, then*

$$d_m(A',B') = d_m(A,B)\sqrt{\frac{\cos_m^2\alpha+\sin_m^2\alpha}{\cos_m^2(\alpha+\theta)+\sin_m^2(\alpha+\theta)}} \tag{14}$$

Proof. Since all translations preserve the m-distance, the line segment AB can be translated to the line segment OX such that O is the origin. Let the line segment OX' be the image of OX under rotation with the angle θ, and let $d_m(A,B) = d_m(O,X) = k$ and $d_m(O,X') = k'$. If α is the reference angle of θ, then $X = (k\cos_m\alpha, k\sin_m\alpha)$ and $X' = (k'\cos_m(\alpha+\theta), k'\sin_m(\alpha+\theta))$. Since $d_E(O,X) = d_m(O,X')$, one gets

$$k'\sqrt{\cos_m^2(\alpha+\theta)+\sin_m^2(\alpha+\theta)} = k\sqrt{\cos_m^2\alpha+\sin_m^2\alpha}$$

and

$$d_m(A',B') = d_m(A,B)\sqrt{\frac{\cos_m^2\alpha+\sin_m^2\alpha}{\cos_m^2(\alpha+\theta)+\sin_m^2(\alpha+\theta)}}. \qquad \square$$

The following corollary shows how one can find the generalized m-length of a line segment, after a rotation with an angle θ in standard position:

Corollary 1 *If the line segment AB is parallel to the x-axis, then*

$$d_m(A',B')=\frac{d_m(A,B)}{(a'\max\{1,|m|\}+b'\min\{1,|m|\})\sqrt{\cos_m^2\theta+\sin_m^2\theta}} \tag{15}$$

Proof. Since $\alpha=0$, proof is obvious. □

In [13], an area formula for a triangle is given in the plane with the generalized m-metric (see also [11]). In the following theorem, the area of a triangle is given by using the trigonometric functions in $\mathbb{R}_m^2$.

Theorem 2 *Let ABC be any triangle in $\mathbb{R}_m^2$, and let θ be the angle between the line segments AC and BC. Then the area $\mathcal{A}$ of the triangle ABC can be given by the following formula:*

$$\mathcal{A}=\frac{1}{2}d_m(A,C)d_m(B,C)\operatorname{msin}\theta. \tag{16}$$

Proof. Let $d_m(A,C)=k$ and $d_m(B,C)=k'$. We can take the vertex C as the origin, and $A=(k\cos_m\alpha,k\sin_m\alpha)$ and $B=(k'\cos_m(\alpha+\theta),k'\sin_m(\alpha+\theta))$, without loss of generality. Thus, we have $d_E(A,C)=k\sqrt{\cos_m^2\alpha+\sin_m^2\alpha}$ and $d_E(B,C)=k'\sqrt{\cos_m^2(\alpha+\theta)+\sin_m^2(\alpha+\theta)}$. Also, it is easy to show that if γ is in standard position, then $\cos_m\gamma=\cos\gamma\sqrt{\cos_m^2\gamma+\sin_m^2\gamma}$ and $\sin_m\gamma=\sin\gamma\sqrt{\cos_m^2\gamma+\sin_m^2\gamma}$. Thus, one gets the equation

$$m\sin\theta=\sin\theta\sqrt{\cos_m^2\alpha+\sin_m^2\alpha}\sqrt{\cos_m^2(\alpha+\theta)+\sin_m^2(\alpha+\theta)}. \tag{17}$$

If we use the values of $d_E(A,C)$, $d_E(B,C)$ and $\sin\theta$ in the formula $\mathcal{A}=\frac{1}{2}d_E(A,C)d_E(B,C)\sin\theta$, we get the area formula in the plane with the generalized m-metric:
$\mathcal{A}=\frac{1}{2}d_m(A,C)d_m(B,C)\operatorname{msin}\theta$. □

References

[1] Z. AKÇA, R. KAYA, On Taxicab Trigonometry, *J. Inst. Math. Comput. Sci. Math. Ser.)* **10**(**3**) (1997), 151–159.

[2] A. BAYAR, S. EKMEKÇI, On the Chinese-Checker Sine and Cosine Functions, *Int. J. Math. Anal.* **1**(**3**) (2006), 249–259.

[3] A. BAYAR, On Trigonometric Functions in Maximum Metric, *KoG* **12** (2008), 45–48.

[4] A. BAYAR, S. EKMEKÇI, M. ÖZCAN, On Trigonometric Functions and Cosine and Sine Rules in Taxicab Plane, *Int Electron. J. Geom.* **2**(**1**) (2009), 17–24.

[5] A. BAYAR, S. EKMEKÇI, Z. AKÇA, On the Plane Geometry with Generalized Absolute Value Metric, *Math. Probl. Eng.* **2008** (2008), Art. ID 673275, 8 pp.

[6] R. BRISBIN, P. ARTOLA, Taxicab Trigonometry, *Pi Mu Epsilon J.* **8**(**3**) (1985), 249–259.

[7] G. CHEN, *Lines and Circles in Taxicab Geometry*, Master Thesis, Department of Mathematics and Computer Science, University of Central Missouri, 1992.

[8] H.B. ÇOLAKOĞLU, Concerning the Alpha Distance, *Algebras Groups Geom.* **28** (2011), 1–14.

[9] H.B. ÇOLAKOĞLU, Ö. GELIŞGEN, R. KAYA, Pythagorean Theorems in the alpha Plane, Math. Commun. **14**(**2**) (2009), 211–221.

[10] H.B. ÇOLAKOĞLU, R. KAYA, A Generalization of Some Well-Known Distances and Related Isometries, *Math. Commun.* **16**(**1**) (2011), 21–35.

[11] H.B. ÇOLAKOĞLU, Ö. GELIŞGEN, R. KAYA, Area Formulas for a Triangle in the Alpha Plane, *Math. Commun.* **18** (2013), 123–132.

[12] S. EKMEKÇI, Z. AKÇA, A.K. ALTINTAŞ, On Trigonometric Functions And Norm In The Generalized Taxicab Metric, *Math. Sci. Appl. E-Notes* **3**(**2**) (2015), 27–33.

[13] Ö. GELIŞGEN, T. ERMIŞ, Area Formulas For A Triangle In The m-Plane, *Konuralp J. Math.* **2**(**2**) (2014) 85–95.

[14] E.F. KRAUSE, *Taxicab Geometry*, Addison-Wesley, Menlo Park, California, 1975; Dover Publications, New York, 1987.

[15] K. MENGER, *You Will Like Geometry*, Guidebook of Illinois Institute of Technology Geometry Exhibit, Museum of Science and Industry, Chicago, Illinois, 1952.

[16] H. MINKOWSKI, *Gesammelte Abhandlungen*, Chelsa Publishing Co. New York, 1967.

[17] M. ÖZCAN, S. EKMEKÇI, A. BAYAR, A Note on the Variation of the Taxicab Lengths Under Rotations, *Pi Mu Epsilon J.* **11**(**7**) (2002), 381–384.

[18] K. THOMPSON, T. DRAY, Taxicab Angles and Trigonometry, *Pi Mu Epsilon J.* **11**(**2**) (2000), 87–97.

[19] S. TIAN, Alpha Distance-A Generalization of Chinese Checker Distance and Taxicab Distance, *Missouri J. Math. Sci.* **17**(**1**) (2005), 35–40.

Harun Barış Çolakoğlu
e-mail: hbcolakoglu@akdeniz.edu.tr

Akdeniz University
Vocational School of Technical Sciences
C-9, 07070, Pınarbaşı, Antalya, Turkey

Original scientific paper
Accepted 31. 10. 2017.

EMA JURKIN
MARIJA ŠIMIĆ HORVATH
VLADIMIR VOLENEC

On Brocard Points of Harmonic Quadrangle in Isotropic Plane

On Brocard Points of Harmonic Quadrangle in Isotropic Plane

ABSTRACT

In this paper we present some new results on Brocard points of a harmonic quadrangle in isotropic plane. We construct new harmonic quadrangles associated to the given one and study their properties dealing with Brocard points.

Key words: isotropic plane, harmonic quadrangle, Brocard points

MSC2010: 51N25

O Brocardovim točkama harmoničnog četverokuta u izotropnoj ravnini

SAŽETAK

U radu se prikazuju neki novi rezultati o Brocardovim točkama harmoničnog četverokuta u izotropnoj ravnini. Konstruiraju se novi harmonični četverokuti pridruženi danom četverokutu, te se proučavaju njihova svojstva vezana uz Brocardove točke.

Ključne riječi: izotropna ravnina, harmonični četverokut, Brocardove točke

1 Introduction

The geometry of harmonic quadrangle has been discussed in [3]. The *harmonic quadrangle* is a cyclic quadrangle $ABCD$ (see [5]) with the following property: the point of intersection of the tangents at the vertices A and C lies on the line BD, and the intersection point of the tangents at the vertices B and D lies on the line AC. If one of the requests is fulfilled, the other one automatically follows. The quadrangle $ABCD$ is chosen to have $y = x^2$ as a circumscribed circle and the vertices $A = (a, a^2), B = (b, b^2), C = (c, c^2)$, and $D = (d, d^2)$, with a, b, c, d being mutually different real numbers, where $a < b < c < d$. In that case, sides of $ABCD$ are

$$\begin{array}{ll} AB \ldots y = (a+b)x - ab, & DA \ldots y = (a+d)x - ad, \\ BC \ldots y = (b+c)x - bc, & AC \ldots y = (a+c)x - ac, \\ CD \ldots y = (c+d)x - cd, & BD \ldots y = (b+d)x - bd. \end{array} \tag{1}$$

and tangents to $y = x^2$ at A, B, C, D are

$$\begin{array}{ll} \mathcal{A} \ldots y = 2ax - a^2, & \mathcal{B} \ldots y = 2bx - b^2, \\ \mathcal{C} \ldots y = 2cx - c^2, & \mathcal{D} \ldots y = 2dx - d^2. \end{array} \tag{2}$$

Equations (1) and (2) can be found within Lemma 1 in [5]. In that paper the diagonal triangle of a cyclic quadrangle was introduced where diagonal points $U = AC \cap BD$, $V = AB \cap CD$ and $W = AD \cap BC$ are given by

$$\begin{aligned} U &= \left(\frac{ac - bd}{a - b + c - d}, \frac{ac(b+d) - bd(a+c)}{a - b + c - d} \right), \\ V &= \left(\frac{ab - cd}{a + b - c - d}, \frac{ab(c+d) - cd(a+b)}{a + b - c - d} \right), \\ W &= \left(\frac{ad - bc}{a - b - c + d}, \frac{ad(b+c) - bc(a+d)}{a - b - c + d} \right). \end{aligned} \tag{3}$$

Taking $ac = bd = -k^2, k > 0$ we deal with harmonic quadrangle in a standard position. As every harmonic quadrangle can be represented in the standard position, in order to prove geometric facts for each harmonic quadrangle, it is sufficient to give a proof for the standard harmonic quadrangle. The diagonal points given by (3) in the case of

standard position turn into

$$U=(0,k^2),\quad V=\left(\frac{ab-cd}{a+b-c-d},-k^2\right),$$
$$W=\left(\frac{ad-bc}{a-b-c+d},-k^2\right). \tag{4}$$

Due to Theorem 1 in [3] more characterizations of harmonic quadrangles among the cyclic ones are given.

Theorem 1 *Let $ABCD$ be an allowable cyclic quadrangle with vertices $A=(a,a^2)$, $B=(b,b^2)$, $C=(c,c^2)$, $D=(d,d^2)$, sides (1) and tangents of its circumscribed circle $y=x^2$ at its vertices are given by (2). These are the equivalent statements:*

1. *the point $T_{AC}=\mathcal{A}\cap\mathcal{C}$ is incident with the diagonal BD;*
2. *the point $T_{BD}=\mathcal{B}\cap\mathcal{D}$ is incident with the diagonal AC;*
3. *the equality*

$$d(A,B)\cdot d(C,D)=-d(B,C)\cdot d(D,A) \tag{5}$$

holds;

4. *the equality*

$$2(ac+bd)=(a+c)(b+d) \tag{6}$$

holds.

In the sequel we will deal with Brocard points of these quadrangles defined in [3] and show several properties of them connected to the harmonic quadrangles associated to $ABCD$. For that purpose the following lemma will be very useful.

Lemma 1 *Let $ABCD$ be an allowable cyclic quadrangle in the standard position with vertices $A=(a,a^2)$, $B=(b,b^2)$, $C=(c,c^2)$, $D=(d,d^2)$. The following equalities are valid*

$$ab+k^2=k(b-a),\qquad bc+k^2=k(c-b),$$
$$cd+k^2=k(d-c),\qquad da+k^2=k(a-d).$$

Proof. Let us prove $ab+k^2=k(b-a)$. Taking (see [3])

$$\frac{(a-c)(b-d)}{a+c-b-d}=-2k \tag{7}$$

in

$$-2k(a-b)-2ab=2k^2$$

we get

$$\frac{-a^2b+ab^2-a^2d+b^2c-4abc+4abd+abc-abd+acd-bcd}{a-b+c-d}$$
$$=2k^2,$$

i.e.

$$\frac{-a^2b+ab^2-a^2d+b^2c-4k^2(a-b)}{a-b+c-d}+k^2=2k^2.$$

After employing $(a+c)(b+d)=-4k^2$ from [3], the upper equality turns into

$$\frac{-a^2b+ab^2-a^2d+b^2c+(a+c)(b+d)(a-b)}{a-b+c-d}+k^2=2k^2.$$

Immediately,

$$\frac{k^2(a-b+c-d)}{a-b+c-d}+k^2=2k^2$$

follows and the claim of Lemma is proved. □

Further on we will always deal with the harmonic quadrangle in the standard position.

2 Brocard points

There is an interesting result discussed in [3]: whole family of harmonic quadrangles can be obtained out of the given harmonic quadrangle. Namely, let $ABCD$ be a harmonic quadrangle. Lines a',b',c',d' are taken in a way to be incident to vertices A,B,C,D, respectively, and make equal angles to the sides AB,BC,CD,DA, respectively. The quadrangle formed by lines a',b',c',d' is a harmonic quadrangle as well. Furthermore, denoting obtained quadrangle by $A'B'C'D'$, the ratios of the corresponding sides of given quadrangle $ABCD$ and obtained quadrangle $A'B'C'D'$ are equal. Only in one case, points A',B',C',D' coincide with one point P_1, the first *Brocard point*. In similar manner, the second Brocard point P_2 is obtained as well. In the latter case lines P_2A, P_2B, P_2C, and P_2D form the equal angles with the sides AD,DC,CB, and BA, respectively. Brocard points are of the form

$$P_1=\left(k,3k^2\right),\quad P_2=\left(-k,3k^2\right). \tag{8}$$

The Brocard points can easily be constructed by using the fact that

$$P_1=WM_{AC}\cap VM_{BD},\quad P_2=VM_{AC}\cap WM_{BD} \tag{9}$$

where M_{AC}, M_{BD} are midpoints of the line segments $\overline{AC}$, $\overline{BD}$, respectively.

The Euclidean case of Theorem 2 can be found in [1], and the Euclidean analogue of Theorem 3 is stated in [2] and [4].

Theorem 2 *Let $ABCD$ be a harmonic quadrangle and P_1, P_2 its Brocard points. The following equality holds:*

$$d(A,P_1)\cdot d(B,P_1)\cdot d(C,P_1)\cdot d(D,P_1) = d(A,P_2)\cdot d(B,P_2)\cdot d(C,P_2)\cdot d(D,P_2).$$

Proof. Since

$$\begin{aligned} &d(A,P_1)\cdot d(B,P_1)\cdot d(C,P_1)\cdot d(D,P_1)\\ &\quad = (k-a)(k-b)(k-c)(k-d)\\ &\quad = \left(k^2-k(a+c)+ac\right)\left(k^2-k(b+d)+bd\right)\\ &\quad = k^2(a+c)(b+d) = -4k^4 \end{aligned}$$

and

$$\begin{aligned} &d(A,P_2)\cdot d(B,P_2)\cdot d(C,P_2)\cdot d(D,P_2)\\ &\quad = (-k-a)(-k-b)(-k-c)(-k-d)\\ &\quad = \left(k^2+k(a+c)+ac\right)\left(k^2+k(b+d)+bd\right)\\ &\quad = k^2(a+c)(b+d) = -4k^4 \end{aligned}$$

the theorem is proved. □

Theorem 3 *Let $ABCD$ be a harmonic quadrangle and P_1, P_2 its Brocard points. The four points $AP_1\cap BP_2$, $BP_1\cap CP_2$, $CP_1\cap DP_2$, $DP_1\cap AP_2$ lie on a circle, that is incident with the points U, P_1, P_2, M_{AC} and M_{BD} as well. Furthermore, they are parallel with the midpoints of the line segments AB, BC, CD and DA, respectively.*

Proof. Due to Theorem 5 in [3] the circle incident to the points U, P_1, P_2, M_{AC} and M_{BD} is given by

$$y = 2x^2 + k^2. \tag{10}$$

Let us take for example the point $AP_1\cap BP_2$. Lines AP_1 and BP_2 have the equations (see Theorem 4 in [3])

$$\begin{aligned} y &= (a+b+2k)x - a(2k+b),\\ y &= (b+a-2k)x - b(-2k+a). \end{aligned}$$

Thus, the point $AP_1\cap BP_2$ is of the form

$$\left(\frac{a+b}{2}, k(b-a)+\frac{a^2+b^2}{2}\right).$$

Due to Lemma 1 the equality $k(b-a) = ab+k^2$ is valid, and therefore the point $AP_1\cap BP_2$ is incident to (10). □

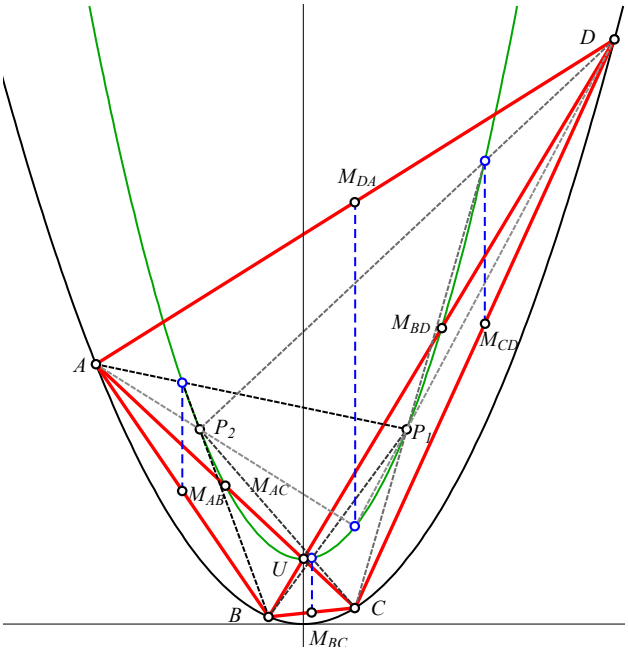

Figure 1: *Visualization of Theorem 3*

In the sequel we will study two quadrangles associated to the given harmonic quadrangle $ABCD$. Let A^i, B^i, C^i, D^i be the intersection points of its circumscribed circle $y = x^2$ with the lines AP_i, BP_i, CP_i, DP_i, respectively, $i = 1, 2$. According to [3] (Theorem 4, for $h = -2k$), the line AP_1 has the equation $y = (a+b+2k)x - a(2k+b)$. Hence, A^1 has coordinates $\left(b+2k, (b+2k)^2\right)$. Similarly, we get the other intersections:

$$\begin{aligned} A^1 &= \left(b+2k,(b+2k)^2\right),\ B^1 = \left(c+2k,(c+2k)^2\right),\\ C^1 &= \left(d+2k,(d+2k)^2\right),\ D^1 = \left(a+2k,(a+2k)^2\right), \end{aligned} \tag{11}$$

and

$$\begin{aligned} A^2 &= \left(d-2k,(d-2k)^2\right),\ B^2 = \left(a-2k,(a-2k)^2\right),\\ C^2 &= \left(b-2k,(b-2k)^2\right),\ D^2 = \left(c-2k,(c-2k)^2\right). \end{aligned} \tag{12}$$

Some interesting properties of the obtained quadrangles are stated in Theorems 4-9 that follow. The authors haven't found their Euclidean counterparts in the literature available to them, but they are convinced in their validity in the Euclidean plane as well.

Theorem 4 *The quadrangles $A^1B^1C^1D^1$ and $A^2B^2C^2D^2$, associated to the harmonic quadrangle $ABCD$, are harmonic quadrangles as well.*

Proof. From (11) we get equations (see Theorem 4 in [3])

$$\begin{aligned} d(A^1,B^1)\cdot d(C^1,D^1) &= (c-b)(a-d) = d(B,C)\cdot d(D,A),\\ d(B^1,C^1)\cdot d(D^1,A^1) &= (d-c)(b-a) = d(C,D)\cdot d(A,B). \end{aligned}$$

Obviously, $d(A^1,B^1)\cdot d(C^1,D^1) = -d(B^1,C^1)\cdot d(D^1,A^1)$ precisely when $d(A,B)\cdot d(C,D) = -d(B,C)\cdot d(D,A)$. Therefore, $A^1B^1C^1D^1$ is a harmonic quadrangle. Similar procedure gives the proof for $A^2B^2C^2D^2$. □

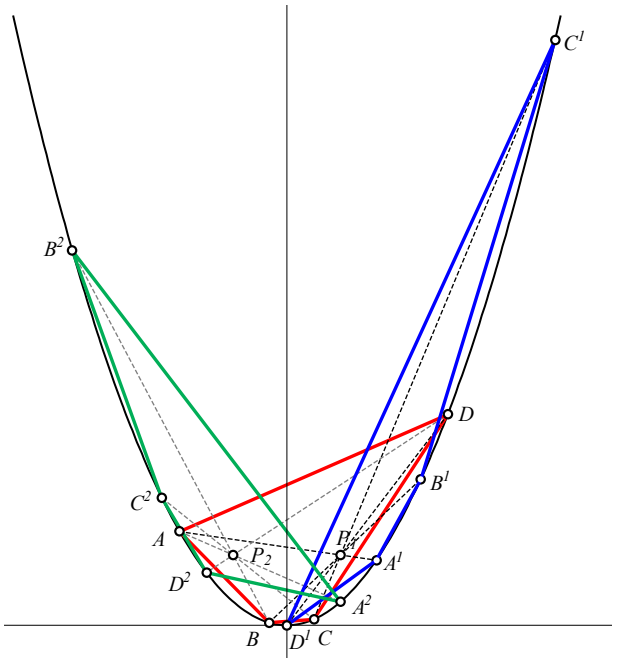

Figure 2: *Harmonic quadrangles $A^1B^1C^1D^1$ and $A^2B^2C^2D^2$.*

Theorem 5 *For the quadrangles $A^1B^1C^1D^1$ and $A^2B^2C^2D^2$ associated to the harmonic quadrangle $ABCD$ the equalities*

$$\angle(D^2A^2,A^2B^2) = -\angle(AB,BC) = \angle(B^1C^1,C^1D^1),$$
$$\angle(A^2B^2,B^2C^2) = -\angle(BC,CD) = \angle(C^1D^1,D^1A^1),$$
$$\angle(B^2C^2,C^2D^2) = -\angle(CD,DA) = \angle(D^1A^1,A^1B^1),$$
$$\angle(C^2D^2,D^2A^2) = -\angle(DA,AB) = \angle(A^1B^1,B^1C^1),$$

and

$$d(A^1,B^1) = d(B,C) = d(C^2,D^2),$$
$$d(B^1,C^1) = d(C,D) = d(D^2,A^2),$$
$$d(C^1,D^1) = d(D,A) = d(A^2,B^2),$$
$$d(D^1,A^1) = d(A,B) = d(B^2,C^2)$$

hold.

Proof. Let us prove $\angle(D^2A^2,A^2B^2) = -\angle(AB,BC)$. From (12) we get

$$A^2B^2 \quad \ldots \quad y = (d+a-4k)x-(d-2k)(a-2k),$$
$$A^2D^2 \quad \ldots \quad y = (d+c-4k)x-(d-2k)(c-2k),$$

and therefore, $\angle(D^2A^2,A^2B^2) = a-c$. The equality $\angle(AB,BC) = c-a$, obtained from (1), completes the first part of the proof.
The second part of the theorem follows directly from (11) and (12). □

Theorem 6 *For the quadrangles $A^1B^1C^1D^1$ and $A^2B^2C^2D^2$ associated to the harmonic quadrangle $ABCD$ the following statements on their diagonal points $U^i = A^iC^i\cap B^iD^i$, $i=1,2$, are valid:*

1. *$d(U^1,U) = d(U,U^2)$.*
2. *The connection line U^1U^2 is parallel to the connection lines P^1P^2 and VW.*
3. *The points U^1, U^2 are incident with the lines UP_1, UP_2, respectively.*

Proof. Directly from (11) and (12) the coordinates of U^1, U^2 are obtained to be

$$U^1 = (2k,5k^2), \quad U^2 = (-2k,5k^2).$$

Thus, $d(U^1,U) = -2k = d(U,U^2)$.
The connection line U^1U^2 has the equation $y = 5k^2$ and it is parallel to the lines P^1P^2 and VW having the equations $y = 3k^2$ and $y = -k^2$.
The last part of the theorem holds since the coordinates of the points U,U^1,P_1 satisfy the equation $y = 2kx+k^2$, while the coordinates of the points U,U^2,P_2 satisfy the equation $y = -2kx+k^2$. □

Theorem 7 *The diagonal points $V^i = A^iB^i\cap C^iD^i$ and $W^i = A^iD^i\cap B^iD^i$ of the quadrangles $A^iB^iC^iD^i$ are incident with the lines VP_i and WP_i, respectively, $i=1,2$.*

Proof. Let us prove that $V^1 = A^1B^1\cap C^1D^1$ is incident with VP_1, i.e. V^1,V,P_1 are collinear points. From (3) and (11) we get

$$V^1 = \left(\frac{ad-bc}{a-b-c+d}+2k, 4k\frac{ad-bc}{a-b-c+d}+3k^2\right).$$

Now, the slopes of the lines VP_1 and V^1P_1 are obtained to be

$$\frac{-4k^2(a+b-c-d)}{ab-cd-k(a+b-c-d)}, \quad \frac{4k(ad-bc)}{ad-bc+k(a-b-c+d)},$$

respectively, and are equal precisely when

$$-k(a+b-c-d)[ad-bc+k(a-b-c+d)] = (ad-bc)[ab-cd-k(a+b-c-d)]$$

i. e.

$$-k^2(a+b-c-d)(a-b-c+d) = (ad-bc)(ab-cd).$$

This is true since

$$-k^2(a^2-2ac+c^2-b^2+2bd-d^2)$$
$$=-a^2k^2+d^2k^2+b^2k^2-c^2k^2.$$

The other three collinearities can be proved in a similar way. □

Theorem 8 *Let $M_{A^iC^i}$ and $M_{B^iD^i}$ be the midpoints of the line segments A^iC^i and B^iD^i, respectively, $i=1,2$. Then the following quadruples of points are collinear: $\{M_{A^1C^1},V,M_{BD},P_1\}$, $\{M_{B^1D^1},W,M_{AC},P_1\}$, $\{M_{A^2C^2},W,M_{BD},P_2\}$, $\{M_{B^2D^2},V,M_{AC},P_2\}$.*

Proof. Let us prove the claim of Theorem for the quadruple of points $\{M_{A^1C^1},V,M_{BD},P_1\}$. According to (9) the points V,M_{BD},P_1 are collinear. Therefore, it is sufficient to show that the points $M_{BD}\left(\frac{b+d}{2},\frac{b^2+d^2}{2}\right)$, $M_{A^1C^1}\left(\frac{b+d+4k}{2},\frac{(b+2k)^2+(d+2k)^2}{2}\right)$, and $P_1(k,3k^2)$ are collinear. Their coordinates satisfy the equation $y=(b+d+2k)x-(b+d)k+k^2$.
Indeed,

$$(b+d+2k)\frac{b+d}{2}-(b+d)k+k^2$$
$$=\frac{(b+d)^2}{2}+(b+d)k-(b+d)k+k^2=\frac{b^2+d^2}{2}.$$

Similarly,

$$(b+d+2k)\frac{b+d+4k}{2}-(b+d)k+k^2$$
$$=\frac{(b+d)^2}{2}+2k(b+d)+k(b+d)+4k^2-(b+d)k+k^2$$
$$=\frac{(b+2k)^2+(d+2k)^2}{2}$$

and

$$(b+d+2k)k-(b+d)k+k^2=3k^2.$$

The other three collinearities can be proved in a similar way. □

Theorem 9 *Let P_1^i and P_2^i be Brocard points of the quadrangle $A^iB^iC^iD^i$, $i=1,2$. Then the second Brocard point P_2^1 of the quadrangle $A^1B^1C^1D^1$ coincides with P_1, while the first Brocard point P_1^2 of the quadrangle $A^2B^2C^2D^2$ coincides with P_2.*

Proof. According to (9), $P_2^1=V^1M_{A^1C^1}\cap W^1M_{B^1D^1}$. Now, from Theorems 7-8 we get $P_2^1=VM_{BD}\cap WM_{AC}=P_1$.
Similarly,
$P_1^2=W^2M_{A^2C^2}\cap V^2M_{B^2D^2}=WM_{BD}\cap VM_{AC}=P_2$. □

By using two Brocard points of the given quadrangle $ABCD$ we constructed two new quadrangles. We can continue that procedure and, by using the Brocard points of the obtained quadrangles, construct further four quadrangles. Actually, we will get only two new quadrangles, since two of them coincide with the referent quadrangle $ABCD$. Indeed, if we use $A^1B^1C^1D^1$ and its first Brocard point, we will get a new quadrangle, but if we use its second Brocard point, which is P_1, then we will get $ABCD$. So, in each step of this procedure we have to use the first Brocard points, or we always have to use the second Brocard points.
Some computations verify that if we start a pattern with the quadrangle $ABCD$ in the step 0, and the quadrangle $A^1B^1C^1D^1$ in the step 1, then the first Brocard point in the step n has the coordinates $\left((2n+1)k,(2n+1)^2k^2+2k^2\right)$. Therefore, we conclude that all Brocard points of the quadrangles associated to the quadrangle $ABCD$ lie on the circle $y=x^2+2k^2$.

We will now focus on the other two quadrangles associated to the given harmonic quadrangle $ABCD$. Let the quadrangles $A^3B^3C^3D^3$ and $A^4B^4C^4D^4$ be defined in the following way: The lines l_{AB}, l_{BC}, l_{CD}, l_{DA} incident with the diagonal point U and parallel to AB, BC, CD, DA, respectively, intersect the sides of the quadrangle $ABCD$ in eight points

$$A^3=l_{AB}\cap AD, \qquad A^4=l_{AD}\cap AB,$$
$$B^3=l_{BC}\cap AB, \qquad B^4=l_{AB}\cap BC,$$
$$C^3=l_{CD}\cap BC, \qquad C^4=l_{BC}\cap CD,$$
$$D^3=l_{AD}\cap CD, \qquad D^4=l_{CD}\cap AD.$$

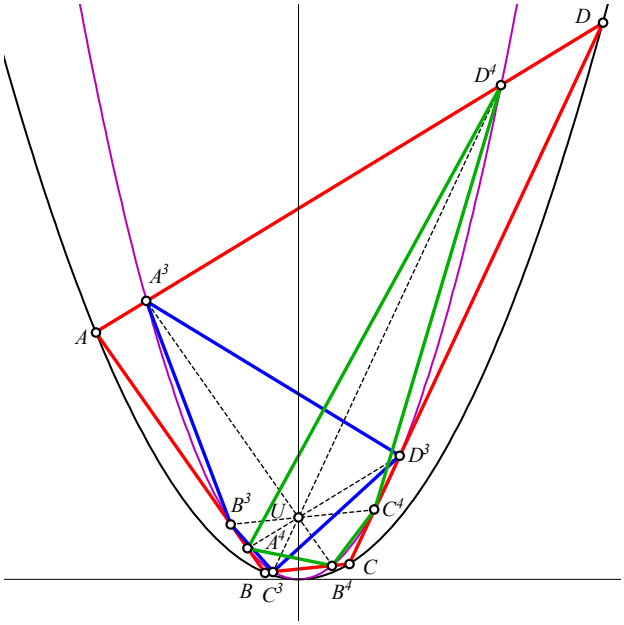

Figure 3: *Harmonic quadrangles $A^3B^3C^3D^3$ and $A^4B^4C^4D^4$*

It was shown in [3] that the constructed eight points lie on a circle $y = 2x^2$. The properties of the quadrangles $A^3B^3C^3D^3$ and $A^4B^4C^4D^4$ in the Euclidean plane have been discussed in [4]. Here we present the similar study for the isotropic plane.
Since the lines l_{AB} and AD are given by

$$\begin{aligned} l_{AB} &\quad ... \quad y = (a+b)x + k^2, \\ AD &\quad ... \quad y = (a+d)x - ad, \end{aligned}$$

the first coordinate of their intersection point A^3 is $\frac{ad+k^2}{d-b}$. According to Lemma 1, it equals $\frac{k(a-d)}{d-b}$. Similarly, all intersection points are obtained as

$$\begin{aligned} A^3 &= \left(\frac{k(a-d)}{d-b}, 2\left(\frac{k(a-d)}{d-b}\right)^2\right), \qquad (13) \\ B^3 &= \left(\frac{k(b-a)}{a-c}, 2\left(\frac{k(b-a)}{a-c}\right)^2\right), \\ C^3 &= \left(\frac{k(c-b)}{b-d}, 2\left(\frac{k(c-b)}{b-d}\right)^2\right), \\ D^3 &= \left(\frac{k(d-c)}{c-a}, 2\left(\frac{k(d-c)}{c-a}\right)^2\right) \end{aligned}$$

and

$$\begin{aligned} A^4 &= \left(\frac{k(b-a)}{b-d}, 2\left(\frac{k(b-a)}{b-d}\right)^2\right), \\ B^4 &= \left(\frac{k(c-b)}{c-a}, 2\left(\frac{k(c-b)}{c-a}\right)^2\right), \\ C^4 &= \left(\frac{k(d-c)}{d-b}, 2\left(\frac{k(d-c)}{d-b}\right)^2\right), \\ D^4 &= \left(\frac{k(a-d)}{a-c}, 2\left(\frac{k(a-d)}{a-c}\right)^2\right). \end{aligned}$$

Theorem 10 *For the quadrangles $A^iB^iC^iD^i$, $i = 3,4$, the equalities*

$$\frac{d(A^i,B^i)}{d(A,B)} = \frac{d(B^i,C^i)}{d(B,C)} = \frac{d(C^i,D^i)}{d(C,D)} = \frac{d(D^i,A^i)}{d(D,A)} = \frac{1}{2} \qquad (14)$$

and

$$\begin{aligned} &\angle(D^iA^i, A^iB^i) = \angle(DA, AB), \\ &\angle(A^iB^i, B^iC^i) = \angle(AB, BC), \\ &\angle(B^iC^i, C^iD^i) = \angle(BC, CD), \\ &\angle(C^iD^i, D^iA^i) = \angle(CD, DA) \end{aligned}$$

hold.

Proof. In order to show (14) is valid, we give a proof for $\frac{d(A^3,B^3)}{d(A,B)} = \frac{1}{2}$. Indeed,

$$\begin{aligned} d(A^3,B^3) &= \frac{k(b-a)}{a-c} + \frac{k(a-d)}{b-d} \\ &= k\frac{(b-a)(b-d)+(a-c)(a-d)}{(a-c)(b-d)} \\ &= k\frac{(a-b)(a-b+c-d)}{(a-c)(b-d)} = k\frac{(a-b)(a-b+c-d)}{-2k(a-b+c-d)} \\ &= \frac{b-a}{2} = \frac{d(A,B)}{2} \end{aligned}$$

Further on, let us prove $\angle(A^3B^3, B^3C^3) = \angle(AB, BC)$. Out of (13) the slopes of the lines A^3B^3 and B^3C^3 are obtained to be

$$2k\left(\frac{a-d}{d-b} + \frac{b-a}{a-c}\right), \quad 2k\left(\frac{b-a}{a-c} + \frac{c-b}{b-d}\right),$$

respectively. Thus,

$$\begin{aligned} \angle(A^3B^3, B^3C^3) &= \frac{2k(a-b+c-d)}{b-d} = \frac{-(a-c)(b-d)}{b-d} \\ &= c-a = \angle(AB, BC). \end{aligned}$$ □

Theorem 11 *The quadrangles $A^3B^3C^3D^3$ and $A^4B^4C^4D^4$ are harmonic quadrangles as well.*

Proof. It follows directly from (14) and Theorem 1. □

Theorem 12 *Let $U^i = A^iC^i \cap B^iD^i$, be the diagonal points of the quadrangles $A^iB^iC^iD^i$, $i = 3,4$. The following statements are valid:*

1. *The diagonal point U is the midpoint of the line segment U^3U^4.*
2. *The connection line U^3U^4 is parallel to the connection lines P_1P_2 and VW.*

Proof. From (14) we get the equation of the line A^3C^3

$$y = -\frac{2k(a+b-c-d)}{b-d}x + \frac{-2k^2(b-c)(a-d)}{(b-d)^2}.$$

By using $2(a-d)(b-c) = (a-c)(b-d)$, it turns into

$$y = -\frac{2k(a+b-c-d)}{b-d}x - \frac{k^2(a-c)}{b-d}.$$

Similarly, we get the equation of the line B^3D^3 as

$$y = -\frac{2k(a-b-c+d)}{a-c}x - \frac{k^2(b-d)}{a-c}.$$

Therefore, their intersection has coordinates $U^3 = \left(-\frac{k}{2}, k^2\right)$. Analogously, the diagonal point $U^4 = A^4C^4 \cap B^4D^4 = \left(\frac{k}{2}, k^2\right)$ is obtained. The point $U(0,k^2)$ is obviously the midpoint of the points U^3 and U^4.
The line U^3U^4 is given by the equation $y = k^2$, and therefore, parallel to the connection lines P_1P_2 and VW. □

Theorem 13 *Let $V^i = A^iB^i \cap C^iD^i$, $W^i = A^iD^i \cap B^iD^i$ be the diagonal points of the quadrangles $A^iB^iC^iD^i$, $i = 3,4$. Then the points V^3, W^4 are incident with BD, and the points V^4, W^3 are incident with AC.*

Proof. To prove the theorem, we will show that V^3 lies on BD. The other statements can be shown in the similar manner.
Out of (13), elementary, but long calculation results with coordinates of $V^3 = A^3B^3 \cap C^3D^3$ in the form

$$V^3 = \left(\frac{c-a}{a+b-c-d}k, \frac{a-b-c+d}{a+b-c-d}k^2\right) \tag{15}$$

The equality $ab - bc - cd + da = 2k(b-d)$ that can be obtained from Lemma 1 will be used to prove that coordinates given by (15) satisfy the equation $y = (b+d)x - bd$ of the line BD. Indeed,

$$\begin{aligned}(b+d)\frac{(c-a)k}{a+b-c-d} - bd &= \frac{(bc-ab+cd-ad)k}{a+b-c-d} + k^2 \\ &= \frac{-2k^2(b-d)}{a+b-c-d} + k^2 = \frac{a-b-c+d}{a+b-c-d}k^2.\end{aligned}$$ □

Theorem 14 *Let $M_{A^iC^i}$ and $M_{B^iD^i}$ be the midpoints of the line segments A^iC^i and B^iD^i, respectively, $i = 3,4$. Then $M_{A^iC^i}$ are incident with AC, and B^iD^i are incident with BD, $i = 3,4$.*

Proof. Let us for example prove that $M_{A^3C^3}$ is incident with AC. It is sufficient to prove that the coordinates of the midpoint

$$M_{A^3C^3} = \left(\frac{a+b-c-d}{d-b}\frac{k}{2}, \frac{(a-d)^2+(c-b)^2}{(d-b)^2}k^2\right) \tag{16}$$

satisfy the equation $y = (a+c)x - ac$ of the line AC. Indeed,

$$\frac{(a+c)(a+b-c-d)k}{2(d-b)} + k^2 = k^2\frac{(a-d)^2+(c-b)^2}{(d-b)^2}$$

precisely when

$$\frac{(a+c)(a+b-c-d)}{2(d-b)}k = k^2\frac{(a-d)^2+(c-b)^2-(d-b)^2}{(d-b)^2}.$$

This is true if and only if

$$\frac{(a+c)(a+b-c-d)}{d-b} = 2k\frac{(a-d)^2+(c-b)^2-(d-b)^2}{(d-b)^2},$$

which is, by using (7), equivalent to

$$\begin{aligned}&(a+c)(a+b-c-d)(a-b+c-d) \\ &\quad = (a-c)(a^2+c^2-2ad-2bc+2bd).\end{aligned}$$

Taking $ac = bd = -k^2$, we get

$$(a+c)(d^2-b^2) = -4k^2(d-b).$$

This is valid due to $(a+c)(b+d) = -4k^2$. □

Theorem 15 *Let P_1^i and P_2^i be Brocard points of the quadrangle $A^iB^iC^iD^i$, $i = 3,4$. Then $P_1^3 = U$, $P_2^3 = P_2$ and $P_1^4 = P_1$, $P_2^4 = U$.*

Proof. The facts $P_1^3 = U$ and $P_2^4 = U$ follow directly from Theorems 13 and 14. Indeed, $P_1^3 = W^3M_{A^3C^3} \cap V^3M_{B^3D^3} = AC \cap BD = U$ and $P_2^4 = V^3M_{A^3C^3} \cap W^3M_{B^3D^3} = BD \cap AC = U$.
It is left to prove $P_2^3 = P_2$ and $P_1^4 = P_1$. For the illustration, we will prove $P_2^3 = P_2$. It is sufficient to show that P_2 lies both on $V^3M_{A^3C^3}$ and $W^3M_{B^3D^3}$. Let us check that it lies on $V^3M_{A^3C^3}$, i. e. that P_2, V^3, $M_{A^3C^3}$ are collinear points.
From (8) and (15) we get the following equation of the line P_2V^3:

$$y = \frac{-2k(a+2b-c-2d)}{b-d}(x+k) + 3k^2. \tag{17}$$

From

$$\begin{aligned}&\frac{-2k(a+2b-c-2d)}{b-d}\left(\frac{a+b-c-d}{d-b}\frac{k}{2} + k\right) + 3k^2 \\ &= \frac{k^2}{(b-d)^2}(a+2b-c-2d)(a-b-c+d) + 3k^2 \\ &= \frac{k^2}{(b-d)^2}\left(a^2+b^2+c^2+d^2-2ac-2bd+ab-ad-bc+cd\right) \\ &= \frac{k^2}{(b-d)^2}\left(a^2-2ad+d^2+b^2-2bc+c^2\right) \\ &= \frac{k^2}{(b-d)^2}\left((a-d)^2+(b-c)^2\right)\end{aligned}$$

we conclude that the midpoint $M_{A^3C^3}$ with coordinates (16) is incident with the line P_2V^3. □

We can start a construction of a sequence of quadrangles with the quadrangle $ABCD$ in step 0, and quadrangle $A^4B^4C^4D^4$ in step 1. Some computations verify that a quadrangle constructed in step n has Brocard points $(k, 3k^2)$ and $\left(\left(1-\frac{1}{2^{n-1}}\right)k, \left(3-\frac{n}{2^{n-2}}\right)k^2\right)$. Obviously, all quadrangles in the sequence have the same first Brocard point $P_1 = (k, 3k^2)$, while their second Brocard points approach the point P_1.

References

[1] A. BERNHART, Polygons of Pursuit, *Scripta Math.* **24** (1959), 23–50.

[2] F.G.W. BROWN, The Brocard and Tucker Circles of a Cyclic Quadrangles, *Proc. Edinb. Math. Soc.* **36** (1917), 61–83.

[3] E. JURKIN, M. ŠIMIĆ HORVATH, V. VOLENEC, J. BEBAN-BRKIĆ, Harmonic Quadrangle in Isotropic Plane, *Turk. J. Math.*, to appear.

[4] E.M. LANGLEY, A Note on Tucker's Harmonic Quadrilateral, *Math. Gaz.* **11** (1923), 306–309.

[5] V. VOLENEC, J. BEBAN-BRKIĆ, M. ŠIMIĆ, Cyclic Quadrangle in the Isotropic Plane, *Sarajevo J. Math.* **7**(**20**) (2011), 265–275.

Ema Jurkin
orcid.org/0000-0002-8658-5446
e-mail: ema.jurkin@rgn.hr

Faculty of Mining, Geology and Petroleum Engineering, University of Zagreb

Pierottijeva 6, HR-10000 Zagreb, Croatia

Marija Šimić Horvath
orcid.org/0000-0001-9190-5371
e-mail: marija.simic@arhitekt.hr

Faculty of Architecture, University of Zagreb

Kačićeva 26, HR-10000 Zagreb, Croatia

Vladimir Volenec
e-mail: volenec@math.hr

Faculty of Science, University of Zagreb

Bijenička cesta 30, HR-10000 Zagreb, Croatia

Original scientific paper
Accepted 5. 11. 2017.

IVA KODRNJA
HELENA KONCUL

The Loci of Vertices of Nedian Triangles

The Loci of Vertices of Nedian Triangles

ABSTRACT

In this article we observe nedians and nedian triangles of ratio η for a given triangle. The locus of vertices of the nedian triangles for $\eta \in \mathbb{R}$ is found and its correlation with isotomic conjugates of the given triangle is shown. Furthermore, the curve on which lie vertices of a nedian triangle for fixed η, when we iterate nedian triangles, is found.

Key words: triangle, cevian, nedian, nedian triangle, isotomic conjugate

MSC2010: 51M04, 51N20

Geometrijsko mjesto vrhova nedijalnog trokuta

SAŽETAK

U ovom članku proučavaju se nedijane i nedijalni trokuti omjera η za dani trokut. Određuju se geometrijska mjesta vrhova nedijalnih trokuta za $\eta \in \mathbb{R}$ te ih se povezuje s pojmom izotomično konjugiranih točaka danog trokuta. Nadalje, određuje se krivulja na kojoj leže vrhovi nedijalnih trokuta za čvrsti η kada se iteriraju nedijalni trokuti.

Ključne riječi: trokut, cevian pravac, nedijalni pravac, nedijalni trokut, izotomično konjugirana točka

1 Introduction

The triangle is one of the first simple figures that mathematicians have studied but, as we can see in [9], it is still an interesting topic. There are numerous triangle points, lines, circles, conics, cubics, transformations, other specific triangles etc. that can be attached in a certain way to a single triangle. These elements can be repeated on the same triangle whereby then they can create a structure without an end. In this article we will add some interesting facts about the nedian triangles to the triangle geometry.

Definition 1 *Let a triangle $\triangle ABC$ be given and $\eta \in \mathbb{R}$. Let A_η, B_η and C_η be the points on the lines BC, CA and AB respectively, such that*

$$\begin{aligned} |AC_\eta| : |AB| &= \eta, \\ |BA_\eta| : |BC| &= \eta, \\ |CB_\eta| : |CA| &= \eta, \end{aligned} \tag{1}$$

is valid, assuming the sides have counterclockwise orientation. Then the cevians AA_η, BB_η and CC_η are called ***nedians of ratio*** η.

The segments are observed as oriented segments such that $|AB| = -|BA|$.

Definition 2 *Let a triangle $\triangle ABC$ be given and $\eta \in \mathbb{R}$ then the triangle $\triangle A_1B_1C_1$ is called the* **nedian triangle of ratio** η *of the given triangle $\triangle ABC$, whereby*

$$\begin{aligned} A_1 &= AA_\eta \cap CC_\eta, \\ B_1 &= BB_\eta \cap AA_\eta, \\ C_1 &= CC_\eta \cap BB_\eta. \end{aligned} \tag{2}$$

The nedian triangle of ratio 0 is the given triangle $\triangle ABC$ and the nedian triangle of ratio 1 is the triangle $\triangle BCA$. For $\eta = 1/2$, the points $A_{1/2}$, $B_{1/2}$ and $C_{1/2}$ are midpoints of sides of the triangle $\triangle ABC$, the nedians are the medians of the triangle $\triangle ABC$ which are concurrent at the centroid G

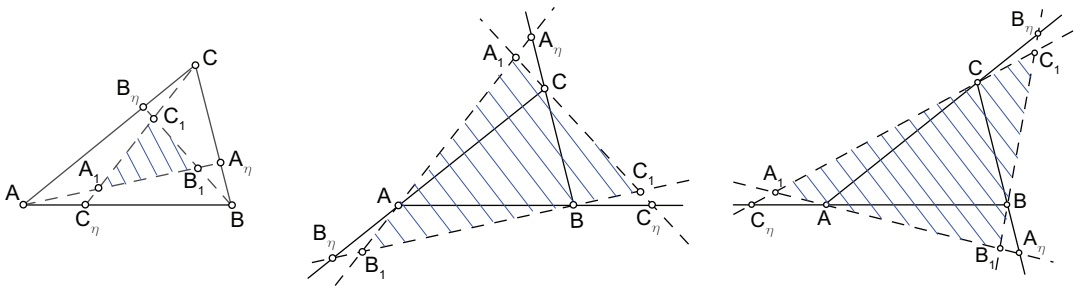

Figure 1: *Nedian triangle $\triangle A_1B_1C_1$ of ratio $\eta = \frac{1}{3}, \frac{7}{5}, -\frac{2}{5}$ of triangle $\triangle ABC$*

of the triangle $\triangle ABC$. Thus, the nedian triangle of ratio $1/2$ is deformed to a point (special case).

We can also define the nedian triangle of ratio $\eta = \infty$ for a given triangle $\triangle ABC$. The points A_∞, B_∞ and C_∞ are the points at infinity of the lines BC, CA and AB respectively. Accordingly, the nedians are the lines through the vertices of the triangle $\triangle ABC$ parallel to the opposite triangle side, i.e. the nedians are the exmedians of the given triangle, ([4], pp. 175-176). Let the intersections of nedians be denoted with G_A, G_B, G_C (see Fig. 2), thus the triangle $\triangle G_A G_B G_C$ is the nedian triangle of ratio ∞. Furthermore, in terms of triangle geometry, the exmedians form the anticomplementary triangle of the given triangle, whose vertices are called exmedian points of the given triangle, ([4], p. 176, [9]).

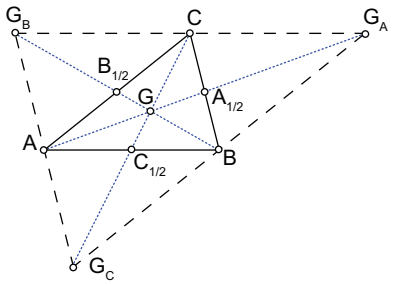

Figure 2: *Nedian triangle $\triangle G_A G_B G_C$ of ratio ∞*

The terminology for the nedian triangles comes from [6, 7], where J. Satterly observes the triangle we now call nedian triangle of ratio $1/n$, obtained by dividing the side of a given triangle in n parts. As he states, 'the name recalls the n', and the similarity to the medians. In [2], H.R. Chillingworth discusses that the ratio can be any real number.

Remark 1 *We will abide by the term nedian triangle from [6, 7], even though we could call it nedial triangle, and the nedian triangle the triangle whose sides have the same lengths as the nedians, i.e. $|AA_\eta|$, $|BB_\eta|$, $|CC_\eta|$. This terminology would follow the notion of the medial ([3], p. 18) and the median ([4], p. 282) triangle of a given triangle.*

Let $A(x_A, y_A)$, $B(x_B, y_B)$ and $C(x_C, y_C)$ be the vertices of a given triangle $\triangle ABC$, then the points A_η, B_η and C_η from Definition 1 have the following coordinates

$$\begin{aligned} A_\eta &= ((x_C - x_B)\eta + x_B, (y_C - y_B)\eta + y_B), \\ B_\eta &= ((x_A - x_C)\eta + x_C, (y_A - y_C)\eta + y_C), \\ C_\eta &= ((x_B - x_A)\eta + x_A, (y_B - y_A)\eta + y_A), \end{aligned} \tag{3}$$

and the vertices of the nedian triangle $\triangle A_1 B_1 C_1$ of ratio η have the coordinates

$$\begin{aligned} A_1 &= \Big(\frac{\eta^2 x_C + (\eta-1)^2 x_A - \eta(\eta-1)x_B}{\eta^2-\eta+1}, \frac{\eta^2 y_C + (\eta-1)^2 y_A - \eta(\eta-1)y_B}{\eta^2-\eta+1}\Big), \\ B_1 &= \Big(\frac{\eta^2 x_A + (\eta-1)^2 x_B - \eta(\eta-1)x_C}{\eta^2-\eta+1}, \frac{\eta^2 y_A + (\eta-1)^2 y_B - \eta(\eta-1)y_C}{\eta^2-\eta+1}\Big), \\ C_1 &= \Big(\frac{\eta^2 x_B + (\eta-1)^2 x_C - \eta(\eta-1)x_A}{\eta^2-\eta+1}, \frac{\eta^2 y_B + (\eta-1)^2 y_C - \eta(\eta-1)y_A}{\eta^2-\eta+1}\Big). \end{aligned} \tag{4}$$

2 The affine transformation

For every two triangles in the same plane we can find an affine transformation that maps one triangle into the other triangle. Affine transformations have 6 degrees of freedom. They preserve affine properties such as parallelism and ratios of lengths as well as projective properties such as cross-ratios and concurrence, ([1] in 2.3.3, 3.3.2, 3.5.1).

Definition 3 The standard triangle *is the triangle with the vertices $A(0,0)$, $B(1,0)$ and $C(0,1)$.*

The affine transformation that maps the standard triangle into its nedian triangle of ratio η has the matrix

$$SN_\eta = \begin{pmatrix} \frac{(2\eta-1)(\eta-1)}{\eta^2-\eta+1} & \frac{(2\eta-1)\eta}{\eta^2-\eta+1} & -\frac{(\eta-1)\eta}{\eta^2-\eta+1} \\ -\frac{(2\eta-1)\eta}{\eta^2-\eta+1} & -\frac{2\eta-1}{\eta^2-\eta+1} & \frac{\eta^2}{\eta^2-\eta+1} \\ 0 & 0 & 1 \end{pmatrix}. \tag{5}$$

The affine transformation for a general triangle can be found by composing transformation (5) and the transformation that maps the standard triangle into the general one, which has the following matrix

$$SG = \begin{pmatrix} -x_A + x_B & -x_A + x_C & x_A \\ -y_A + y_B & -y_A + y_C & y_A \\ 0 & 0 & 1 \end{pmatrix}. \tag{6}$$

Since the centroid is an affine invariant, we can state the following

Theorem 1 *The centroid of all nedian triangles of a given triangle is the centroid of the given triangle.*

Another property of affine transformations is that they multiply the area of a given figure by $|\det(T_{aff})|$, where T_{aff} is the transformation matrix. Thus, in our example, the ratio of the area of the nedian triangle of ratio η and the area of the standard triangle equals

$$|\det(SN_\eta)| = \frac{(2\eta-1)^2}{\eta^2-\eta+1}. \tag{7}$$

3 Locus of vertices of the nedian triangles

Theorem 2 *Vertices of all nedian triangles of ratio* η *of a given triangle* $\triangle ABC$ *lie on three ellipses such that they intersect at the centroid of the triangle* $\triangle ABC$*, each of the ellipse passes through an exmedian point and two vertices of the triangle* $\triangle ABC$ *and is tangent to two sides of the triangle* $\triangle ABC$*.*

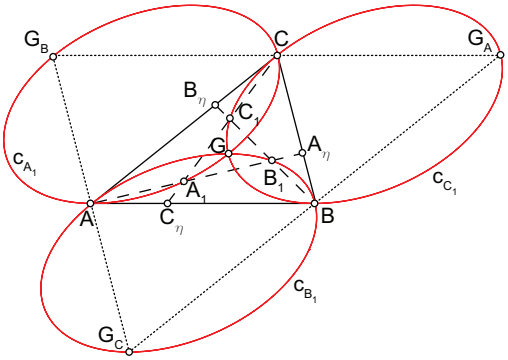

Figure 3: *Locus of vertices of nedian triangles*

Proof. For a given triangle $\triangle ABC$ the ratios (1) define 3 pairs of projective pencils $(A)\,\overline{\wedge}\,(B)$, $(B)\,\overline{\wedge}\,(C)$, $(C)\,\overline{\wedge}\,(A)$. The result of a pair of projective pencils is a conic which passes through the vertices of the pencils. Furthermore, for

i) $\eta = 0$,
$AB \in (A) \to BC \in (B)$,
$BC \in (B) \to CA \in (C)$,
$CA \in (C) \to AB \in (A)$,

ii) $\eta = 1$,
$AC \in (A) \to BA \in (B)$,
$BA \in (B) \to CB \in (C)$,
$CB \in (C) \to AC \in (A)$,

iii) $\eta = 1/2$,
$AA_{1/2} \in (A) \to BB_{1/2} \in (B)$,
$BB_{1/2} \in (B) \to CC_{1/2} \in (C)$,
$CC_{1/2} \in (C) \to AA_{1/2} \in (A)$,

iv) $\eta = \infty$,
$AA_\infty \in (A) \to BB_\infty \in (B)$,
$BB_\infty \in (B) \to CC_\infty \in (C)$,
$CC_\infty \in (C) \to AA_\infty \in (A)$,

whereby from (i) and (ii) follows that each conic is tangent to one pair of lines on which lie the triangle sides, from (iii) that each conic passes through the centroid G of the triangle $\triangle ABC$. Furthermore from (iv) follows that each conic passes through a vertex of the nedian triangle $\triangle G_A G_B G_C$ of ratio ∞, i.e. through an exmedian vertex of the given triangle $\triangle ABC$.

Each pair of projective pencils determines two ranges of points on the line at infinity with no real double points, therefore the conics are ellipses. □

For the standard triangle from (3) and (4) follows

$$A_\eta = (1-\eta,\eta),\ B_\eta = (0,1-\eta),\ C_\eta = (\eta,0), \tag{8}$$

$$\begin{aligned} A_1 &= \Big(\frac{-\eta^2+\eta}{\eta^2-\eta+1}, \frac{\eta^2}{\eta^2-\eta+1}\Big),\\ B_1 &= \Big(\frac{\eta^2-2\eta+1}{\eta^2-\eta+1}, \frac{-\eta^2+\eta}{\eta^2-\eta+1}\Big),\\ C_1 &= \Big(\frac{\eta^2}{\eta^2-\eta+1}, \frac{\eta^2-2\eta+1}{\eta^2-\eta+1}\Big). \end{aligned} \tag{9}$$

Points A_1, B_1, and C_1 are the parametrization of the ellipses in Theorem 2, denoted with $c_{A_1}, c_{B_1}, c_{C_1}$ (see Fig. 3), whose equations in terms of affine point coordinates are obtained by eliminating the parameter η. This yields:

$$\begin{aligned} c_{A_1} &: x^2+y^2+xy-y=0,\\ c_{B_1} &: x^2+y^2+xy-x=0,\\ c_{C_1} &: x^2+y^2+xy-2x-2y+1=0. \end{aligned} \tag{10}$$

The equations of those ellipses can be found for a general triangle with the inverse of the transformation (6).

4 Isotomic conjugates of a triangle

Definition 4 *If two cevians from a triangle vertex are intersecting the opposite side in points that are equidistant from its midpoint then they are called* ***isotomic lines*** *of the triangle and the points are called* ***isotomic points*** *of the triangle, ([5], p. 126).*

Definition 5 *Let a point P and a triangle* $\triangle ABC$ *be given. Then the isotomic lines of the cevians for the point P are concurrent at a point* $\overline{P}$*. The points P and* $\overline{P}$ *are called* ***isotomic conjugates*** *of the triangle* $\triangle ABC$*, ([4], pp. 157-158, [5], p. 127).*

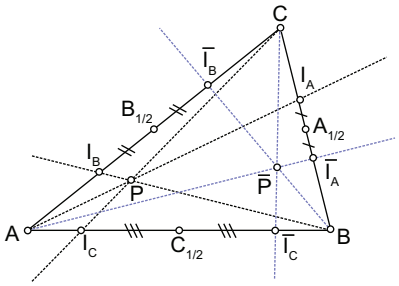

Figure 4: *Isotomic conjugates P and* $\overline{P}$ *of triangle* $\triangle ABC$

In ([4], pp. 157-158), ([5], p. 127) and [8] can be found various properties of the isotomic conjugates of a triangle, but here we will point out only the following:

- self-isotomic points of a triangle $\triangle ABC$ are the centroid G and the exmedian points G_A, G_B, G_C of the triangle $\triangle ABC$
- self-isotomic lines are the medians m_a, m_b, m_c and exmedians e_a, e_b, e_c of the triangle $\triangle ABC$
- the isotomic conjugate of the line at infinity for the triangle $\triangle ABC$ is the Steiner ellipse s
- every conic through points $AGBG_C$, $BGCG_A$ or $CGAG_B$ is self-isotomic. Each of these family of conics contains an special ellipse, denoted with s_c, s_a and s_b, which is a translation of the Steiner ellipse by the vector $\overrightarrow{CG}$, $\overrightarrow{AG}$ or $\overrightarrow{BG}$, respectively. Furthermore ellipses s_a, s_b and s_c are tangent to the triangle sides which are opposite to the vertices that the corresponding ellipse passes through.

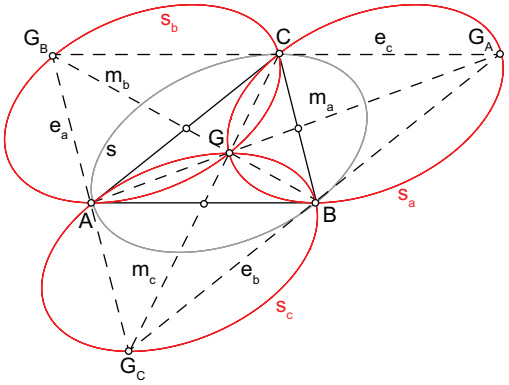

Figure 5: *Steiner ellipse s and self-isotomic elements of triangle $\triangle ABC$*

Theorem 3 *The vertices of all nedian triangles of a given triangle lie on the self-isotomic ellipses of the given triangle.*

Proof. Let the isotomic conjugate of the vertex B_1 of a nedian triangle be denoted with $\overline{B_1}$ and the intersections of cevians through $\overline{B_1}$ with lines AB, BC and CA be denoted with $\overline{C_\eta}$, $\overline{A_\eta}$ and $\overline{B_\eta}$ respectively. Then the points A_η, $\overline{A_\eta}$ and B_η, $\overline{B_\eta}$ are isotomic points of the triangle $\triangle ABC$, thus

$$|A_\eta A_{1/2}| = |A_{1/2}\overline{A_\eta}| \;\Rightarrow\; |BA_\eta| = |\overline{A_\eta}C|, \qquad (11)$$
$$|B_\eta B_{1/2}| = |B_{1/2}\overline{B_\eta}| \;\Rightarrow\; |CB_\eta| = |\overline{B_\eta}A|.$$

On the other hand the point B_1 is a vertex of a nedian triangle and therefore from Definition 1 and a simple calculation follows

$$|B\overline{A_\eta}| : |BC| = 1-\eta, \qquad (12)$$
$$|C\overline{B_\eta}| : |CA| = 1-\eta,$$

hence, $\overline{B_1}$ is a vertex of a nedian triangle when ratio is $1-\eta$ for every $\eta \in \mathbb{R}\cup\{\infty\}$. Analogously we can conclude for vertices A_1, C_1 and its isotomic conjugates, therefore the ellipses on which lie vertices of the nedian triangles are self-isotomic. □

From Theorem 2., Theorem 3. and properties of the special self-isotomic ellipses of a triangle we can conclude the following statement

Corollary 1 *The three ellipses on which lie the vertices of all nedian triangles of a given triangle are congruent.*

4.1 Equilateral triangle and its nedian triangle

Theorem 4 *The nedian triangle of ratio η of an equilateral triangle is equilateral.*

Proof. From $\triangle AA_\eta B \cong \triangle BB_\eta C \cong \triangle CC_\eta A$ follows $|AA_\eta| = |BB_\eta| = |CC_\eta|$. The ratios of segments on nedians can be computed and we obtain ratios

$$\frac{|A_1B_1|}{|AA_\eta|} = \frac{|B_1C_1|}{|BB_\eta|} = \frac{|C_1A_1|}{|CC_\eta|} = \frac{2\eta-1}{\eta^2-\eta+1}, \qquad (13)$$

hence $|A_1B_1| = |B_1C_1| = |C_1A_1|$. □

Proposition 1 *Vertices of all nedian triangles of an given equilateral triangle lie on three circles such that each passes through the centroid, two vertices and an exmedian point of the given triangle.*

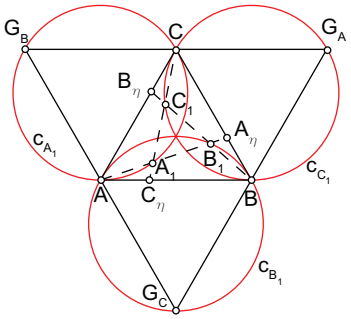

Figure 6: *Locus of vertices of nedian triangles of equilateral triangle*

Proof. W.l.o.g., due to the affine transformations, we will prove this statement for the equilateral triangle $A(-\frac{\sqrt{3}}{2},-\frac{1}{2}), B(\frac{\sqrt{3}}{2},-\frac{1}{2}), C(0,1)$. From Theorem 2 the locus of vertices of the nedian triangles are passing through through the centroid, two vertices and an exmedian point of the given triangle. The Steiner ellipse for the triangle $\triangle ABC$ is the circle with equation $x^2+y^2=1$. Then by Theorem 3 the conics on which the vertices of the nedian

triangle lie are circles with following equations

$$\begin{aligned} c_{A_1} &: \left(x+\frac{\sqrt{3}}{2}\right)^2+\left(y-\frac{1}{2}\right)^2=1,\\ c_{B_1} &: x^2+(y+1)^2=1,\\ c_{C_1} &: \left(x-\frac{\sqrt{3}}{2}\right)^2+\left(y-\frac{1}{2}\right)^2=1. \end{aligned} \tag{14}$$

The same conclusion can be made if we apply the affine transformation on (10) which maps the standard triangle to the chosen equilateral triangle. □

5 Iterations in the standard triangle

We will explore what happens when we repeat the process of finding a nedian triangle. For a fixed η, the triangle $\triangle A_nB_nC_n$, $n \geq 0$ is defined as the nedian triangle of the triangle $\triangle A_{n-1}B_{n-1}C_{n-1}$ such that the triangle $\triangle A_0B_0C_0$ is the given triangle.

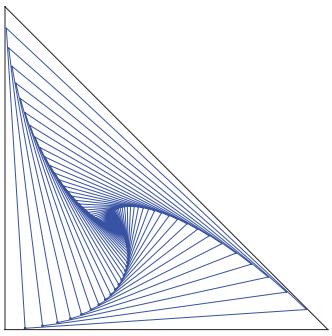

Figure 7: *First 50 iterations with* $\eta = 1/16$

To simplify the computations, we will work with the standard triangle. We will show that points A_n, $n \geq 0$ (see Fig. 8) lie on a curve and give its parametric equation.

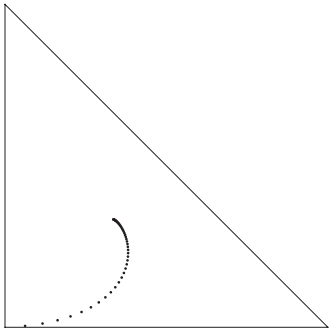

Figure 8: *Points* A_n *with* $\eta = 1/16$

We will observe the affine transformation (5) using barycentric coordinates. In this case, the transformation matrix for the nedian triangle of ratio η, as we can see from (4) is given by:

$$Q = \frac{(\eta-1)^2}{\eta^2-\eta+1}Q_1, \tag{15}$$

where

$$Q_1 = \begin{pmatrix} 1 & t & t^2 \\ t^2 & 1 & t \\ t & t^2 & 1 \end{pmatrix}, \quad t = \frac{1}{1-\eta}. \tag{16}$$

The eigenvalues of the matrix Q_1 are

$$\begin{aligned} \lambda_1 &= -\frac{1}{2}(t^2-t-2)+\frac{\sqrt{3}}{2}(t^2-t)i,\\ \lambda_2 &= -\frac{1}{2}(t^2-t-2)-\frac{\sqrt{3}}{2}(t^2-t)i,\\ \lambda_3 &= t^2+t+1. \end{aligned} \tag{17}$$

If we denote by $\sigma = -\frac{1}{2}+\frac{\sqrt{3}}{2}i$, which satisfies $\sigma^6 = 1$, the eigenvectors for Q_1 are

$$(1,\bar{\sigma},\sigma),(1,\sigma,\bar{\sigma}),(1,1,1). \tag{18}$$

If M is the matrix whose columns are the eigenvectors (18), then we can write

$$Q_1 = MDM^{-1}, \tag{19}$$

where D is the diagonal matrix

$$D = \begin{pmatrix} \lambda_1 & 0 & 0 \\ 0 & \lambda_2 & 0 \\ 0 & 0 & \lambda_3 \end{pmatrix}. \tag{20}$$

The triangle $A_nB_nC_n$, i. e. the n-th iteration of the nedian triangle, will be obtained by the transformation

$$Q_1^n = MD^nM^{-1}. \tag{21}$$

To find the equations of the curve which passes through the points A_n, $n \geq 0$, we have to make (21) continuous in the variable n. This can be done in the following way. Let us write the matrix D as $\exp D_1$, where D_1 is a diagonal matrix whose entries are $\ln\lambda_i$. From (17) we can compute that λ_1, λ_2 and λ_3 are never negative real numbers, so we can choose the principal logarithm branch.
This way, we have

$$\begin{aligned} Q^r &= \left(\frac{(\eta-1)^2}{\eta^2-\eta+1}\right)^r Q_1^r\\ Q^r &= \left(\frac{(\eta-1)^2}{\eta^2-\eta+1}\right)^r M\exp rD_1M^{-1}, \end{aligned} \tag{22}$$

where r is any real number.

The matrix $\exp rD_1$ is the matrix

$$\begin{pmatrix} \lambda_1^r & 0 & 0 \\ 0 & \lambda_2^r & 0 \\ 0 & 0 & \lambda_3^r \end{pmatrix}. \tag{23}$$

The trajectory of the point A, for $r \in \mathbb{R}$ will be a curve, and all the points A_n, $n \geq 1$, lie on this curve.
The affine coordinates (x,y) of the point on the curve can be obtained from barycentric coordinates as the elements of the matrix $Q^r = (q_{ij}^r)$

$$x = q_{12}^r, \quad y = q_{13}^r, \tag{24}$$

and from this we get parametric equations of the curve.
To find these equations and to prove that x and y are real numbers, we write λ_1, λ_2 in the trigonometric form as

$$\begin{aligned} \lambda_1 &= r_\lambda(\cos\varphi_\lambda + i\sin\varphi_\lambda), \\ \lambda_2 &= r_\lambda(\cos\varphi_\lambda - i\sin\varphi_\lambda), \end{aligned} \tag{25}$$

such that

$$\begin{aligned} r_\lambda &= \frac{1}{4}\sqrt{3(t^2-t)^2 + (-t^2-t+2)^2} \\ \varphi_\lambda &= \arctan\left(\frac{\sqrt{3}(t^2-t)}{-t^2-t+2}\right) \end{aligned} \tag{26}$$

Then follows

$$\lambda_1^r = r_\lambda^r(\cos r\varphi_\lambda + i\sin r\varphi_\lambda). \tag{27}$$

From (24) we have

$$\begin{aligned} x &= \frac{1}{3}\left(\frac{(\eta-1)^2}{\eta^2-\eta+1}\right)^r (\bar{\sigma}\lambda_1^r + \sigma\lambda_2^r + \lambda_3^r), \\ y &= \frac{1}{3}\left(\frac{(\eta-1)^2}{\eta^2-\eta+1}\right)^r (\sigma\lambda_1^r + \bar{\sigma}\lambda_2^r + \lambda_3^r). \end{aligned} \tag{28}$$

These expressions are real, and substituting the trigonometric form of λ_1, λ_2 we get the following parametric equation for the curve which passes through A_n, $n \geqslant 0$

$$\begin{aligned} x &= \frac{1}{3}\left(\frac{(\eta-1)^2}{\eta^2-\eta+1}\right)^r \left(r_\lambda^r(\sqrt{3}\sin r\varphi_\lambda - \cos r\varphi_\lambda) + \lambda_3^r\right), \\ y &= \frac{1}{3}\left(\frac{(\eta-1)^2}{\eta^2-\eta+1}\right)^r \left(r_\lambda^r(\sqrt{3}\sin r\varphi_\lambda + \cos r\varphi_\lambda) + \lambda_3^r\right). \end{aligned} \tag{29}$$

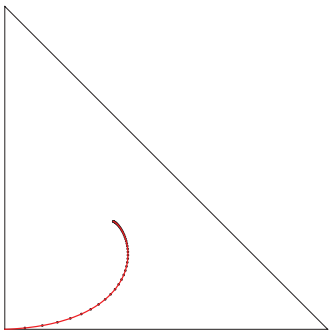

Figure 9: *First 50 iterations with* $\eta = 1/16$

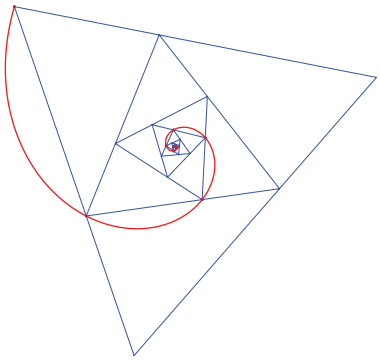

Figure 10: *First 10 iterations with* $\eta = 3$ *for equilateral triangle*

Acknowledgement

The authors would like to thank Professor Tomislav Došlić for providing the idea for this paper.

References

[1] D.A. Brannan, M.F. Esplen, J.J. Gray, *Geometry*, Cambridge University Press, New York, 2012.

[2] H.R. Chillingworth, A further note on the nedians of a plane triangle, *Gaz. Math.*, **40**/331 (1956), 52–53.

[3] H.S. Coxeter, S.L. Greitzer, *Geometry revisited*, The Mathematical Association of America, Washingthon D.C., 1967.

[4] R.A. Johnson, *Advanced Euclidean geometry: An elementary treatise on the geometry of the triangle and the circle*, Dover Publications Inc., New York, 1960.

[5] D. Palman, *Trokut i kružnica*, Element, Zagreb, 1994.

[6] J. Satterly, The nedians of a plane triangle, *Gaz. Math.*, **38**/324 (1954), 111–113.

[7] J. SATTERLY, The nedians, the nedian triangle and the aliquot triangle of a plane triangle, *Gaz. Math.*, **40**/332 (1956), 109–113.

[8] S. SIGUR, Where are the conjugates?, *Forum Geom.*, **5** (2005), 1–15.

[9] C. KIMBERLING, Encyclopedia of Triangle Centers, `http://faculty.evansville.edu/ck6/encyclopedia/ETC.html`

Iva Kodrnja
orcid.org/0000-0003-3976-41665
e-mail: ikodrnja@grad.hr

Helena Koncul
orcid.org/0000-0002-6890-7835
email: hkoncul@grad.hr

Faculty of Civil Engineering, University of Zagreb,
10 000 Zagreb, Kačićeva 26, Croatia

Original scientific paper
Accepted 8. 11. 2017.

GUNTER WEISS

Non-standard Aspects of Fibonacci Type Sequences

Dedicated to Hellmuth Stachel on the occasion of his 75th birthday

Non-standard Aspects of Fibonacci Type Sequences

ABSTRACT

Fibonacci sequence and the limit of the quotient of adjacent Fibonacci numbers, namely the Golden Mean, belong to general knowledge of almost anybody, not only of mathematicians and geometers. There were several attempts to generalize these fundamental concepts which also found applications in art and architecture, as e.g. number series and quadratic equations leading to the so-called "Metallic means" by V. DE SPINADEL [8] or the cubic "plastic number" by VAN DER LAAN [5] resp. the "cubi ratio" by L. ROSENBUSCH [7]. The mentioned generalisations consider series of integers or real numbers. "Non-standard aspects" now mean generalisations with respect to a given number field or ring as well as visualisations of the resulting geometric objects. Another aspect concerns Fibonacci type resp. Padovan type combinations of given start objects. Here it turns out that the concept "Golden Mean" or "van der Laan Mean" also makes sense for vectors, matrices and mappings.

Key words: generalized Fibonacci sequence, Golden Mean, non-Euclidean geometry, number field, ring

MSC2010: 51Mxx

Nestandardni pristupi nizovima Fibonaccijevog tipa

SAŽETAK

Fibonaccijev niz i zlatni rez, limes kvocijenata susjednih Fibonaccijevih brojeva, su pojmovi poznati ne samo matematičarima i geometričarima, već gotovo svima. Oni svoju primjenu nalaze u umjetnosti i arhitekturi. Poznato je nekoliko pokušaja poopćenja ovih pojmova, kao što su nizovi brojeva i kvadratne jednadžbe koje rezultiraju takozvanim "metalnim rezovima" V. DE SPINADEL [8], ili kubni "plastični broj" VAN DER LAANA [5], odnosno "kubni omjer" L. ROSENBUSCHA [7]. Spomenuta se poopćenja odnose na nizove cijelih ili realnih brojeva. "Nestandardnim pristupima" ovdje smatramo poopćenja u odnosu na dano polje ili prsten brojeva, kao i na vizualizaciju dobivenih geometrijskih objekata. Idući se pristup odnosi na Fibonaccijev, odnosno Padovanov tip kombinacija danih početnih objekata. Pokazuje se da pojam zlatnog reza ili van der Laanovog reza ima smisla promatrati i za vektore, matrice i preslikavanja.

Ključne riječi: popćeni Fibonaccijev niz, zlatni rez, neeuklidska geometrija, polje brojeva, prsten

1 Introduction

There exists already a huge set of references concerning the Fibonacci sequence and the Golden Mean and some generalisations of these concepts, most of them only repeating results of former works, such that it seems to be hopeless to add something essentially new to that topic. We shall start with basic facts about the Fibonacci sequence and the limit of adjacent Fibonacci numbers, namely the Golden Mean. Subsequently, we shall have a short look at the main traces of existing generalisations of these basic properties and concepts before adding another generalisation type. Finally, it will turn out that these proposed additional points of view are very natural and they are unifying consequences of what is already known.

2 Basic facts about Fibonacci sequences and the Golden Mean

The Fibonacci sequence is based on the recursive definition

$$F_{n+1} = F_n + F_{n-1}, (n \in \mathbb{N}), \quad F_1 = 1, \quad F_0 = 0. \tag{1}$$

Therewith, one receives the standard representation $\{\mathbf{0}, \mathbf{1}, 1, 2, 3, 5, 8, 13, 21, 34, 55, 89, \dots\}$.

The limit of adjacent Fibonacci numbers for $n \to \infty$ is, therefore,

$$\phi := \lim_{n\to\infty} \frac{F_{n+1}}{F_n} = \lim_{n\to\infty} \frac{F_n + F_{n-1}}{F_n} = 1 + \lim_{n\to\infty} \frac{F_{n-1}}{F_n} = 1 + \frac{1}{\phi}, \tag{2}$$

and ϕ solves the quadratic equation

$$x^2 - x - 1 = 0. \tag{3}$$

Remark 1 *This limit is independent of the two start elements, i.e.* 0 *and* 1 *can be replaced by any numbers* $a_0, a_1 \in \mathbb{R}$ *(not both* 0*). By recursion we receive* $a_n = F_n a_1 + F_{n-1} a_0$*, and obviously we get*

$$\lim_{n\to\infty} \frac{a_n}{a_{n-1}} = \lim_{n\to\infty} \frac{\left(\frac{F_n}{F_{n-1}} a_1 + a_0\right) F_{n-1}}{\left(\frac{F_{n-1}}{F_{n-2}} a_1 + a_0\right) F_{n-2}} = \frac{\phi a_1 + a_0}{\phi a_1 + a_0} \phi = \phi.$$

In the following we will interpret a_{n+1} as a special linear combination, say a "Fibonacci combination", of the pair of start elements a_0, a_1. To present an example we remind to the "Lucas numbers", which use the start elements $\mathbf{2}, \mathbf{1}$ (see e.g. [4]).

Remark 2 *The Golden Mean value* ϕ *is the well-known result of the periodic continuous fraction*

$$\phi = 1 + \cfrac{1}{1 + \cfrac{1}{1 + \cfrac{1}{1 + \ddots}}} = 1{,}618\ldots \tag{4}$$

Remark 3 *The classical Greek point of view intersects a given segment* $[A,B]$ *(of length 1) into two segments M (the maior) and m (the minor) such that*

$$m : M = M : 1 = 1 - M : M$$

Therewith, it follows the quadratic condition

$$M^2 + M - 1 = 0, \tag{3'}$$

which has the positive solution $M = 0{,}618\cdots = \frac{1}{\phi}$*. This value is also considered as the "Golden Mean" and it suits to the line of numbers with* $A := 0$*,* $B := 1$*,* $M := 0{,}618\ldots$*, while the affine ratio* $R(M,A,B)$ *is the negative of this value.*

Remark 4 *It is possible to directly calculate the* n^{th} *Fibonacci number* F_n *as*

$$F_n = \frac{(1+\sqrt{5})^n - (1-\sqrt{5})^{-n}}{2^n \sqrt{5}}. \tag{5}$$

There is an obvious connection of F_n *to the Pascal triangle, (Fig. 1 and [15]) that leads to an expression for* F_n *also as a sum of binomial coefficients as*

$$F_n = \sum_{p+q=n-2} \binom{p}{q}.$$

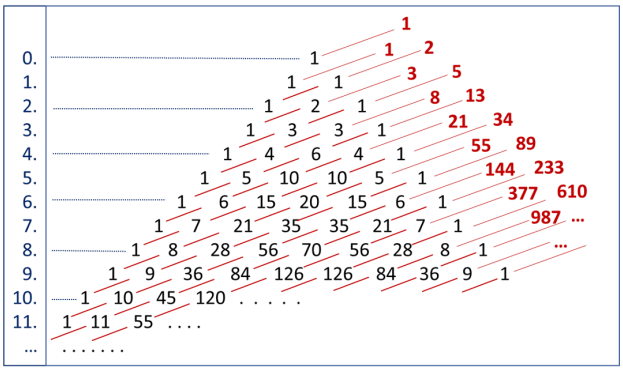

Figure 1: *The Fibonacci numbers* F_n *can be received as transversal sums of binomial coefficients as indicated in the Pascal triangle.*

Remark 5 *The Fibonacci sequence* $\{\mathbf{0},\mathbf{1},1,2,3,5,8,\ldots\}$ *can be interpreted as an approximation of the geometric sequence* $\{1,\phi,\phi^2,\phi^3,\phi^4,\ldots\}$*. By the way, Lucas numbers are an even better approximation of this geometric sequence (c.f. [15]).*

We conclude this chapter noticing that the Golden Mean can be connected

(i) with the Fibonacci sequence,

(ii) with the quadratic equation (3), and

(iii) with the periodic continued fraction (4).

Generalisations of the Golden Mean are based on each of these mentioned connections.

3 Some known generalisations of the Fibonacci sequence and the Golden Mean

a) Generalisations of the Fibonacci sequence

As an example we mention the *Padovan sequence*, which leads to van der Laan's *plastic number* as a 3D-generalisation of the Golden Mean:
By replacing (1) by the rule

$$P_{n+1} = P_{n-1} + P_{n-2} \tag{6}$$

and using the start elements $\mathbf{0},\mathbf{1},\mathbf{1}$ we get the "Padovan standard sequence" $\{\mathbf{0},\mathbf{1},\mathbf{1},1,2,2,3,4,5,7,9,12,16,21,28,37,\ldots\}$. The limit of the ratio of consecutive Padovan numbers $P_{n+1} : P_n$ is the (positive) solution ψ of the cubic equation

$$x^3 - x - 1 = 0. \tag{7}$$

This solution $\psi = 1{,}324717958\ldots$ is called "van der Laan's plastic number", as he used it as a 3D-replacement for the Golden Mean in his architectural design (see [5], [6], [10], and [16]).

Remark 6 *Using arbitrary start values a_0, a_1, a_2 (not all $a_i = 0$) we get the recursion formula*

$$a_{n+1} = P_{n-3}a_0 + P_{n-1}a_1 + P_{n-2}a_2, \tag{8}$$

and again the limit of the quotient of consecutive numbers a_{n+1}, a_n is van der Laan's plastic number ψ. As an example one could mention the "Perrin sequence", which uses the start elements $\mathbf{3},\mathbf{0},\mathbf{2}$ instead of $\mathbf{0},\mathbf{1},\mathbf{1}$.

Remark 7 *The Padovan sequence can also be connected to the Pascal triangle by choosing a special "skew" direction for summing up binomial coefficients, similar to the Fibonacci case Fig. 1, c.f. [16]. This gives rise to a procedure to construct other maybe interesting sequences derived from the Pascal triangle.*

Remark 8 *To calculate the polynomial (7) one can use the linear mapping, which maps the vector $(P_n, P_{n-1}, P_{n-2})^\top$ to the vector $(P_{n+1}, P_n, P_{n-1})^\top$:*

$$\begin{pmatrix} P_{n+1} \\ P_n \\ P_{n-1} \end{pmatrix} = \begin{pmatrix} 0 & 1 & 1 \\ 1 & 0 & 0 \\ 0 & 1 & 0 \end{pmatrix} \begin{pmatrix} P_n \\ P_{n-1} \\ P_{n-2} \end{pmatrix} \quad \Longrightarrow$$

$$char.Pol.: \begin{vmatrix} -x & 1 & 1 \\ 1 & -x & 0 \\ 0 & 1 & -x \end{vmatrix} = 0 = -x^3 + x + 1. \tag{9}$$

b) Generalisations of the equation defining the Golden Mean

V. de Spinadel's Metallic Means

A simple way to define generalisations of the Golden Mean deals with (positive) solutions of quadratic equations by allowing arbitrary (positive or negative) integer coefficients for the characteristic equation

$$x^2 - px - 1 = 0, \quad \text{or} \quad x^2 - x - q = 0, \quad (p,q \in \mathbb{Z}), \tag{10}$$

c.f. [8] and [9]. For the solutions of (10) with $p = 2,3,4,\ldots$ V. Spinadel coined the concepts "Silver Mean" σ_2, "Bronze Mean" σ_3, "Copper Mean" σ_4 resp. "Metallic Mean" σ_p for general $p \in \mathbb{N}$. The Silver Mean $\sigma_2 := 1+\sqrt{2}$ occurs as the affine ratio of the 2nd diagonal of a regular octagon to its side and is, therefore, omnipresent in medieval architecture.

The Metallic Means take the values of periodic continued fractions of type

$$\sigma_p = p + \cfrac{1}{p + \cfrac{1}{p + \cfrac{1}{p + \ddots}}}, \quad p \in \mathbb{N}. \tag{11}$$

Obviously, problems in physics, mathematics, and geometry, which result in a quadratic equation with rational or especially integer coefficients can be interpreted as applications of what can be called the "Generalised Metallic Means Family", c.f. [14], where the authors generalise a result of G. Odom [3] connecting the Golden Mean to an equilateral triangle and its circumcircle, see Fig. 2, to regular polyhedra and their circum-sphere.

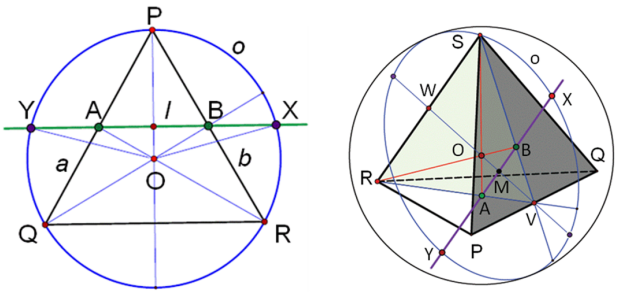

Figure 2: *Odom's discovery of the Golden Mean (left) and one of many possible generalisations (right).*

Generalising the equation (3) to irreducible equations of higher degree

H. van der Laan seems to be the first following this idea with using the cubic equation (7) for defining what he called the "plastic number" $\psi = 1,324717958\ldots$. But independent of him L. Rosenbusch [7] (see also [10]), too, looked for a 3D-analogue of the Golden Mean which he called "cubi ratio" $\rho := 0,6823278040\ldots$, and which is the (positive) solution of the cubic equation

$$x^3 + x - 1 = 0. \tag{7'}$$

Putting $y := \frac{1}{x}$ in (7) and (7') we get the equations $y^3 \pm y^2 - 1 = 0$, and a somehow natural generalisation of the equations (7) and (7') would be

$$x^d \pm x - 1 = 0 \quad \text{or} \quad x^d \pm x^{d-1} \pm \cdots \pm x - 1 = 0.$$

As many of the classical geometric problems from the ancient Greeks lead to cubic equations, one could consider general cubic equations, too, and construct the Fibonacci type sequence to it. This means to reconstruct the linear mapping (9) to a given characteristic polynomial

$$x^3 - px^2 - qx - r = 0, \quad (p,q,r \in \mathbb{R}), \tag{12}$$

with real solution x_0. As (12) is of degree $d = 3$, we put $S_{n+1} = aS_{n-2} + bS_{n-1} + cS_n$. Division by S_{n-2} and calculating the limits for $n \to \infty$ gives $x_0^3 = a + bx_0 + cx_0^2$, and we find $a := r$, $b := q$, $c := p$. Note that a Fibonacci type sequence should have at least two non-zero values a, b, c. These considerations can be formulated as

Result 1: Given an (irreducible) polynomial $P[x]$ of degree d, then it is possible to construct a Fibonnacci type sequence $\{\ldots, P_{n-d}, P_{n-d+1}, \ldots, P_{n-1}, P_n, \ldots\}$ to it, such that

$P[x]=0$ is the characteristic polynomial of the linear mapping

$$\{P_{n-d},P_{n-d+1},\dots,P_{n-1},P_n\}\mapsto\{P_{n-d+1},\dots,P_{n-1},P_n,P_{n+1}\}.$$

If the sequence P_{n+1}/P_n is convergent, then the limit $\lim_{n\to\infty} P_{n+1}/P_n$ is a (real) solution of $P[x]=0$. Therewith, we get an additional method to find Zeros of a polynomial, besides the well-known and more general methods "regula falsi" and "Newtons method".

Remark 9 *By a Tschirnhaus-Bring-Jerrard transform [1] it is always possible to transform an equation* $x^d + p_1x^{d-1} + p_2x^{d-2} + \dots + p_{d-1}x + p_d = 0$ *into one with* $p_1 = p_2 = 0$. *For a cubic equation this would result in* $x^3 = q$, *which is not a proper form for constructing a Fibonacci type sequence.*
As an example, the equation $x^3 = 2$, *describing the classical problem of doubling the cube, can be solved via the cubic equation* $y^3 - y^2 + y - \frac{1}{3} = 0$ *with* $y = \frac{1-x}{x}$.
Another example is the trisection of an angle α*: Putting* $x = \tan\alpha$, $a = \tan 3\alpha$ *the corresponding cubic equation becomes* $x^3 - 3ax^2 - 3x + a = 0$.
The Cubus Simus, the "snub cube", resp. the regular heptagon are connected to the cubic equations $x^3 + x^2 + 3x - 1 = 0$ *resp.* $x^3 + x^2 - 2x - 1 = 0$, *while* $x^3 - x^2 + 2x - 1 = 0$ *describes the axis-ratio of quarter-ellipses of a* C^2*-continuous bi-arc spiral consisting of such quarter ellipses. The latter equation can be transformed into (7) by the Tschirnhaus-Bring-Jerrard transformation and thus relates to van der Laan's Plastic Number* ψ *(c.f. [14]).*

c) Continued fractions and their iterations

A theorem by Euler-Lagrange states that periodic continued fractions only lead to quadratic equations. This means that such fractions only can take values of the Generalized Metallic Means Family. From the decimal representation of, e.g., van der Laan's Plastic Number ψ, one could calculate finite approximations of the surely non periodic continued fraction of ψ. But one could generalise the concept "periodic continuous fraction" using reals instead of natural numbers as coefficients and iterate such a fraction as e.g.

$$a_{i+1} = a_i + \cfrac{1}{a_i + \cfrac{1}{a_i + \cfrac{1}{a_i + \ddots}}}, \quad a_i \in \mathbb{R}, \quad a_0 = 1. \tag{13}$$

In [12] the limit of this special sequence of periodic continued fractions is considered and turns out to be $\sqrt{2}/2$. This iteration process can also be seen as a sequence of quadratic equations (10) where the coefficient p is consecutively replaced by the (positive) solution of the former equation.

4 Fibonacci sequences and finite structures

a) Elliptic and spherical Geometry

In [13] visualisations of the Fibonacci sequence and the Golden Mean in non-Euclidean geometries were shown with one exception: the elliptic geometry. The elliptic lenght L of a line is π, and thus finite!
There seem to be two "natural" possibilities to handle Fibonacci numbers F_n^{el} in elliptic resp. spherical geometry:

(i) $F_n^{el} := F_n mod L.$

(ii) $F_n^{el} := F_n \cdot \frac{L}{F_{n+1}}$.

The way (i) seems not to be considered yet, while (ii) can be used to define the well-known "Golden Angle" as

$$\alpha := 2\pi - \lim_{n\to\infty} 2F_n^{el} = 137{,}520^\circ. \tag{14}$$

The usual definition of the Golden Angle devides the circumference of the unit circle into two angle-segments $2\pi-\alpha$ and α such that $(2\pi-\alpha):\alpha=\phi$. Obviously (ii) connects this definition to the circular model of the elliptic line. For the first stages $n=1,2,3$, of (ii) one may observe that the ratio of the regular $(n+1)$-gon's side s_{n+1} to its n-diagonal d_n takes remarkable values $r_n = d_n : s_{n+1}$, see Fig. 3: For the regular pentagon this ratio is the well-known Golden Mean, for the regular octagon it is the Silver Mean! As for $n\to\infty$ this ratio $r_n\to\infty$ it seems more reasonable to calculate the ratios $R_n = d_n : ((n-1)\cdot s_{n+1})$ and their limit θ

$$\theta := \lim_{n\to\infty} R_n = \lim_{n\to\infty} \frac{F_{n-1}\cdot\sin\left(\frac{\pi}{F_{n+1}}\right)}{\pi\cdot\frac{F_{n-1}}{F_{n+1}}} = \frac{\sin\left(\pi/\phi^2\right)}{\pi/\phi^2}$$
$$= 0{,}78185913047\dots \tag{15}$$

which is somehow a "golden" number, too.

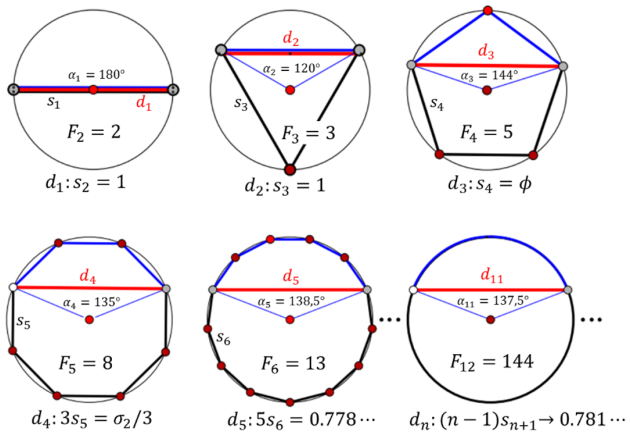

Figure 3: *F_{n+1}-gons and the ratios of diagonals d_n (red) and sides s_{n+1} (blue).*

b) Finite fields and Fibonacci numbers

We consider the Galois fields $GF(p)$, p prime, $p \in \mathbb{N}$. Here it seems to be natural to use the way (i) of the former subchapter (a) to define Fibonacci numbers F_n^p:

$$F_n^p := F_n \; mod p = F_{n-1}^p + F_{n-2}^p. \tag{16}$$

Obviously the sequence of Fibonacci numbers F_n^p is periodic. The behaviour shall be visualised by the following examples:

$p = 5$: **0**, **1**, 1, 2, 3, 0, 3, 3, 1, 4, 0, 4, 4, 3, 2, 0, 2, 2, 4, 1, **0**, **1**, 1, …
Lenght of period is 20, all numbers of $GF(5)$occur.

$p = 7$: **0**, **1**, 1, 2, 3, 5, 1, 6, 0, 6, 6, 5, 4, 2, 6, 1, **0**, **1**, 1, …
Lenght of period is 16, all numbers of $GF(7)$ occur.

$p = 11$: **0**, **1**, 1, 2, 3, 5, 8, 2, 10, 1, **0**, **1**, 1, …
Lenght of period is 10, not all numbers of $GF(11)$ occur! (4, 6, 7, 9 do not occur.)
Other start elements, e.g. 4, 6: **4**, **6**, 10, 5, 4, 9, 2, 0, 2, 2, **4**, **6**, …
Again the length of period is 10. There are four numbers of $GF(11)$ that do not occur: 1, 3, 7, 8.

$p = 13$: **0**, **1**, 1, 2, 3, 5, 8, 0, 8, 8, 3, 11, 1, 12, 0, 12, 12, 11, 10, 8, 5, 0, 5, 5, 10, **2**, **1**, 3, 4, 7, 11, 5, 3, 8, 11, 6, 4, 10, 1, 11, 5, 3, 8, 11, 6, 4, 10, 1, 11, 12, 10, 9, 6, 2, 8, 10, 5, 2, 7, 9, 3, 12, **2**, **1**, 3, 4, 7, …
Lenght of period is 28 with 25 elements before the period, all numbers of $GF(13)$ occur!

$p = 17$: **0**, **1**, 1, 2, 3, 5, 8, 13, 4, 0, 4, 4, 8, 12, 3, 15, 1, 16, 0, 16, 16, 15, 14, 12, 9, 4, 13, 0, 13, 13, 9, 5, 14, 2, 16, 1, **0**, **1**, 1, …
Lenght of period is 36. There are three numbers of $GF(17)$ that do not occur: 7, 10, 11.

Trying to apply this method (16) also to a circle by taking $L = 360°$ and e.g. $10°$ as unit, one could consider Fibonacci numbers modulo 36, too:

*mod*36: **0**, **1**, 1, 2, 3, 5, 8, 13, 21, 34, 19, 17, 0, 17, 17, 34, 15, 13, 28, 5, 33, 2, 35, 1, **0**, **1**, 1, …
Lenght of period is 23, only 15 numbers occur, 21 numbers are "gaps".

Remark 10 *As the quotient $F_{n+1}^p / F_n^p \in \{0, 1, \ldots, p-1\}$ is periodical, the limit does not make sense.*

One could also consider the way (i) of subchapter (a) and calculate Fibonacci numbers modulo π:

mod π: **0**, **1**, 1, 2, 3, 1.8584…, 1.7168..., 0.4336..., 2.1502..., 2.5840..., 1.5929..., …

As π is transcendent and irrational, this sequence is not periodic.

Conclusion: The presented examples of Galois fields $GF(p)$ show that Fibonacci sequences are periodic independent of the pair of start values. As the set of Fibonacci numbers is countable, Fibonacci numbers modulo π must generate "gaps" in the interval $[0, \pi) \subset \mathbb{R}$. Here the questions arise, whether there occurs an attractor or not, and, whether there occur finite intervals as gaps or not.

5 Fibonacci sequences consisting of complex numbers

In Sec. 2. we mentioned that one can generalize the concept Fibonacci sequences by $a_n = F_n a_1 + F_{n-1} a_0$ with a_0, a_1 as general start values. Let us now take $a_0 := z_0$, $a_1 := z_1 \in \mathbb{C}$ and consider e.g. $z_0 := 1$, $z_1 := i$ as the pair of start values. We visualize the sequence $\{z_n\}$ in the Gauss plane (which is endowed with a Cartesian frame), see Fig. 4: The Fibonacci numbers $z_n = F_n + iF_{n+1}$ with odd index n are points of a branch of an equilateral hyperbola c, while the numbers with even index n belong to a branch of the conjugate hyperbola c'. Those hyperbolas have equations

$$y^2 - xy - x^2 = \mp 1. \tag{17}$$

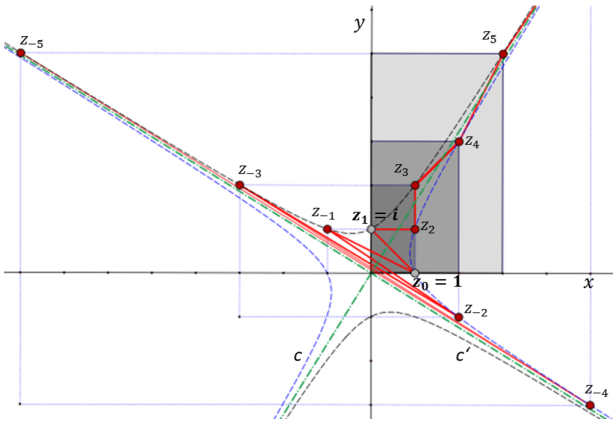

Figure 4: *The complex Fibonacci sequence to start values* $z_0 = (1,0)$, $z_1 = (0,1)$.

The stereographic projection $\cdot^\sigma$ of these hyperbolas (17) onto the Riemann sphere Σ obviously gives a pair of Viviani curves $c^\sigma, c'^\sigma \subset \Sigma$ with common tangents in their common double point U, which also acts as the centre of the stereographic projection. Thereby, the stereographic images of the "Fibonacci points" z_n of the Gauss plane belong to one loop of each of the two Viviani curves.

Calculating $z = \lim z_{n+1}/z_n$ leads to the complex quadratic equation $z^2 - z - 1 = 0$ with real coefficients. Its solutions

$s_1 = a_1 + ib_1$, $s_2 = a_2 + ib_2$ fulfil

$$s_1 s_2 = 1 + 0.i, \quad s_1 + s_2 = 1 + 0.i$$
$$\Longrightarrow \quad s_2 = 1/s_1 = \frac{a_1 - ib_1}{a_1^2 + b_1^2}$$
$$\Longrightarrow \quad a_1 + ib_1 + \frac{a_1 - ib_1}{a_1^2 + b_1^2} = 1 + 0.i$$
$$\Longrightarrow \quad b_{1,2} = 0, \quad a_{1,2} = \frac{1}{2}(1 \pm \sqrt{5})$$
$$\Longrightarrow \quad s_1 = \phi + 0.i, \quad s_2 = -\phi^{-1} + 0.i.$$

Result 2: Independent of the complex start elements, the limit $z = \lim z_{n+1}/z_n$ of the quotient returns at the (real) Golden Mean ϕ.

Remark 11 *From arbitrary (different) start values z_0, z_1 we get $z_n = F_n z_1 + F_{n-1} z_0$, ($n \in \mathbb{Z}$). We may speak of z_n being a "Fibonacci combination" of z_0, z_1. Consequently, it follows that the Fibonacci points z_n belong to a straight line, if $z_1 = z_0 \cdot r_1$, $r_1 \in \mathbb{R}$. In this case the stereographic image on the Riemann sphere Σ is circular.*

Remark 12 *We might relate $\mathbb{C}$ to the two-dimensional vector space $\mathbb{R}^2$, as indicated by its visualisation in the Gauss plane. Then the expression $z = \lim z_{n+1}/z_n$ must be replaced by $\|\vec{z}\| = \lim \|\vec{z_{n+1}}\|/\|\vec{z_n}\|$. A short calculation shows that this limit again takes the value $\phi \in \mathbb{R}$.*

Remark 13 *Replacing $\mathbb{C}$ by the ring D of dual numbers $d := a + \varepsilon b$, ($\varepsilon^2 = 0$, $a,b \in \mathbb{R}$) or the ring A of double numbers $h := a + jb$, ($j^2 = 1$, $a,b \in \mathbb{R}$) does not change the visualisation of Fibonacci numbers in the respective Gauss plane. Figure 4 can be considered as a visualisation of dual or double Fibonacci numbers as well. As far as a Fibonacci number is not a zero divisor in D resp. A, the quotients d_{n+1}/d_n resp. h_{n+1}/h_n make sense and their limits for $n \to \infty$ are again $\phi \in \mathbb{R}$. We show this for the case of Fibonacci dual numbers $d_{n+1} = F_n d_1 + F_{n-1} d_0$:*

$$d = \lim_{n\to\infty} \frac{d_{n+1}}{d_n} = \lim_{n\to\infty} \frac{F_n d_1 + F_{n-1} d_0}{F_{n-1} d_1 + F_{n-2} d_0} = \phi \cdot \frac{\phi d_1 + d_0}{\phi d_1 + d_0}$$
$$= \begin{cases} \phi & \text{for} \quad \phi d_1 + d_0 \notin N = \{0 + \varepsilon b, b \in \mathbb{R}\} \\ - & \text{for} \quad \phi(a_1 + \varepsilon b_1) + a_0 + \varepsilon b_0 \in N \end{cases}$$

From the last equation follows that the condition for a not declared limit reads as

$$\phi a_1 + a_0 \in N, \quad b_1, b_0 \in \mathbb{R} \quad \text{arbitrary.} \tag{18}$$

The stereographic images of the pair of conjugate equilateral hyperbolas (17) passing through the Fibonacci dual numbers are points of curves of degree 4 on a quadratic cylinder, while Fibonacci double numbers belong to curves on a one-sheeted hyperboloid, c.f. [2].

6 Fibonacci type sequences defined as vector combinations

Remark 12 in gives a hint how to define Fibonacci type sequences of vectors:

Recursive definition: Given a set of initial vectors $\{v_0, v_1, \ldots, v_p\} \subset \mathbb{R}^k$, $p,k \in \mathbb{N}$ and a set of scalars $\{r_0, \ldots, r_p\}$, then

$$v_{p+r+1} := r_0 v_{0+q} + r_1 v_{1+q} + \cdots + r_p v_{p+q}, \quad q \in \mathbb{N}_0. \tag{19}$$

The sequence obviously can be extended to negative values of $q \in \mathbb{Z}$.
A Fibonnacci type combination of two independent vectors gives "Fibonacci vectors" of a two-dimensional vector space. The Padovan combinations (6) and (8) (i.e., in (19) we put $r_0 = 1, r_1 = 1, r_2 = 0$) applied to three independent start vectors delivers "Padovan vectors" of a 3-space, which are recursively defined by

$$v_n = v_{n-1} + v_{n-2} = P_{n-2} v_0 + P_n v_1 + P_{n-1} v_2. \tag{20}$$

We present an example using the basis vectors of $\mathbb{R}^3$ as the start vector triplet, i.e

$$v_0 = (1,0,0)^\top, \quad v_1 = (0,1,0)^\top, \quad v_2 = (0,0,1)^\top,$$

such that (20) becomes

$$v_{n+1} = (P_{n-3}, P_{n-1}, P_{n-2})^\top. \tag{21}$$

For the following visualisations in Figure 5, it seems to be necessary to calculate the Padovan numbers at least for $-40 \le n \le 19$, see Table 1 :

Table 1: *List of Padovan numbers for $-40 \le n \le 19$*

-40 . . . -31	145	-89	56	-7	-33	49	-40	16	9
-30 . . . -21	-24	25	-15	1	10	-14	11	-4	-3
-20 . . . -11	7	-7	4	0	4	-3	1	1	-2
-10 . . . -1	2	-1	0	1	-1	1	0	0	1
0 . . . 9	**0**	**1**	**1**	1	2	2	3	4	5
10 . . . 19	7	9	12	16	21	28	37	49	65

Remark 14 *The Padovan numbers resp. vectors with negative index n are recursively defined by*

$$Q_{m+1} = Q_{m-2} - Q_m, \quad (m = -n) \quad \text{resp.} \quad v_{m+1} = v_{m-2} - v_m. \tag{22}$$

Thereby, it follows that $\lim_{m\to\infty} \frac{Q_{m-1}}{Q_m} = \frac{1}{\Psi}$ is a solution of $y^3 + y^2 - 1 = 0$.

Remark 15 *The (real) vector* $(1,\psi^2,\psi)^\top$, $\psi = 1,32\ldots$ *the van der Laan number, points to* v_∞. *Equation (7) for van der Laan's Plastic Number* $x_1 = \psi$ *has two complex conjugate solutions of the quadratic equation*

$$x^2 + \psi x + (\psi^2 - 1) = 0, \tag{23}$$

$$x_{2,3} = \frac{1}{2}\cdot(-\psi \pm \sqrt{4-3\psi^2}) \approx -0,662359 \pm i\cdot 1,12456. \tag{24}$$

The correspoding complex vectors $(1,x_{2,3}^2,x_{2,3})^\top$ *represent complex ideal points of the spiral set of points described by (21) for* $m \to \infty$, *see Fig. 5 visualising the top view of that point set. The star-shaped blue polygon tends to a pentagram for* $m \to \infty$. *(The black, almost straight lined polygon describes the top view of the first n points,* $n > 2$.*) One might calculate the angle* $\alpha := \angle(v_{n-1} - v_n)(v_{n+1} - v_n)$ *of the limit 3D-pentagram's spikes. It turns out that one gets*

$$\cos\alpha = \frac{\psi(2\psi-1)}{\psi^2+\psi+1} \quad \Longrightarrow \quad \alpha \approx 68,0\ldots^\circ.$$

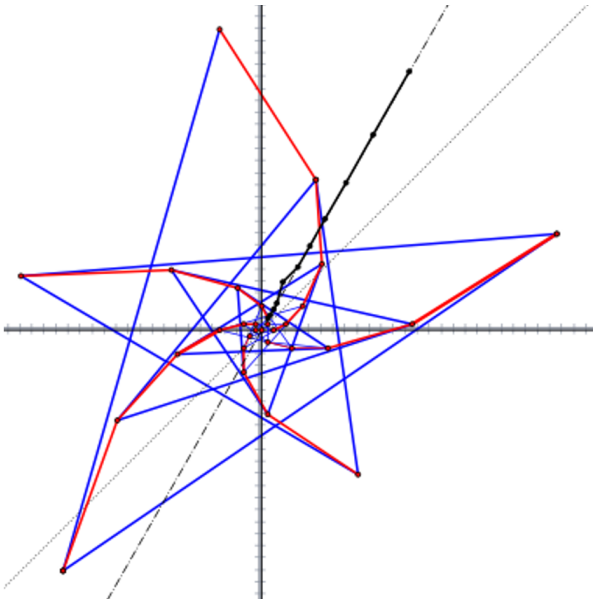

Figure 5: *Top view of the Padovan type point set resulting from (20).*

Remark 16 *Obviously one can interpret the set of vectors* v_n *(19) as homogeneous coordinates of points of a projective space* $\pi = \mathrm{P}(\mathbb{R}^k)$. *Again we focus on the example of Padovan vectors as treated above. We replace the vector symbol* v_n *by the symbol* V_n *for projective points and continue the "Padovan example" above rewriting (21) as*

$$V_{n+1} = (P_{n-3}, P_{n-1}, P_{n-2})\mathbb{R}. \tag{25}$$

7 Normed Fibonacci combinations and Conclusion

The interpretation in Remark 16 stimulates to consider Fibonacci or Padovan type combinations of *Matrices* or even (algebraic) *equations* too. The Fibonacci combination of e.g. two such geometric objects Obj_0, Obj_1 of the same type results in a set of objects belonging to a pencil

$$Obj_n = F_n Obj_1 + F_{n-1} Obj_0. \tag{26}$$

Similarly, the Padovan-combination of three such objects results in a set of these objects belonging to a two-parameter manifold. As one can interpret the coefficients F_n, F_{n-1} in (26) as *projective coordinates* within the pencil of objects, the limit object Obj_∞ for $n \to \infty$ also makes sence. As an example we show this situation for the Fibonacci combination of two circles c_0, c_1:

$$c_0 \ldots (x-m_0)^2 + y^2 = r_0^2, \qquad c_1 \ldots (x-m_1)^2 + y^2 = r_1^2,$$

$$\begin{pmatrix} m_0^2 - r_0^2 & -m_0 & 0 \\ -m_0 & 1 & 0 \\ 0 & 0 & 1 \end{pmatrix}, \qquad \begin{pmatrix} m_1^2 - r_1^2 & -m_1 & 0 \\ -m_1 & 1 & 0 \\ 0 & 0 & 1 \end{pmatrix}.$$

To receive the normed equation for the circle c_n we have to "norm" the Fibonacci combination as in (26):

$$c_n = \frac{F_{n-1}}{F_{n-1}+F_n} c_0 + \frac{F_n}{F_{n-1}+F_n} c_1, \tag{27}$$

and we get

$$c_\infty = \frac{1}{\phi^2} c_0 + \frac{1}{\phi} c_1. \tag{28}$$

Using power rules for ϕ, we receive the normed equation for that limit circle c_∞

$$c_\infty \ldots \left(x - \left(\frac{m_0}{\phi^2} + \frac{m_1}{\phi}\right)\right)^2 + y^2 = \frac{r_0^2}{\phi^2} + \frac{r_1^2}{\phi} - \frac{1}{\phi^3}(m_0 - m_1)^2. \tag{29}$$

From (29), we read off that the center M_∞ of c_∞ divides the segment between the centres M_0, M_1 of c_0, c_1 in the Golden Ratio. Note that the radius r_∞ and thus c_∞ can be complex, if c_0, c_1 span a hyperbolic pencil of circles! In case c_∞ is real, it must intersect the circles of the elliptic pencil of circles conjugate to that spanned by c_0, c_1 orthogonally. In case c_0, c_1 span an elliptic or parabolic pencil of circles, c_∞ has to pass throught the basis point(s) of that pencil. So it is easy to construct c_∞ to a given pair c_0, c_1, see Fig. 6.

In the following, we focus on the norming process used in (27) and we will speak of "normed Fibonacci combinations" of two (geometric) objects.

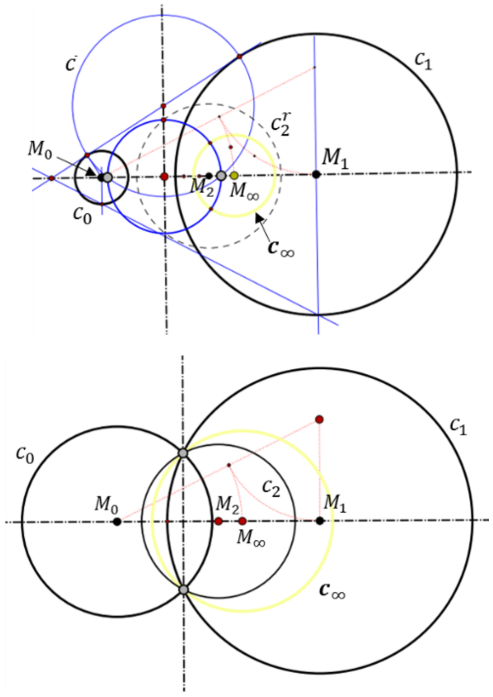

Figure 6: *Limit circle c_∞ to The Fibonacci combination of two circles c_0, c_1.*
top: c_0, c_1 span a hyperbolic pencil of circles, $\overline{c}$ is a circle of the (elliptic) conjugate pencil, c_∞ is real, but c_2 is imaginary with the "real representative" c_2^r.
bottom: c_0, c_1 span an elliptic pencil of circles. All circles c_n are real.

a) Let the given objects Obj_0, Obj_1 be $(n \times m)$-matrices. For $n = m$, they can be interpreted as the coordinate representation of collineations, while for $n > m$ they represent linear mappings. A Fibonacci combination (26) of such matrices represents a collineation resp. a linear mapping which depends on the ratio $F_n : F_{n-1}$ and the two initial matrices Obj_i. Thus, the resulting mapping also has the "normed Fibonacci representation"

$$Obj_n = \frac{F_{n-1}}{F_{n+1}} Obj_0 + \frac{F_n}{F_{n+1}} Obj_1 \tag{30}$$

and we call Obj_n the "n^{th} Fibonacci mean" of Obj_0 and Obj_1. For the object Obj_∞ the name "Golden Mean of Obj_0 and Obj_1" could be coined.

b) Let the given objects Obj_0, Obj_1 be vectors, the coordinates of which fulfil a (quadratic) condition, then the coordinates of the Fibonacci or Padovan type combination Obj_n will not fulfil this condition anymore! Examples of such vectors are, e.g., the Plücker coordinates of lines of a projective 3-space, the spear- and cycle- resp. circle-coordinates in Laguerre, Möbius, and Liegeometry (see [2]). Here a "norming" of the resulting vector Obj_n analogue to that used in (25) would allow to extend the concept "pencil" or "two-parameter manifold" as well as "Fibonacci mean" and "Padovan mean" also to these cases.

For example, in the case of Line Geometry the Fibonacci combination of two skew lines g_0, g_1 results in a set of linear complexes within the pencil of linear complexes spanned by g_0, g_1. Here the norming process could consider the axes a_n of these complexes Obj_n, if the space of action is the projective closure of the Euclidean 3-space. As the set of axes of a pencil of linear complexes comprises the rulings of a Plücker conoid, the axis a_∞ of the "limit complex" Obj_∞ is a line "in Golden Ratio" between g_0 and g_1. We might call a_∞ the Golden Mean line of the lines g_0 and g_1.

c) Coming back to numbers we put $Obj_i := \log q_i$. Now (30) becomes

$$\log q_n = \frac{F_{n-1}}{F_{n+1}} \log q_0 + \frac{F_n}{F_{n+1}} \log q_1, \tag{31}$$
$$n \in \mathbb{N}, \quad q_0, q_1 \in \mathbb{R}^+,$$

what means that

$$q_n = \sqrt[F_{n+1}]{q_0^{F_{n-1}} \cdot q_1^{F_n}} \tag{32}$$

and finally

$$q_\infty = q_0^{1/\phi^2} \cdot q_1^{1/\phi} \tag{33}$$

Hereby, we receive as a final

Result 3: The *geometric mean* of two (ordered) numbers q_0, q_1 can be interpreted as the *third normed Fibonacci mean* q_3 of these numbers, while q_∞ is their *Geometric Golden Mean*.

Concluding remark. The presented material does not at all cover all possibilities to generalise the Fibonacci sequence. By focussing on both, the Fibonacci sequence and the Padovan sequence the material connects to known facts which are seen from a perhaps new point of view. Obviously the presented methods can be applied to any Fibonacci (resp. Padovan) type sequence. It might be worth to treat the sequence leading to V. de Spinadel's Silver Mean more explicite and in the above presented way.

Acknowledgement

The author thanks Ema Jurkin and the reviewer(s) for their valuable support and suggestions.

References

[1] V.S. ADAMCHOK, D.J. JEFFREY, Polynomial Transformations of Tschirnhaus, Bring and Jerard, *ACM SIGSAM Bulletin* **37**(**3**) (2003), 90–94.

[2] W. BENZ, *Vorlesungen über Algebren*, (Grundlehren der math. Wiss., Vol. 197), Springer-Verlag Berlin, 1973.

[3] H.S.M. COXETER, Problem E3007 (due to G. ODOM), American Math. Monthly 1983.

[4] M. HAZEWINKE, Lucas polynomials, in *Encyclopedia of Mathematics*, Springer Science + Buisiness Media B.V. Kluwer Academic Publishers, 2001.

[5] R. PADOVAN, Dom Hans van der Laan and the Plastic Number, *Nexus Network Journal* **4**(**3**), *Architecture and Mathematics* (2002), 181–193.

[6] A. REDONDO-BUITRAGO, Sobre los systemas de proporciones áureo y plastic y sus generalisaciones, *Journ. Mathematics & Design* **9**(**1**) (2009), 15–34.

[7] L. ROSENBUSCH, Räumliche Proportionen, in *Geometry, Art, and Science 06*, ed. O. NIEWIADOMSKI, Hauschild Verlag, 2007.

[8] V.W. DE SPINADEL, The Family of Metallic Means, *Visual Mathematics* **1**(**3**) (1999).

[9] V.W. DE SPINADEL, Golden and Metallic Means in Modern Mathematics and Physics, *Proc. 13th ICGG 2008*, Dresden, Germany, 2008.

[10] V.W. DE SPINADEL, G. WEISS, Remarks to classical cubic problems and the Mean Values of van der Laan and Rosenbusch, *Proc. 14th ICGG*, Kyoto, Japan, 2010.

[11] G. WEISS, Ratios and Mean Values: A Topic in Art, Architecture, and Mathematics, *Proc. 29th Conf. on Geom. & Graph.*, Doubice, Czech Republic, 2009.

[12] G. WEISS, Remarks on Fractions, Fractals, and Golden Sections, *Journ. Mathematics & Design* **8**(**2**) (2008).

[13] G. WEISS, S. MICK, Non-standard Visualisations of Fibonacci Numbers and the Golden Mean, *KoG* **18** (2014), 34–42.

[14] G. WEISS, V.W. DE SPINADEL, From George Odom to a New System of Metallic Means, *Journ. Mathematics & Design* **13** (2014), 71–85.

[15] Wikipedia, `https://en.wikipedia.org/wiki/Fibonacci-number`

[16] Wikipedia, `https://en.wikipedia.org/wiki/Padovan_sequence`

Gunter Weiss
e-mail: weissgunter@hotmail.com

University of Technology Vienna,
Karlsplatz 13, 1040 Vienna, Austria

University of Technology Dresden,
Helmholtzstrße 10, 01069 Dresden, Germany

Original scientific paper
Accepted 8. 12. 2017.

BORIS ODEHNAL

Generalized Conchoids

Generalized Conchoids

ABSTRACT

We adapt the classical definition of conchoids as known from the Euclidean plane to geometries that can be modeled within quadrics. Based on a construction by means of cross ratios, a generalized conchoid transformation is obtained. Basic properties of the generalized conchoid transformation are worked out. At hand of some prominent examples - line geometry and sphere geometry - the actions of these conchoid transformations are studied. Linear and also non-linear transformations are presented and relations to well-known transformations are disclosed.

Key words: conchoid transformation, line geometry, sphere geometry, cross ratio, regulus, Dupin cyclide, Laguerre transformation, equiform transformation, inversion

MSC2010: 14J26, 51C99, 51N05, 51N15, 51N35, 53A05, 53A17, 74N10, 93B17

Poopćene konhoide

SAŽETAK

Prilagođavamo klasičnu definiciju konhoida iz euklidske ravnine geometrijama definiranim kvadrikama. Postiže se poopćena konhoidna transformacija koja se temelji na konstrukciji pomoću dvoomjera. Proučavaju se osnovna svojstva ovakve transformacije. Djelovanje poopćene konhoidne transformacije se proučava na nekim istaknutim primjerima kao što su pravčasta i sferna geometrija. Prikazuju se linearne i nelinearne transformacije te su opisane veze s dobro poznatim transformacijama.

Ključne riječi: konhoidna transformacija, pravčasta geometrija, sferna geometrija, dvoomjer, sustav izvodnica, Dupinova ciklida, Laguerrova transformacija, ekviformna transformacija, inverzija

1 Introduction

The well-known construction of conchoids is usually applied to curves in the Euclidean plane $\mathbb{R}^2$. Several conchoids of simple and elementary curves in the Euclidean plane are known and have undergone intensive investigations, see for example [4, 6, 10, 11, 16, 22].
The conchoid construction uses a *focus* F and a *directrix* l (with $F \notin l$ in case of a straight line l). Then, a value $d \in \mathbb{R}$ is chosen and the conchoid c_d of l with respect to F is defined as

$$c_d := \{X_d : \overline{X_d X} = d, X_d \in [X,F], \forall X \in l\} \tag{1}$$

where $\overline{X_d X}$ denotes the Euclidean distance of the segment $X_d X$ and $[F,X]$ means the line spanned by F and X. A special example is obtained by choosing l as a straight line which yields the one-parameter family of Nikomedes's conchoids. Pascal's limaçon is the conchoid of a circle l with $F \in l$, see [6, 11, 22]. Fig. 1 shows some members from the Nikomedes family. In Euclidean geometry it makes a difference whether the *distance* d is equipped with a sign or not. So, the conchoid c_d has either one or two branches depending on whether d is signed or not.

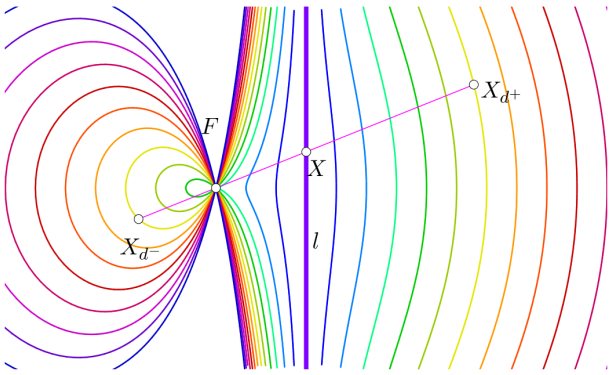

Figure 1: *Some conchoids of a straight line l with respect to the focus F.*

In the following, the mapping $X \mapsto X_d$ shall be called the *conchoid transformation*. It is clearly seen that the conchoid transformation defined via (1) can be applied to arbitrary submanifolds of any metric space. Thus, the conchoid transformation has been applied to surfaces in Euclidean three-space $\mathbb{R}^3$ in [13, 14, 15, 17, 18] in order to construct new classes of surfaces admitting rational parametrizations, and thus, making them accessible to the algorithms implemented in CAD systems. In [8], a special affine version of a line geometric conchoid transformation was presented. Conchoids on the Euclidean unit sphere were studied from the algebraic and constructive point of view in [12].

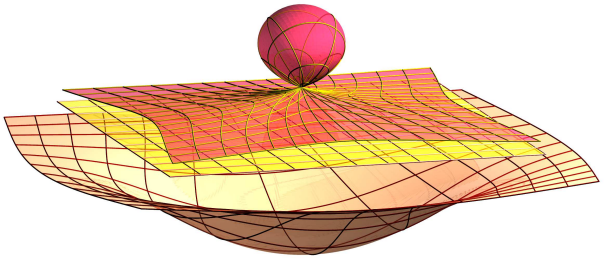

Figure 2: *The conchoid of a plane with respect to a point is a surface of revolution with Nikomedes's conchoid for its meridian curve.*

None of the constructions presented in [13, 14, 15] preserves the type of the geometric object that undergoes the conchoid transformation. The conchoids of planes and spheres become some algebraic surfaces that somehow imitate the features of the conchoids known from the Euclidean plane, see Fig. 2. Ruled surfaces transform to arbitrary surfaces which, in general, carry maybe only a finite number of straight lines, cf. [13].

In this paper, we adapt the conchoid construction such that it applies to various geometries that can be modeled within quadrics. This is especially the case for the geometry of lines and spheres in three-dimensional spaces which can be modeled within Plücker's and Lie's quadric. So, we are able to find conchoids within certain classes of geometric objects: Lines or spheres can be mapped to lines and spheres. Consequently, ruled surfaces and channel surfaces are transformed to such surfaces. As a by product, rational parametrizations are also preserved.

However, this concept is not restricted to line and sphere geometry, but these are taken as examples in order to show how the generalized conchoid transformation acts. The group of Euclidean motions can be treated in Study's quadric model and also Möbius geometry can be realized on a sphere, further, isotropic geometries and Laguerre geometry also have quadric models and the generalized conchoid transformation can be used there. We shall not discuss these latter four in detail.

Section 2 is dedicated to the generalized conchoid construction and its basic properties. The special cases of line and sphere geometric conchoid transformations are discussed in Sections 3 and 4. In both sections, we treat linear conchoid transformations and special types of quadratic transformations.

2 The generalized conchoid transformation

Let $\mathbb{F}$ be an arbitrary commutative field with $\operatorname{char}\mathbb{F} \neq 2$. Further, let $\mathbb{F}^{n+1}$ be the $(n+1)$-dimensional vector space on $\mathbb{F}$ and $\mathbb{P}^n(\mathbb{F})$ be the projective space of n dimensions over $\mathbb{F}^{n+1}$. A quadric $Q \subset \mathbb{P}^n(\mathbb{F})$ can be defined by prescribing a symmetric bilinear form $\Omega: \mathbb{F}^{n+1} \times \mathbb{F}^{n+1} \to \mathbb{F}$. With $\mathbf{x}$ we denote the homogeneous coordinate vector of a point $X \in \mathbb{P}^n(\mathbb{F})$ and the equation of the quadric Q is then $\Omega(\mathbf{x},\mathbf{x}) = 0$. In the following, lower case bold letters denote the coordinate vectors while capitals denote the points, *i.e.*, the point P has the coordinate vector $\mathbf{p}$.

Assume that we are given three points P_i ($i \in \{0,1,2\}$) in a quadric $Q \in \mathbb{P}^n(\mathbb{F})$. The line $[P_0,P_1]$ shall not be contained in the quadric and the plane $\pi = [P_0,P_1,P_2]$ shall not be tangent to Q. Further, $f := \pi \cap Q$ shall be a regular conic in Q. Then, there is always a uniquely defined point P_δ that forms the cross ratio $\delta = \operatorname{cr}(P_0,P_1,P_2,P_\delta)$ with P_0, P_1, and P_2. Now, we give

Definition 1 *To any triple (P_0,P_1,P_2) of three different points in a quadric $Q \subset \mathbb{P}^n(\mathbb{F})$ and to any value $\delta \in \mathbb{F} \cup \{\infty\}$ there exists a uniquely defined fourth point P_δ such that $\operatorname{cr}(P_0,P_1,P_2,P_\delta) = \delta$ provided that $[P_0,P_1] \not\subset Q$, $\pi = [P_0,P_1,P_2]$ is not tangent to Q, and $\operatorname{char}\mathbb{F} \neq 2$.*
We call P_δ the δ-conchoid transformation *of P_2 with respect to the* foci *P_0 and P_1.*

Later, we will apply the thus generalized conchoid construction to points in ruled quadrics. Therefore, we do not exclude the case of collinear points P_0, P_1, and P_2. Moreover, four points in a quadric do not have to be coplanar in order to assign a cross ratio to them.

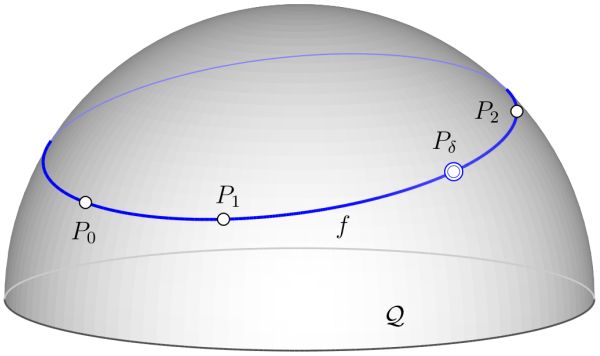

Figure 3: *The generalized conchoid transformation acting on a quadric.*

By means of a stereographic projection to the Gauss plane, we obtain four points that can be identified with four complex numbers and the definition of a cross ratio of these four points is straight forward, see [2].

Remark 1 *1. None of the three points P_0, P_1, P_2 is distinguished. In fact, any two points P_i and P_j ($i \neq j$) out of the three initial points can be considered the foci of the conchoid transformation. Then, P_δ is the conchoid transform of P_k ($k \neq i, j$) with respect to P_i and P_j.*

2. Changing the roles of the given points does not really change the conchoid transformation. Only the cross ratio δ may turn into one of the six values δ, δ^{-1}, $1-\delta$, $(1-\delta)^{-1}$, $\delta(\delta-1)^{-1}$, $(\delta-1)\delta^{-1}$.

3. In the case $\mathrm{char}\,\mathbb{F} = 3$, only the cross ratio $\delta = 2$ yields a conchoid transform $P_\delta \neq P_0, P_1, P_2$. Since any projective line, and thus, any projective conic carries four points in this case, the conchoid transform P_δ of any three (collinear or con-conic) points is the remaining fourth point. Furthermore, 2 is its additive inverse, P_δ makes P_0, P_1, P_2 a harmonic quadruple. Therefore, the conchoid transform P_δ of P_i with respect to P_j and P_k (with $i \neq j,k$ and $j \neq k$) is the harmonic conjugate of P_i with respect to P_j and P_k.

We can give a coordinate representation of the generalized conchoid transformation in $\mathbb{P}^n(\mathbb{F})$ which is helpful for further investigations:

Theorem 1 *Let $\mathbb{F}^{n+1}$ be the $(n+1)$-dimensional vector space on the commutative field $\mathbb{F}$ with $\mathrm{char}\,\mathbb{F} \neq 2$. Assume that $\Omega: \mathbb{F}^{n+1} \times \mathbb{F}^{n+1} \to \mathbb{F}^{n+1}$ is a symmetric non-degenerate bilinear form defining a quadric $\mathcal{Q} \subset \mathbb{P}^n(\mathbb{F})$ by $\mathcal{Q}: \Omega(\mathbf{x},\mathbf{x}) = 0$.*
Then, the conchoid transformation $P_2 \mapsto P_\delta$ as explained in Def. 1 can be given in terms of homogeneous point coordinates in $\mathbb{P}^n(\mathbb{F})$ as

$$\mathbf{p}_\delta = \delta(\delta-1)\Omega_{12}\mathbf{p}_0 + (1-\delta)\Omega_{02}\mathbf{p}_1 + \delta\Omega_{01}\mathbf{p}_2 \qquad (2)$$

*where $\delta \in \mathbb{F} \cup \{\infty\}$, $\mathbf{p}_i$ ($i \in \{0,1,2\}$) are the homogeneous coordinates of the points P_i, $\Omega_{ij} := \Omega(\mathbf{p}_i, \mathbf{p}_j)$, and neither pair $(\mathbf{p}_i, \mathbf{p}_j)$ is conjugate with regard to $\mathcal{Q}$ (*i.e.*, $\Omega_{ij} \neq 0$).*

Proof. We prove Thm. 1 by constructing the coordinate representation given in (2). In the end, we shall arrive at a parametrization of the conic $f = [P_0, P_1, P_2] \cap \mathcal{Q}$ with

$$\mathrm{cr}(P_0, P_1, P_2, P_\delta) = \delta.$$

For that, we observe

$$\mathrm{cr}(P_0, P_1, P_2, P_\delta) = \mathrm{cr}(T_{P_0}, [P_0,P_1], [P_0,P_2], [P_0,P_\delta]) = \delta$$

where T_{P_0} is the tangent of f at P_0 (see Fig. 4), *i.e.*, the intersection of the tangent hyperplane $T_{P_0}\mathcal{Q}$ of $\mathcal{Q}$ at P_0 with the plane $[P_0, P_1, P_2]$. The lines T_{P_0}, $[P_0,P_1]$, $[P_0,P_2]$, $[P_0,P_\delta]$ from the pencil about P_0 establish the stereographic projection $f \to [P_1, P_2]$ which preserves cross ratios. If further $T_0 := T_{P_0} \cap [P_1,P_2]$ and $P'_\delta := [P_0,P_\delta] \cap [P_1,P_2]$, then $\mathrm{cr}(P_0,P_1,P_2,P_\delta) = \mathrm{cr}(T_0,P_1,P_2,P'_\delta) = \delta$.

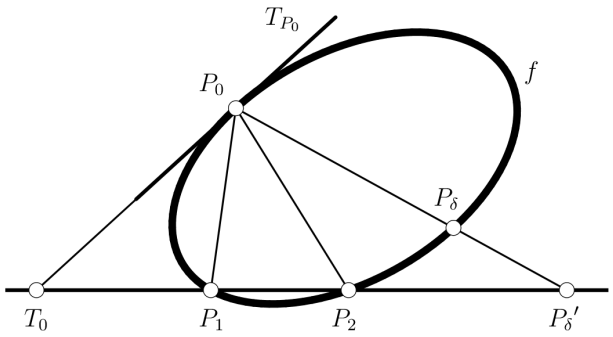

Figure 4: *The stereographic projection $f \to [P_1, P_2]$ yields a parametrization of the conic f by means of the cross ratio δ.*

The point T_0 is found as the common point of $T_{P_0}\mathcal{Q}$: $\Omega(\mathbf{p}_0, \mathbf{x}) = 0$ and the line $\mathbf{g}_{12}(\lambda,\mu) = \lambda\mathbf{p}_1 + \mu\mathbf{p}_2$ (with $(\lambda,\mu) \in \mathbb{F}^2 \setminus \{(0,0)\}$). This yields

$$\mathbf{t}_0 = -\Omega_{02}\mathbf{p}_1 + \Omega_{01}\mathbf{p}_2.$$

Obviously, $\mathbf{t}_0 \neq \mathbf{p}_i$ for $\Omega_{0i} \neq 0$ for $i \in \{1,2\}$, by assumption. Now, the pairs $(-\Omega_{02}, \Omega_{01})$, $(1,0)$, $(0,1)$ are homogeneous coordinates of T_0, P_1, P_2 on the line $[P_1,P_2]$, and thus, we find P'_δ with $\mathrm{cr}(T_0,P_1,P_2,P'_\delta) = \delta$ as

$$\mathbf{p}'_\delta = (1-\delta)\Omega_{02}\mathbf{p}_1 + \delta\Omega_{01}\mathbf{p}_2.$$

The stereographic projection $[P_1,P_2] \to \mathcal{Q}$, and thus, also onto f with center P_0 sends P'_δ to P_δ. Since $P_\delta = \mathcal{Q} \cap [P_0, P'_\delta] \setminus \{P_0\}$, we find $\mathbf{p}_\delta = \mathbf{p}'_\delta + \delta(\delta-1)\Omega_{12}\mathbf{p}_0$ which completes the proof. □

The coordinate representation

$$\mathbf{p}_\delta: \mathbb{F} \cup \{\infty\} \to \mathcal{Q}$$

of P_δ given in (2) is a parametrization of the conic $f \subset \mathcal{Q}$. Hence, $\Omega(\mathbf{p}_\delta, \mathbf{p}_\delta) = 0 \forall \delta \in \mathbb{F} \cup \{\infty\}$. We shall call f the *fiber* (conic) of the conchoid transformation.
From the definition of the generalized conchoid transformation and the analytic representation (2), we can easily conclude:

Corollary 1 *The generalized conchoid transformation is involutive if, and only if, the cross ratio equals $\delta = -1$.*

Proof. Geometrically speaking: If P_δ is the conchoid transform of P_2 with $\delta=-1$ and, if transformed with $\delta=-1$ once again, then we obtain P_2 back. □

Remark 2 *If* $\mathrm{char}\,\mathbb{F}=3$*, then the non-trivial* ($\delta\neq 0,1,\infty$) *generalized conchoid transformation is always involutive.*

None of the points $\mathbf{p}_i$ is geometrically distinguished which is expressed in (2) by the fact that the coordinate representation of $\mathbf{p}_\delta$ is a trilinear form: It is linear in each $\mathbf{p}_i$. This gives rise to the following:

Corollary 2 *1. The generalized conchoid transformation on a quadric Q can be extended to an automorphic collineation κ of Q.*

2. The collineation κ has the fixed points P_0 and P_1 corresponding to the two eigenvalues $\delta^2\Omega_{01}$ and Ω_{01}.

3. The polar space F of $f:=[P_0,P_1]$ with regard to Q is fixed point wise and corresponds to the eigenvalue $\delta\Omega_{01}$.

Proof.

1. Consider $\mathbf{p}_2$ in (2) as the variable point $\mathbf{x}$. Then, we observe that each summand depends only linearly on $\mathbf{x}$: The first two coefficients in the linear combination are $\Omega(\mathbf{p}_1,\mathbf{x})$ and $\Omega(\mathbf{p}_0,\mathbf{x})$ and neither is multiplied with $\mathbf{x}$. Also the last summand depends only linearly on $\mathbf{x}$, since Ω_{01} is independent of $\mathbf{x}$. Since $\mathbf{p}_2=\mathbf{x}\mapsto\mathbf{p}_\delta$ is homogeneous and linear in $\mathbf{x}$ and $\mathbf{p}_\delta\in Q$ ($\forall\delta\in\mathbb{F}\cup\{\infty\}$), it is an automorphic collineation of Q.

2. By letting either $\mathbf{p}_2=\mathbf{p}_0$ or $\mathbf{p}_2=\mathbf{p}_1$ in (2), we see that the conchoid transformation returns either $\mathbf{p}_\delta=\delta^2\Omega_{01}\mathbf{p}_0$ or $\mathbf{p}_\delta=\Omega_{01}\mathbf{p}_1$.

3. The three-dimensional polar space F of $f=[P_0,P_1]$ with regard to the quadric $Q:\ \Omega(\mathbf{x},\mathbf{x})=0$ is given by the homogeneous linear equations

$$F:\ \Omega(\mathbf{p}_0,\mathbf{x})=\Omega(\mathbf{p}_1,\mathbf{x})=0. \tag{3}$$

With (2), $\mathbf{x}\mapsto\mathbf{x}_\delta$ and reads

$$\mathbf{x}_\delta=\delta(\delta-1)\Omega_{1\mathbf{x}}\mathbf{p}_0+(1-\delta)\Omega_{0\mathbf{x}}\mathbf{p}_1+\delta\Omega_{01}\mathbf{x} \tag{4}$$

with $\Omega_{i\mathbf{x}}:=\Omega(\mathbf{p}_i,\mathbf{x})$ for $i=0,1$. Inserting (3) into (4), we infer $\mathbf{x}_\delta=\delta\Omega_{01}\mathbf{x}$ which holds true for all $\mathbf{x}\in\mathbb{F}^{n+1}\setminus\{\mathbf{o}\}$ subject to (3). □

Remark 3 *The cross ratio itself is a homogeneous coordinate on a projective line or on a conic section (in fact on any rational normal curve). Therefore, we could replace the inhomogeneous parameter δ in* (2) *by the homogeneous parameter $(d_0,d_1)\in\mathbb{F}^2\setminus\{(0,0)\}$ with $\delta=d_1d_0^{-1}$. We omit this since $d_0=0$ causes $\delta=\infty$, $P_\delta=P_0$ which shall be excluded from our considerations.*

3 Line geometric conchoids

3.1 Linear transformations

In this section, we apply the generalized conchoid transformation to the manifold of lines. For that we use the well-known Klein model for the set of lines in a three-dimensional space. Details, exact definitions, properties, and how to compute with Plücker coordinates can found in [9, 19, 20, 23].

We describe lines L in projective three-space $\mathbb{P}^3(\mathbb{F})$ by Plücker coordinates

$$(\mathbf{l};\bar{\mathbf{l}})=(l_1,l_2,l_3;l_4,l_5,l_6)\in\mathbb{F}^6\setminus\{\mathbf{o}\} \tag{5}$$

which can be made homogeneous (see [9, 19, 20, 23]). Thus, they can be interpreted as coordinates of points in a projective space of five dimensions. From the definition of Plücker coordinates of lines in three-space it is clear that these six-tuples satisfy a quadratic relation:

$$M_2^4:\ \tfrac{1}{2}\Omega_L(L,L)=\langle\mathbf{l},\bar{\mathbf{l}}\rangle=l_1l_4+l_2l_5+l_3l_6=0. \tag{6}$$

M_2^4 is a quadric of four dimensions. It is of index two, *i.e.*, the maximum dimension of subspaces contained in M_2^4 equals two. All points on M_2^4 correspond to lines in $\mathbb{P}^3(\mathbb{F})$ and any line can be described by Plücker coordinates satisfying (6). (An affine or a Euclidean specialization is also possible, see [20, 23].)

The polar form $\Omega_L:\ \mathbb{F}^6\times\mathbb{F}^6\to\mathbb{F}$ of M_2^4 can be used to characterize pairs of lines. Two different lines L and M are coplanar if, and only if, $\Omega_L(L,M)=0$, *i.e.*, the corresponding points in $\mathbb{P}^5$ are conjugate with regard to M_2^4.

Since M_2^4 is a regular hyperquadric in $\mathbb{P}^5(\mathbb{F})$, there is a nine-parameter family of conics in it. We have to distinguish between three types of regular conics in Plücker's quadric: (1) the transversal intersection of a two-dimensional subspace $\mathbb{P}^2(\mathbb{F})\subset\mathbb{P}^5(\mathbb{F})$; (2a) a conic in a plane $\mathbb{P}_1^2(\mathbb{F})\subset M_2^4$ (of the first kind); (2b) a conic in a plane $\mathbb{P}_2^2(\mathbb{F})\subset M_2^4$ (of the second kind). In the following, the conic of type (1) is the most important. The points on a conic of that type correspond to one particular one-parameter family of lines in a ruled quadric, *i.e.*, a regulus. The points on the conics mentioned in the cases (2a) and (2b) correspond to the rulings of a quadratic cone or to the tangents of a (planar) conic, see Fig. 5. Consequently, the fibers of the line geometric conchoid transformation are reguli and in some cases the rulings of quadratic cones or the tangents of conics. Fig. 6 shows a typical fiber regulus.

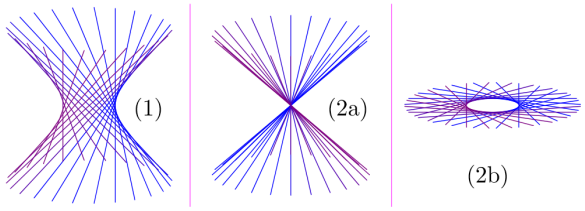

Figure 5: *The three types of reguli.*

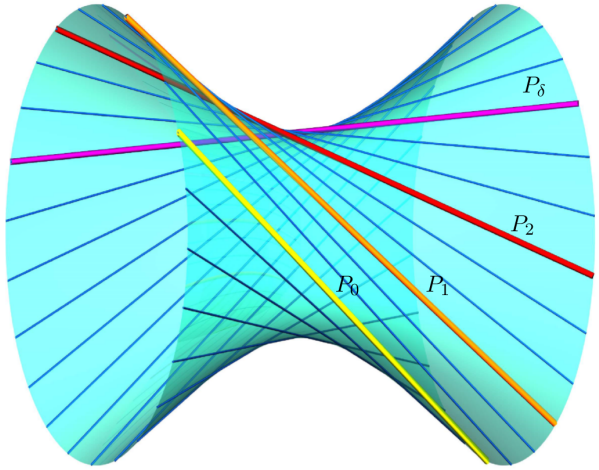

Figure 6: *A regular fiber regulus of the line geometric conchoid transformation.*

Since the line geometric conchoid transformation maps points on Plücker's quadric to points on Plücker's quadric, it preserves lines, and thus, it maps ruled surfaces to ruled surfaces, and even congruences and complexes of lines (two- and three-dimensional submanifolds of M_2^4) to such. By assumption, the case of intersecting focal lines L_0 and L_1 is excluded and so we have:

Theorem 2 *Let L_0 and L_1 be two (skew) lines in $\mathbb{P}^3(\mathbb{F})$ and let $\delta \in \mathbb{F} \cup \{\infty\}$ be a certain fixed value. Then, the line geometric conchoid transformation induces a (regular) automorphic collineation κ of M_2^4 that has a fixed line $f \subset \mathbb{P}^5(\mathbb{F})$ and a fixed three-space $F \subset \mathbb{P}^5(\mathbb{F})$ for its axis. F and f are polar with regard to M_2^4.*

Proof. It is always possible to choose homogeneous coordinates in $P^3(\mathbb{F})$ such that the Plücker coordinates of the focal lines are

$$L_0 = (1,0,0;0,0,0),\ L_1 = (0,0,0;1,0,0),$$

(satisfying $\Omega_L(L_0,L_1) \neq 0$) and $L_2 = (l_1,l_2,l_3;l_4,l_5,l_6)$. We insert into (2) and arrive at

$$L_\delta = (\delta^2 l_1, \delta l_2, \delta l_3; l_4, \delta l_5, \delta l_6). \tag{7}$$

Obviously, the mapping $\kappa: L_2 \mapsto L_\delta$ is a regular collineation with the diagonal matrix $D = \operatorname{diag}(\delta^2,\delta,\delta,1,\delta,\delta)$ for its coordinate representation. The linear mapping described by D fixes the quadratic form Ω_L, and thus, it is an automorphic collineation of M_2^4. The eigenvalues are $t_1 = 1$, $t_2 = \delta^2$, and $t_3 = \delta$ with their algebraic multiplicities $\mu(t_1) = \mu(t_2) = 1$ and $\mu(t_3) = 4$. The fixed points corresponding to 1 and δ^2 are L_0 and L_1, while δ determines the κ-invariant three-space $F: x_1 = x_4 = 0$. The restriction $\kappa|_f$ of κ to the line $f := [L_0,L_1]$ is a hyperbolic projective mapping with two fixed points L_0, L_1 and the coordinate representation $\operatorname{diag}(\delta^2,1)$. The three-space F is fixed pointwise under κ and is polar to f according to Cor. 2. □

Remark 4 *In the case of intersecting focal lines L_0 and L_1, i.e., $\Omega_L(L_0,L_1) = 0$, κ is a projection (singular collineation) onto a one-dimensional subspace of $\mathbb{P}^5(\mathbb{F})$ as can be seen by choosing*

$$L_0 = (1,0,0;0,0,0),\ L_1 = (0,1,0;0,0,0),$$

and $L_2 = (l_1,l_2,l_3;l_4,l_5,l_6)$. With (2), we find $L_\delta = (-\delta l_5, l_4, 0; 0,0,0)$ provided that $\delta \neq 0$ otherwise L_δ is a single point. Now, $L_2 \mapsto L_\delta$ is a projection onto the subspace $x_2 = x_3 = x_5 = x_6 = 0$. Note that f and F are polar with regard to M_2^4.

We take closer look at the induced collineation of the regular (linear) line geometric conchoid transformation. The incidence graph in Fig. 7 shall support our imagination.

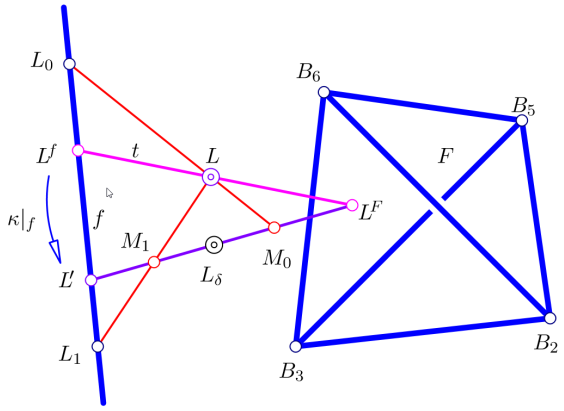

Figure 7: *Action of the collineation induced by the regular (linear) line geometric conchoid transformation.*

Through a generic point $L \in \mathbb{P}^5(\mathbb{F})$ there exists a unique line t that meets f and F. We denote the intersections of t and the fixed spaces f, F by L^f and L^F. The projective mapping $\kappa|_f: f \to f$ sends L^f to a point L' while $\kappa|_F = \mathrm{id}_F$ and L^F remains fixed. Thus, κ maps t to the line $t' = [L',L^F]$. Since κ preserves collinearities, the image L_δ

of L has to be on t'. The projections M_0 and M_1 of L from L_0 and L_1 onto t' satisfy

$$\mathrm{cr}(L', L^F, M_0, L_\delta) = \delta^{-1}, \quad \mathrm{cr}(L', L^F, M_1, L_\delta) = \delta.$$

We are able to show that the automorphic collineations of M_2^4 obtained from the line geometric conchoid transformation are indeed induced by projective collineations $\mathbb{P}^3(\mathbb{F}) \to \mathbb{P}^3(\mathbb{F})$:

Theorem 3 *Any automorphic collineation κ of M_2^4 induced by the line geometric conchoid transformation is induced by a projective collineation $\alpha: \mathbb{P}^3(\mathbb{F}) \to \mathbb{P}^3(\mathbb{F})$.*

Proof. It means no restriction to assume that the focal lines L_0 and L_1 are those used in the proof of Thm. 2. (The coordinate system in $\mathbb{P}^3(\mathbb{F})$ can always be chosen appropriately.) Then, according to the proof of Thm. 2, the automorphic collineation κ of M_2^4 induced by the line geometric conchoid transformation is given by (7) and is described by the diagonal matrix $D := \mathrm{diag}(\delta^2, \delta, \delta, 1, \delta, \delta)$. Now, we have to show that D can be written as the Kronecker product $A \oslash A$ of a (regular) 4×4 matrix A with itself being a the transformation matrix of a collineation $\alpha: \mathbb{P}^3(\mathbb{F}) \to \mathbb{P}^3(\mathbb{F})$. It turns out that $A = \mathrm{diag}(\delta, \delta, 1, 1)$ fulfills the equation $D = A \oslash A$, and thus, the linear mapping given by D describing an automorphic collineation of M_2^4 is really induced by a projective collineation $\alpha: \mathbb{P}^3(\mathbb{F}) \to \mathbb{P}^3(\mathbb{F})$ with coordinate matrix A. □

The factorization of the 6×6 matrix D given in the proof of Thm. 3 may not be unique. However, the uniqueness is not necessary in order to show that the collineation $\kappa: M_2^4 \to M_2^4$ described by D is induced by a collineation $\alpha: \mathbb{P}^3(\mathbb{F}) \to \mathbb{P}^3(\mathbb{F})$ as long as there exists at least one.
Assume now that $\mathbb{F} = \mathbb{R}$ and $\mathcal{R}: I \subset \mathbb{R} \to M_2^4$ is a curve in M_2^4. Then, it corresponds to a ruled surface in $\mathbb{P}^3(\mathbb{R})$. A regular point $R = \mathcal{R}(t_0)$ on this curve corresponds to a regular ruling on the ruled surface in $\mathbb{P}^3(\mathbb{R})$. The regular ruling R is called *torsal* if $\dot{R} = \dot{\mathcal{R}}(t_0)$ fulfills $\Omega_L(\dot{R}, \dot{R}) = 0$. Along a torsal ruling the tangent planes of the ruled surface do not change, see [9, 19].
A ruled surface that consists of torsal rulings only is called *torsal ruled surface* and its parametrization $\mathcal{R}(t)$ satisfies $\Omega_L(\dot{\mathcal{R}}, \dot{\mathcal{R}}) = 0$ besides $\Omega_L(\mathcal{R}, \mathcal{R}) = 0$, both for all $t \in I$.
The term torsal ruled surface covers cylinders, cones, and the surfaces swept by the tangents of a (space) curve (in $\mathbb{P}^3(\mathbb{R})$). Torsal ruled surfaces in Euclidean three-space can be mapped isometrically onto a Euclidean plane, and therefore, these surfaces are called developable. However, torsality is a projective differential geometric property of a ruled surface (see [9, 19, 20, 23]) and we can say:

Corollary 3 *Torsal ruled surfaces are mapped to torsal ruled surfaces under the linear line geometric conchoid transformation.*

Proof. Since torsality of rulings and ruled surfaces is a projective property, it cannot be harmed by the induced automorphic collineation of M_2^4. According to Thm. 3, the latter is induced by a projective collineation in $\mathbb{P}^3$.
We could also prove the corollary by direct calculation. Assume that $\mathcal{R}: I \subset \mathbb{R} \to M_2^4$ is a curve in M_2^4 (*i.e.*, $\Omega_L(\mathcal{R}, \mathcal{R}) = 0 \; \forall t \in I$) all of whose rulings are torsal, *i.e.*, $\Omega_L(\dot{\mathcal{R}}, \dot{\mathcal{R}}) = 0$ for all $t \in I$. Then, we compute $\mathcal{R}_\delta$ with (2), differentiate once with respect to t, and verify that $\Omega_L(\dot{\mathcal{R}}_\delta, \dot{\mathcal{R}}_\delta) = 0$ on $I \subset \mathbb{R}$. □

Some examples shall illustrate the action of the (linear) line geometric conchoid transformation:

Example 1 *The tangents of the curve $(6, 6t, 3t^2, 2t^3) \subset \mathbb{P}^3(\mathbb{R})$ sweep a cubic developable. If we choose $L_0 = (1,0,0;0,0,0)$, $L_1 = (0,0,0;1,0,0)$ and insert into (2), we obtain the cubic developable built by the tangents of the cubic $(6\delta, 6\delta t, 3t^2, 2t^3)$. If we slice $\mathbb{P}^3(\mathbb{F})$ along $x_0 = 0$ (as usual), we see that the two cubics are related by an affine transformation and so are the cubic developables. Fig. 8 shows the initial cubic developable together with three of its line geometric conchoids. We can see that the parametrization of the two cubic curves differ only by a multiplication with the matrix $A = \mathrm{diag}(\delta, \delta, 1, 1)$ given in the proof of Thm. 3.*

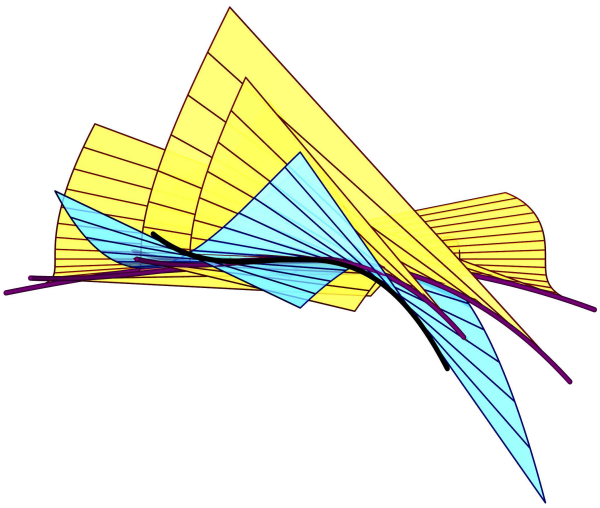

Figure 8: *Some cubic developables being each others line geometric conchoids.*

Example 2 *Assume that the focal lines are $L_0 = (0,-1,2;0,-2,-1)$ and $L_1 = (1,1,3;3,0,-1)$. Further, we choose $\delta = 2/5$ and apply the line geometric conchoid transformation (2) to the set of rulings given by $L_2(t) = (t^2+t, t-t^2, 2, -t-t^2, t^2-t, t^4+t^2)$ and obtain $L_d(t) = (30t^4 - 25t^2 - 85t - 30, 48t^4 + 151t^2 - 79t - 42, 54t^4 + 63t^2 - 57t - 206, 90t^4 + 205t^2 + 25t - 90, 36t^4 + 2t^2 + 82t - 24, -82t^4 - 79t^2 + 21t + 18)$. A part of this*

ruled surface is shown in Fig. 9 together with the focal lines and one fiber regulus.

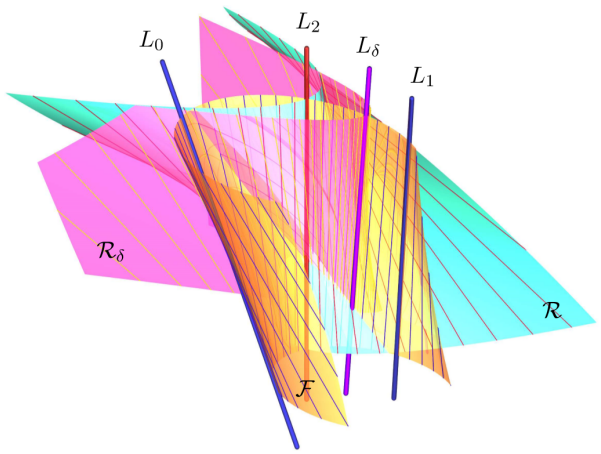

Figure 9: *The conchoid transform of a quartic ruled surface with the two focal lines L_0, L_1, and a fiber regulus $\mathcal{F}$.*

3.2 Quadratic mappings

The line geometric conchoid transformations discussed in the previous section turned out to be linear mappings, *i.e.*, collineations. From that it is a small step to the definition of a quadratic mapping: Assume that one focal line, say L_1, is image of L_2 under a fixed projective transformation and leave L_0 fixed. Then, (2) yields a transformation in terms of Plücker coordinates $(l_1,\dots,l_6)$ that is quadratic in the l_i. A special affine version of such a quadratic line geometric conchoid transformation was studied in [8].
In the following, we shall consider a special Euclidean version of a quadratic line geometric conchoid transformation. For that purpose, we assume that $L_0 = (1,0,0;0,0,0)$ is the fixed and constant first focal line. It means no restriction to assume that L_0 coincides with the x-axis of the coordinate system. The second focal line shall be the *absolute polar* of the line $L_2 = (l_1,l_2,l_3;l_4,l_5,l_6)$ (that is to be transformed) with respect to the absolute polarity of Euclidean geometry, *i.e.*, $L_1 = (0,0,0;l_1,l_2,l_3)$. With (2) we find the coordinate representation of this particular quadratic line geometric conchoid transformation as

$$q: \begin{pmatrix} l_1\\ l_2\\ l_3\\ l_4\\ l_5\\ l_6 \end{pmatrix} \mapsto \begin{pmatrix} \delta(\delta-1)(l_1^2+l_2^2+l_3^2)+\delta l_1^2\\ \delta l_1 l_3\\ \delta l_2 l_3\\ (1-\delta)l_1 l_6+\delta l_3 l_4\\ (1-\delta)l_2 l_6+\delta l_3 l_5\\ l_3 l_6 \end{pmatrix}. \tag{8}$$

The mapping q is degenerate on the field of lines in the ideal plane, *i.e.*, $q(L) = \mathbf{o}$ for all lines $L = (0,0,0;u,v,w)$ with $(u,v,w) \in \mathbb{R}^3 \setminus \{\mathbf{o}\}$.

Torsality is, in general, not preserved under quadratic line geometric conchoid transformations. Surprisingly, we can show the following result (for an arbitrarily chosen first focal line L_0) which holds in Euclidean three-space $\mathbb{R}^3$:

Theorem 4 *The quadratic line geometric conchoid transformation* (8) *maps cylinders to cylinders.*

Proof. Let $L_0 = (\mathbf{l},\bar{\mathbf{l}})$ be the first focal line with constant vectors $\mathbf{l},\bar{\mathbf{l}} \in \mathbb{R}^3 \setminus \{\mathbf{o}\}$ satisfying $\langle \mathbf{l},\bar{\mathbf{l}}\rangle = 0$. Further, let

$$L_2 = (\mathbf{v},\bar{\mathbf{v}}) :\ I \subset \mathbb{R} \to M_2^4$$

be the Plücker representation of the cylinder where the constant vector $\mathbf{v} \in \mathbb{R}^3 \setminus \{\mathbf{o}\}$ points into the direction of the cylinder's rulings and $\bar{\mathbf{v}} : I \subset \mathbb{R} \to \mathbb{R}^3$ is not constant. Naturally, $\langle \mathbf{v},\bar{\mathbf{v}}\rangle = 0$ for all $t \in I$. Then, the second focal line is given by $L_1 = (\mathbf{o},\mathbf{v})$ and is obviously constant. Since we are dealing with lines in Euclidean three-space, we may assume that both $\mathbf{l}$ and $\mathbf{v}$ are unit vectors, *i.e.*, $\langle \mathbf{v},\mathbf{v}\rangle = \langle \mathbf{l},\mathbf{l}\rangle = 1$. With $\Omega_{01} = \Omega_{12} = 1$, $\Omega_{02} = \langle \mathbf{l},\bar{\mathbf{v}}\rangle + \langle \bar{\mathbf{l}},\mathbf{v}\rangle$, and (2), we find

$$L_\delta = \delta(\delta-1)\begin{pmatrix}\mathbf{l}\\ \bar{\mathbf{l}}\end{pmatrix} + (1-\delta)\Omega_{02}\begin{pmatrix}\mathbf{o}\\ \mathbf{v}\end{pmatrix} + \delta\begin{pmatrix}\mathbf{v}\\ \bar{\mathbf{v}}\end{pmatrix}$$

from which we immediately see that the direction vector

$$\mathbf{l}_\delta = \delta(\delta-1)\mathbf{l} + \delta\mathbf{v} \tag{9}$$

is constant since $\mathbf{l},\mathbf{v} \in \mathbb{R}^3$ are constant. Therefore, $L_\delta :\ I \subset \mathbb{R} \to M_2^4$ parametrizes a cylinder. □

Remark 5 *Since the argument* $\mathbf{v}$ *is constant, the quadratic line geometric conchoid transformation turns out to be linear in the case of the cylinder. According to Cor. 3, torsal ruled surfaces are mapped to torsal ruled surfaces.*

It is also possible to verify Thm. 4 via direct computation in terms of coordinates. Then, it is useful to assume that $\mathbf{v} = (0,0,1)$ and the cylinder is erected on the cross section $\mathbf{q} = (q_1,q_2,0) :\ I \subset \mathbb{R} \to \mathbb{R}^3$ in the plane $\langle \mathbf{x},\mathbf{v}\rangle = 0$. Apparently, the cross section of L_δ can be parametrized by

$$\mathbf{q}_\delta = \frac{1-\delta}{\delta l_3}\begin{pmatrix} l_5\\ -l_4\\ 0\end{pmatrix} + \frac{1}{\delta}\begin{pmatrix} q_1\\ q_2\\ 0\end{pmatrix},$$

and thus, the cross section $\mathbf{q}$ of L undergoes an equiform transformation with scaling factor δ^{-1}.
Eq. (9) shows that the direction of the rulings changes. Fig. 10 shows a cylinder of revolution (elliptic cylinder) and its quadratic conchoidal image. The horizontal cross sections of the cylinder are circles and are mapped to circles. The direction of the cylinder's rulings are changed and the image cylinder is again an elliptic cylinder, but with circular horizontal cross sections.

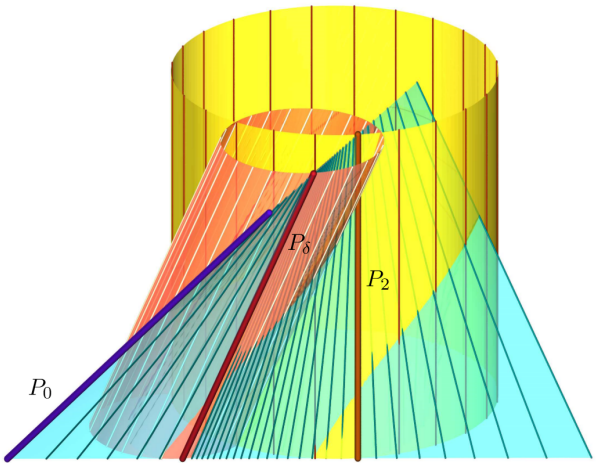

Figure 10: *The quadratic line geometric conchoid transform of a cylinder.*

4 Conchoids in sphere geometry

Many of the results from Sec. 3 dealing with lines can be carried over directly to similar results on spheres. This is mainly based on a mapping that goes back to S. LIE and establishes a one-to-one correspondence between lines and spheres. The mapping is called *Lie's line-sphere-mapping* which is a projective collineation $\mathbb{P}^5(\mathbb{C}) \to \mathbb{P}^5(\mathbb{C})$. Unfortunately, Lie's mapping needs the complex extension of the underlying projective space and mixes up real and complex objects. Therefore, we go a different way and use a coordinatization of the manifold of spheres that was given in [21].

A sphere S in Euclidean three-space $\mathbb{R}^3$ can always be given by its equation in terms of Cartesian coordinates as

$$\begin{aligned} S: (s_6-s_4)(x^2+y^2+z^2)- \\ -2s_1x-2s_2y-2s_3z+(s_6+s_4)=0. \end{aligned} \tag{10}$$

For the moment, we assume that $s_6 - s_4 \neq 0$. By completing to full squares in the sphere's equation, we find the center

$$M = \frac{1}{s_6-s_4}(s_1,s_2,s_3) \tag{11}$$

and the radius R

$$R^2 = \frac{s_1^2+s_2^2+s_3^2+s_4^2-s_6^2}{(s_6-s_4)^2}.$$

With the definition

$$R = \frac{s_5}{s_6-s_4} \tag{12}$$

we find that the six values s_i satisfy the homogeneous quadratic equation

$$L_2^4 : \Omega_S(S,S) := s_1^2+s_2^2+s_3^2+s_4^2-s_5^2-s_6^2 = 0. \tag{13}$$

It is clear that the s_i are homogeneous and an interpretation as homogeneous coordinates of points in a projective five-space is nearby. The coordinates $\mathbf{s} = (s_1,\ldots,s_6) \in \mathbb{R}^6 \setminus \{\mathbf{o}\}$ are called Lie's sphere coordinates. We shall keep in mind that R can be equipped with a sign which can be used to express an orientation of the sphere S. The quadric L_2^4 spans $\mathbb{P}^5(\mathbb{R})$, is of index one, and therefore, it carries straight lines as maximal subspaces. L_2^4 is called Lie's quadric (cf. [5, 7, 20, 21]) and serves as a point model for the set of spheres in Euclidean three-space.

The polar form $\Omega_S : \mathbb{R}^6 \times \mathbb{R}^6 \to \mathbb{R}$ describes the polar system of L_2^4. Assume that S and T are two different spheres (non-proportional Lie coordinates) in oriented contact, *i.e.*, the radii (normal vectors) have equal orientation at the point of contact. Then, S and T are conjugate with regard to L_2^4, or equivalently, $\Omega_S(S,T) = 0$, and *vice versa*.

The two quadrics M_2^4 and L_2^4 are each others collinear image under Lie's line-sphere-mapping, see [5, 7, 20, 21]. However, the collinear transformation does not map real objects to real ones in general and L_2^4 carries only straight lines, while M_2^4 carries two independent families of planes. Since L_2^4 carries at most straight lines, there exists only one type of regular conics in L_2^4. These conics correspond to one-parameter families of spheres enveloping Dupin cyclides. Hence, the fibers of the sphere geometric conchoid transformation are, loosely speaking, Dupin cyclides (cf. Fig. 11). (More precise, but rather lengthy: The fibers of the sphere geometric conchoid transformation are one-parameter families of spheres enveloping Dupin cyclides.)

In analogy to Thm. 2, we can state:

Theorem 5 *Let S_0 and S_1 be two spheres in Euclidean three-space $\mathbb{R}^3$ (not in oriented contact,* i.e., *$\Omega_S(S_0,S_1) \neq 0$) and let $\delta \in \mathbb{R} \cup \{\infty\}$ be a certain fixed value. Then, the sphere geometric conchoid transformation induces a (regular) automorphic collineation λ of L_2^4 that has a fixed line f and a fixed three-space L for its axis. F and f are polar with regard to L_2^4.*

Proof. The proof can be kept short. Without loss of generality, we may assume that the focal spheres are given by

$$\begin{aligned} S_0 &= (0,0,0,-1,1,0), \\ S_1 &= \left(m,0,0,\tfrac{1}{2}(m^2-R^2-1),R,\tfrac{1}{2}(m^2-R^2+1)\right) \end{aligned}$$

are the two focal spheres which are not in oriented contact unless

$$(R-1+m)(R-1-m) = 0.$$

If now $S_2 = (s_1,\ldots,s_6)$ is the sphere to be transformed, then S_δ can be obtained with (2) where Ω is the polar form with the coordinate matrix $\operatorname{diag}(1,1,1,1,-1,-1)$.

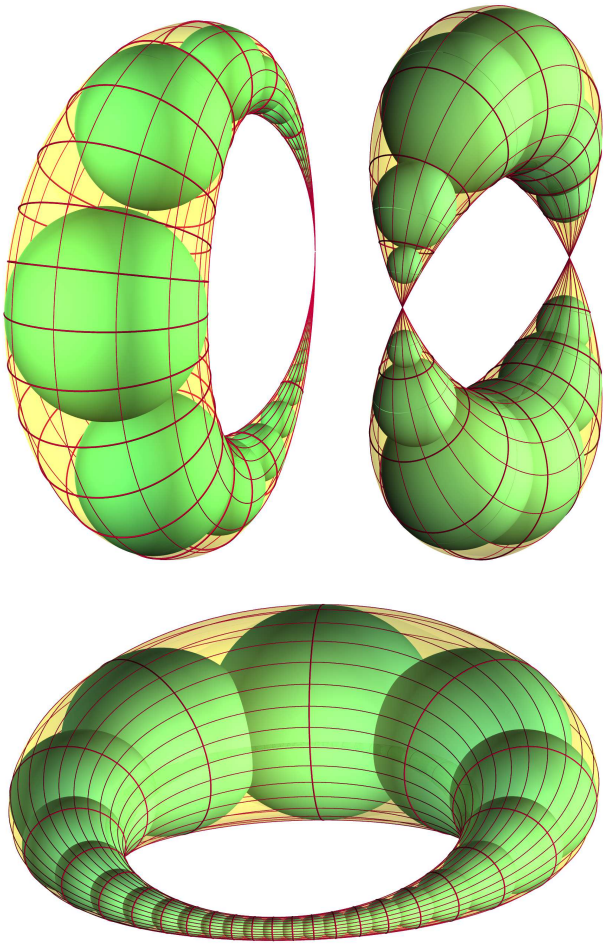

Figure 11: *The fibers of the sphere geometric conchoid construction are Dupin cyclides of any type.*

In the following, we use the abbreviations

$$\rho_1 = R - m - 1, \quad \rho_2 = R - m + 1.$$

The coordinate matrix of the linear mapping $S_2 \mapsto S_\delta$ has the three different eigenvalues $t_1 = \frac{1}{2}\rho_1\rho_2$, $t_2 = \delta^2 t_1$, and $t_3 = \delta t_1$ with the respective algebraic multiplicities $\mu(t_1) = \mu(t_2) = 1$ and $\mu(t_3) = 4$. Then, it is easily verified that the λ-invariant subspaces show the same behavior as those belonging to κ in the proof of Thm. 2. F and f are polar with regard to L_2^4 according to Cor. 2. □

Remark 6 *If the focal spheres S_0 and S_1 are in oriented contact,* i.e., *$\Omega_S(S_0, S_1) = 0$, λ is a projection (singular collineation) onto a one-dimensional subspace of $\mathbb{P}^5(\mathbb{R})$, since then, $(R-1+m)(R-1-m) = \rho_1\rho_2 = 0$ and the coordinate matrix of $S_2 \mapsto S_\delta$ is of rank 2.*

The above chosen coordinatization of the Euclidean spheres covers more than just Euclidean spheres:

1. (Oriented) Euclidean spheres S are characterized by $s_6 - s_4 \neq 0$ (otherwise the quadratic term in (10) would vanish) and $s_5 \neq 0$, and therefore, $R \neq 0$. Especially, the Euclidean unit sphere S^2 has Lie coordinates $(0,0,0,1,1,0)$.

2. (Oriented) planes are characterized by $s_6 - s_4 = 0$. Naturally, the remaining non-vanishing coordinates have to fulfill $s_1^2 + s_2^2 + s_3^2 = s_5^2$. Sometimes, s_5 is set to one and (s_1, s_2, s_3) is then a unit normal vector of the plane

   $$\varepsilon: \; 2s_1x + 2s_2y + 2s_3z - (s_4 + s_6) = 0.$$

3. The hyperplane $s_5 = 0$ meets L_2^4 along the regular three-dimensional quadric $s_1^2 + s_2^2 + s_3^2 + s_4^2 - s_6^2 = 0$ all of whose points correspond to spheres of radius 0. However, spheres of radius 0 can be viewed as points P with coordinates

   $$\mathbf{p} = \left(\frac{s_1}{s_6 - s_4}, \frac{s_2}{s_6 - s_4}, \frac{s_3}{s_6 - s_4} \right),$$

   but should rather be considered as isotropic cones Γ_P of Euclidean geometry with the equation

   $$\Gamma_P: \; \langle \mathbf{x} - \mathbf{p}, \mathbf{x} - \mathbf{p} \rangle = 0.$$

   With $\Gamma_\mathbf{o}$ we denote the isotropic cone with the equation $\langle \mathbf{x}, \mathbf{x} \rangle = 0$ emanating from the origin $\mathbf{o} = (0,0,0)$ of the coordinate system.

4. Finally, the Lie coordinate vector $(0,0,0,1,0,1)$ turns (10) into a false statement, although it describes a point on L_2^4. It is useful to perform the conformal closure by setting

   $$U = (0,0,0,1,0,1).$$

Thus, there are four principal types of elements in Lie geometry and any pair out of these four gives rise to a certain sphere geometric conchoid transformation when used as pair of focal spheres. Depending on the nature of the pairs (S_0, S_1) of focal spheres, the sphere geometric conchoid transformations turn out to be well-known transformations from specific subgroups of the huge group of contact transformations. We are able show the following:

Theorem 6 *1. The sphere geometric conchoid transformation with $S_0 = U$ and $S_1 = \Gamma_\mathbf{o}$ is an equiform transformation, more precisely a similarity with scaling factor δ.*

2. The sphere geometric conchoid transformation with $S_0 = U$ and $S_1 = S^2$ is a Laguerre transformation.

3. The sphere geometric conchoid transformation with $S_0 = \Gamma_\mathbf{o}$ and $S_1 = S^2$ is an inversion.

Proof.

1. It means no restriction to assume that the isotropic cone is centered at the origin of the Cartesian coordinate system. Hence,

   $$U = (0,0,0,1,0,1), \quad \Gamma_{\mathbf{o}} = (0,0,0,1,0,-1).$$

   Inserting $S_0 = U$, $S_1 = \Gamma_{\mathbf{o}}$, and $S_2 = (s_1,\ldots,s_6)$ into (2), we find the induced linear mapping

   $$(s_1,\ldots,s_6) \mapsto (2\delta s_1, 2\delta s_2, 2\delta s_3, (1+\delta^2)s_4+(\delta^2-1)s_6,$$
   $$2\delta s_5, (\delta^2-1)s_4+(1+\delta^2)s_6).$$

   Consequently, spheres with center $\mathbf{m}$ and radius ρ are mapped to spheres with center $\delta\mathbf{m}$ and radius $\delta\rho$, while planes are mapped to planes. Further, points are mapped to points. Fig. 12 shows the action of this mapping.

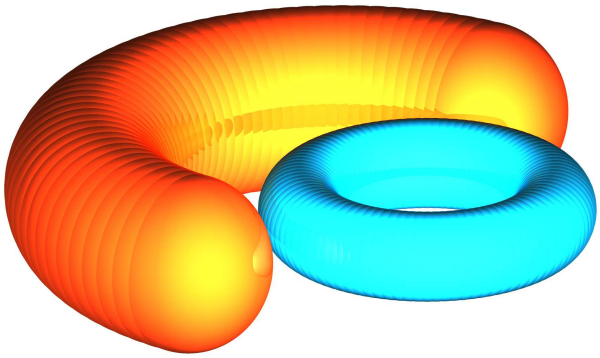

Figure 12: *The action of an equiform transformation on one of the one-parameter families of spheres enveloping a torus.*

2. In this case, we have $S_0 = U$ (like in the previous case) and

   $$S_1 = \mathrm{S}^2 = (0,0,0,1,1,0).$$

   With $S_2 = (s_1,\ldots,s_6)$ and (2), we find the induced linear mapping

   $$(s_1,\ldots,s_6) \mapsto (\delta s_1, \delta s_2, \delta s_3, \delta(\delta-1)(s_4-s_5)+$$
   $$+(\delta-1)s_6+s_4, \delta s_5+(\delta-1)(s_6-s_4),$$
   $$\delta(\delta-1)(s_4-s_5)+\delta s_6).$$

   Obviously, a sphere with center $\mathbf{m}$ and radius ρ is mapped to a sphere with center $\delta\mathbf{m}$ and radius

   $$\frac{\delta s_5+(\delta-1)(s_6-s_4)}{s_6-s_4} = \delta\rho+\delta-1.$$

   Further, a plane with the equation $s_1x+s_2y+s_3z+s_4=0$ with $s_1^2+s_2^2+s_3^2=s_5^2=1$ is mapped to the plane $s_1x+s_2y+s_3z+s_4-1+\delta+\delta\rho=0$ which makes the present sphere geometric conchoid a Laguerre transformation, cf. [3, 5, 7]. Fig. 13 shows how the spheres in a torus change under a Laguerre transformation.

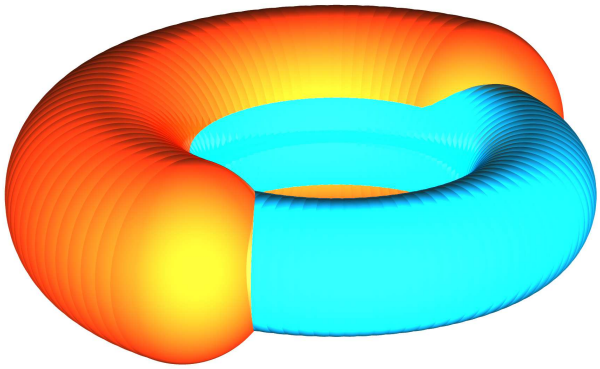

Figure 13: *A Laguerre transformation is applied to one of the one-parameter families of spheres enveloping a torus.*

3. Finally, we choose the focal spheres

   $$S_0 = \Gamma_{\mathbf{o}} = (0,0,0,1,0,-1),$$
   $$S_1 = \mathrm{S}^2 = (0,0,0,1,1,0).$$

   Thus, (2) yields the linear mapping

   $$(s_1,\ldots,s_6) \mapsto (\delta s_1, \delta s_2, \delta s_3, \delta(\delta-1)(s_4-s_5)+$$
   $$+(1-\delta)s_6+s_4, \delta s_5+(1-\delta)(s_4+s_6),$$
   $$\delta(1-\delta)(s_4-s_5)+\delta s_6)$$

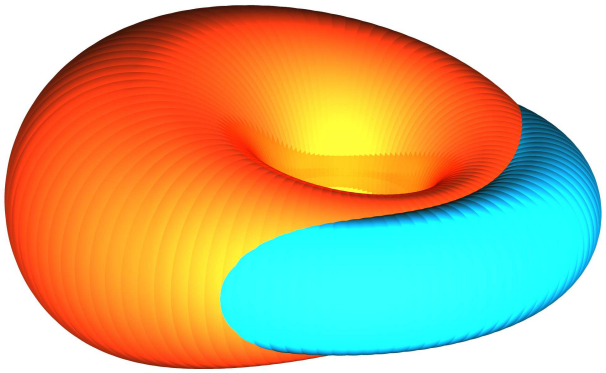

Figure 14: *An inversion maps a one-parameter family of spheres enveloping a torus to a one-parameter family of spheres enveloping a Dupin cyclide.*

which maps spheres with center $\mathbf{m}$ and radius ρ to spheres with center

$$\frac{\delta\mathbf{m}}{\delta(2\rho\delta-2\rho+\delta)+(\rho^2-\langle\mathbf{m},\mathbf{m}\rangle)(\delta-1)^2}$$

and radius

$$\frac{(\langle\mathbf{m},\mathbf{m}\rangle-\rho^2)(\delta-1)-\rho\delta}{(\langle\mathbf{m},\mathbf{m}\rangle-\rho^2)(\delta-1)^2-\delta(2\rho\delta-2\rho+\delta)}.$$

Obviously, this is an inversion as illustrated in Fig. 14. □

4.1 Quadratic mappings

Similar to the case of line geometric conchoid transformations, quadratic sphere geometric conchoid transformations can be defined. Therefore, it is only necessary to let the focal sphere S_1 be a linear image of the sphere S_2 to be transformed. A linear image of S_2 means a linear image of the Lie coordinate vector of the sphere S_2.
We shall have a look at two special types:

Theorem 7 *1. The quadratic sphere geometric conchoid transformation with the first focal sphere $S_0 = \Gamma_{\mathbf{o}}$ and the second focal sphere S_1 being the polar plane of $(0,0,0)$ with respect to $S_2 = (s_1,\dots,s_6)$ is a central similarity with center $(0,0,0)$ and scaling factor $\frac{1}{2}(1-2\delta)\delta^{-2}$, provided that $\delta \neq 0, \frac{1}{2}$.*

2. The quadratic sphere geometric conchoid transformation with the first focal sphere $S_0 = \mathrm{S}^2 = (0,0,0,-1,1,0)$ and the second focal sphere S_1 being the radical plane of S_0 and $S_2 = (s_1,\dots,s_6)$ is a cubic transformation, provided that $\delta \neq 0, 1$.

Proof.

1. The Lie coordinates of the focal spheres are

$$S_0 = (0,0,0,-1,0,1),$$
$$S_1 = (s_1,s_2,s_3,-\frac{1}{2}(s_4+s_6),s_5,-\frac{1}{2}(s_4+s_6))$$

with $s_5^2 = s_1^2+s_2^2+s_3^2$. Then, (2) yields

$$S_\delta = ((1-2\delta)s_1,(1-2\delta)s_2,(1-2\delta)s_3,$$
$$-\frac{1}{2}(\delta^2(s_4-s_6)+s_4+s_6),(1-2\delta)s_5,$$
$$\frac{1}{2}(\delta^2(s_6-s_4)-s_4-s_6))$$

where $s_4+s_6 \neq 0$ is canceled, since $\Omega_{01} = 2\Omega_{02} = \Omega_{12}(s_6-s_4)^{-1}$. This can be expressed by means of the original sphere data of S_2 (center $\mathbf{m} = (m_1,m_2,m_3)$ and radius ρ) via

$$s_1 = m_1,\ s_2 = m_2,\ s_3 = m_3,\ s_5 = \rho, \qquad (14)$$
$$s_4 = \frac{1}{2}\left(\langle\mathbf{m},\mathbf{m}\rangle-\rho^2-1\right),\ s_6 = \frac{1}{2}\left(\langle\mathbf{m},\mathbf{m}\rangle-\rho^2+1\right)$$

and gives the center $\mathbf{m}_\delta$ and radius ρ_δ of the image spheres:

$$\mathbf{m}_\delta = \frac{1-2\delta}{2\delta^2}\mathbf{m},\quad \rho_\delta = \frac{1-2\delta}{2\delta^2}\rho.$$

2. Inserting the Lie coordinates of the two focal spheres

$$S_0 = (0,0,0,-1,1,0),$$
$$S_1 = (s_1,s_2,s_3,\frac{1}{2}(s_6-s_4),s_5,\frac{1}{2}(s_6-s_4)).$$

into (2) yields

$$S_\delta = (s_1((1-2\delta)s_4-s_6),\ s_2((1-2\delta)s_4-s_6),$$
$$s_3((1-2\delta)s_4-s_6),\ \delta((\delta-1)s_4-s_5)(s_4-s_6)-$$
$$-(s_4+s_5)s_6,\ s_5((1-2\delta)s_4-s_6),$$
$$\delta((1-\delta)s_4+s_6)(s_4-s_6)-(s_4-s_5)s_5,$$

which can be reshaped with (14), and finally, (11) and (12) allow us to compute the center and the radius as

$$\mathbf{m}_\delta = \frac{1}{\delta^2}\left((1-\delta)(\langle\mathbf{m},\mathbf{m}\rangle-\rho^2)+\delta\right)\mathbf{m}$$
$$\rho_\delta = \frac{1}{\delta^2}\left((1-\delta)(\langle\mathbf{m},\mathbf{m}\rangle-\rho^2)+\delta\right)\rho.$$

Obviously, $\mathbf{m}_\delta$ is cubic in the coordinates of $\mathbf{m}$ and ρ_δ is cubic in ρ. □

5 Conclusion

The projective models of various geometries allow us to generalize the well-known conchoid transformation as long as a quadric model exists and a cross ratio can be defined. So far we haven't dealt with singular quadrics such as Blaschke's cylinder model for isotropic geometries. The subspaces contained in singular quadrics may cause problems for the generalized conchoid construction.
The sphere model of Möbius geometry could also be a playground for generalized conchoid constructions. Nevertheless, cross ratios of four complex numbers can also be defined and give rise to a generalized conchoid construction in the Gauss plane.
Finally, there is one special quadric serving as a point model for the set of Euclidean motions: It is Study's quadric $S_2^6 \subset \mathbb{P}^6(\mathbb{R})$. Conchoid transformations within Study's quadric may generate special Euclidean motions in Euclidean three space.

Acknowledgement

I have to express my sincere thanks to a careful reviewer whose suggestions helped to improve the paper.

References

[1] A. ALBANO, M. ROGGERO, Conchoidal transform of two plane curves, *Appl. Algebra Eng. Comm. Comp.* **21**(**4**) (2010), 309–328.

[2] W. BENZ, *Vorlesungen über Geometrie der Algebren.* Springer-Verlag, Berlin-Heidelberg-New York, 1973.

[3] W. BLASCHKE, *Vorlesungen über Differentialgeometrie III.* Springer-Verlag, Berlin, 1929.

[4] E. BRIESKORN, H. KNÖRRER, *Plane Algebraic Curves.* Birkhäuser, Basel - Boston - Stuttgart, 2012.

[5] T.E. CECIL, *Lie sphere geometry*, Springer, New York; 2nd ed., 2008.

[6] K. FLADT, *Analytische Geometrie spezieller ebener Kurven*, Akademische Verlagsgesellschaft, Frankfurt am Main, 1962.

[7] O. GIERING, *Vorlesungen über höhere Geometrie.* Vieweg, Braunschweig - Wiesbaden, 1982.

[8] M. HAMANN, B. ODEHNAL, Conchoidal ruled surfaces, *Proc. 15th Int. Conf. Geometry & Graphics*, Aug. 1–5, 2012, Montreal, article No. 089.

[9] J. HOSCHEK, *Liniengeometrie*, Bibliographisches Institut, Zürich, 1971.

[10] J.D. LAWRENCE, *A catalog of special plane curves*, Dover Publications, New York, 1972.

[11] G. LORIA, *Spezielle algebraische und transzendente ebene Kurven*, B.G. Teubner, Leipzig, 1908.

[12] B. ODEHNAL, Conchoids on the Sphere, *KoG* **17** (2014), 43–52.

[13] M. PETERNELL, D. GRUBER, J. SENDRA, Conchoid surfaces of rational ruled surfaces, *Comp. Aided Geom. Design* **28** (2011), 427–435.

[14] M. PETERNELL, D. GRUBER, J. SENDRA, Conchoid surfaces of spheres, *Comp. Aided Geom. Design* **30** (2013), 35–44.

[15] M. PETERNELL, L. GOTTHART, J. SENDRA, J.R. SENDRA, Offsets, Conchoids and Pedal Surfaces, *J. Geom.* **106** (2015), 321–339.

[16] J.G. SEMPLE, *Algebraic Curves*, Clarendon Press, Oxford, 1959.

[17] J.R. SENDRA, J. SENDRA, An algebraic analysis of conchoids to algebraic curves, *Appl. Algebra Eng. Comm. Comp.* **19**(**5**) (2008), 285–305.

[18] J. SENDRA, J.R. SENDRA, Rational parametrization of conchoids to algebraic curves, *Appl. Algebra Eng. Comm. Comp.* **21**(**4**) (2010), 413–428.

[19] R. SAUER, *Projektive Liniengeometrie*, W. de Gruyter & Co., Berlin und Leipzig, 1937.

[20] E.A. Weiss, *Einführung in die Liniengeometrie und Kinematik.* B.G. Teubner, Leipzig und Berlin, 1935.

[21] E.A. WEISS, Die geschichtliche Entwicklung der Lehre von der Geraden-Kugel-Transformation VII, *Deutsche Math.* **3** (1938), 11–35.

[22] H. WIELEITNER, *Spezielle ebene Kurven*, G.J. Göschen'sche Verlagshandlung, Leipzig, 1908.

[23] K. ZINDLER, *Liniengeometrie mit Anwendungen I & II*, G.J. Göschen'sche Verlagshandlung, Leipzig, 1902.

Boris Odehnal
orcid.org/0000-0002-7265-5132
e-mail: boris.odehnal@uni-ak.ac.at

University of Applied Arts Vienna

Oskar-Kokoschka-Platz 2, A-1100 Vienna, Austria

Original scientific paper
Accepted 12. 12. 2017.

N J WILDBERGER

Rational Trigonometry in Higher Dimensions and a Diagonal Rule for 2-planes in Four-dimensional Space

Rational Trigonometry in Higher Dimensions and a Diagonal Rule for 2-planes in Four-dimensional space

ABSTRACT

We extend rational trigonometry to higher dimensions by introducing rational invariants between k-subspaces of n-dimensional space to give an alternative to the canonical or principal angles studied by Jordan and many others, and their angular variants. We study in particular the cross, spread and det-cross of 2-subspaces of four-dimensional space, and show that Pythagoras theorem, or the Diagonal Rule, has a natural generalization for such 2-subspaces.

Key words: rational trigonometry, subspaces, canonical angles, Diagonal rule, spread, cross

MSC2010: 51N25, 14Qxx, 14N20

Racionalna trigonometrija u višim dimenzijama i dijagonalno pravilo za 2-ravnine u 4-dimenzionalnom prostoru

SAŽETAK

Proširujemo racionalnu trigonometriju na više dimenzije tako da uvodimo racionalne invarijante između k-podprostora n-dimenzionalnog prostora. Dajemo alternativu kanonskim ili glavnim kutovima, koje su proučavali Jordan i mnogi drugi, te njihove varijante. Posebno proučavamo križni produkt, raspon i det-križni produkt 2-podprostora 4-dimenzionalnog prostora i pokazujemo da Pitagorin teorem, ili dijagonalno pravilo, ima prirodnu generalizaciju za takve 2-podprostore.

Ključne riječi: racionalna trigonometrija, podprostori, kanonski kutovi, dijagonalno pravilo, raspon, križni produkt

1 Introduction

The notion of "angles" between two subspaces of a Euclidean space has seen many results going back to C. Jordan's foundational work in 1875 [7]. In the last fifty years, this idea has also seen considerable interest from statisticians and numerical analysts, who refer to "canonical or principal angles", as in [1], [2] and [3]. Applications of these "canonical angles" can be found in, for example, [4], [5], [8], [13] and [24].

Let us consider a general dot product space, by which we mean a vector space together with a non-degenerate symmetric bilinear form, or dot product, $u \cdot v$, although traditionally the topic involves only the classical case with the Euclidean inner product. We will refer to a subspace of dimension k as a **k-subspace**.

Then for example in Jordan's theory, two 2-subspaces of four dimensional space determine in general two "angles" θ_1 and θ_2. The first is the smallest "angle" between non-zero vectors in the two spaces, while the second is the smallest "angle" between the orthogonal compliments in each subspace to the vectors creating the first "angle". For example if P is the span of $(1,0,0,0)$ and $(0,1,0,0)$, while R is the span of $(1,0,0,a)$ and $(0,1,0,b)$ for numbers $|a| < |b|$, then the usual description amounts to "angles" θ_1 and θ_2 specified (somewhat loosely) by

$$\cos\theta_1 = \frac{1}{\sqrt{1+a^2}} \qquad \text{and} \qquad \cos\theta_2 = \frac{\sqrt{1+a^2}}{\sqrt{1+a^2+b^2}}.$$

The work of Risteski and Trenčevski [14] suggests that if we multiply the cosines of the "canonical angles", then we

may obtain the cosine of some new "geometrical angle" θ between the two given subspaces. In the special case where $(u_1, u_2, \cdots, u_k)$ and $(v_1, v_2, \cdots, v_k)$ are orthonormal bases of k-dimensional subspaces P and R of R^n, their formula reduces to

$$\cos^2\theta = \det\left(M^T M\right) \tag{1}$$

in terms of the $k \times k$ matrix $M = [u_i \cdot v_j]$, although their original more general formulation had an error which was corrected by Gunawan, Neswan and Setya-Budhi in [6].

The reason that many of these concepts are put in quotes here is that this author is *skeptical* about the current "theory of real numbers" and most claims involving computations that require an "infinite amount" of computing time or power. But we do acknowledge that finite truncations of such procedures can have a very useful applied function. From our point of view even the usual definition of the "angle" between vectors u and v given by

$$\cos\theta = \frac{u \cdot v}{|u|\,|v|}$$

is problematic in the realm of pure mathematics, on account of the "infinite amounts" of work needed to evaluate the square roots implicit in $|u|$ and $|v|$, and then to evaluate an inverse circular function.

We are interested in investigating a framework for pure mathematics that does *not require us to pretend to obtain outputs from unending algorithms or computer programs*.

Now many readers may very well not share this orientation, but we do hope that they can see that it might nevertheless be a legitimate logical position, and might actually steer us in natural and fruitful directions. This in fact leads us to rational trigonometry [15], [16], [17], [18]; to chromogeometry and associated triangle geometry [9], [10] and [19]; and to universal hyperbolic geometry, as in [20], [21], [22] and [23], so there is plenty of evidence that the approach has some merit.

To avoid "angles" therefore, we are going to re-frame the separation between two k-dimensional subspaces in an n-dimensional dot product space using an extension of a fundamental formula of rational trigonometry. Notice that we restrict to this more specific situation here, with subspaces of equal dimension. We will investigate some basic properties of rational invariants obtained from the characteristic polynomial of a cross matrix determined by two such subspaces, and in particular will prove a Pythagorean theorem, or *Diagonal Rule* result, for the special but quite interesting case of 2-subspaces in the four-dimensional Euclidean vector space V^4 of row vectors. The alternate new name for this historically important result reflects the fact that the Old Babylonian culture had a clear understanding of the geometry of a right triangle, more than 1000 years before Pythagoras was born, as discussed for example in [11].

1.1 The basic vector orientation of rational trigonometry

We begin by reviewing the basics of rational trigonometry, which was introduced in the planar situation in the author's book [15], and to more general situations in [16] and [19]. The main initial idea is to replace "transcendental metrical quantities" in Euclidean geometry with purely algebraic quantities. Thus the "distance" $|A,B|$ between two points A and B is replaced by the *quadrance* $Q(A,B)$, which is the sum of squares of the differences between the coordinates, and the "angle" $\theta(l,m)$ between two lines l and m is replaced by the *spread* $s(l,m)$, which may be thought of as the ratio of the opposite quadrance over the hypotenuse quadrance for any right triangle formed by the two lines, or the *cross*, which is the ratio of the adjacent quadrance over the hypotenuse quadrance.

More generally and explicitly, if a vector space over a field is given a symmetric bilinear form, or dot product, $u \cdot v$, then we define the **quadrance** of a vector v to be the number

$$Q(v) \equiv v \cdot v.$$

A vector v is **null** precisely when $Q(v) = 0$. The **cross** between non-null vectors u and v is defined to be the number

$$c(u,v) \equiv \frac{(u \cdot v)^2}{Q(u)\,Q(v)}.$$

The **spread** between u and v is

$$s(u,v) \equiv 1 - c(u,v) = 1 - \frac{(u \cdot v)^2}{Q(u)\,Q(v)}.$$

Since both the cross and spread are invariant under rescaling of either or both of the vectors, these quantities extend to metrical invariants between one-dimensional subspaces, just by considering spanning or direction vectors. So given one-dimensional subspaces l and m with respective spanning vectors u and v, we may define the respective cross and spread between them as $c(l,m) \equiv c(u,v)$ and $s(l,m) \equiv s(u,v)$. These quantities are numbers in the given field.

For the vector space of row vectors of a given dimension n, the Euclidean symmetric bilinear form may be written in linear algebraic terms as

$$u \cdot v = uv^T.$$

A more general symmetric bilinear form is given by

$$u \cdot v = uMv^T$$

for some symmetric $n \times n$ matrix M, which is usually also assumed to be non-degenerate, meaning that $\det M \neq 0$.

Let us make an important additional observation: that since $u \cdot v = v \cdot u$, the (Euclidean) cross may be rewritten in this linear algebraic notation as

$$c(u,v) = \frac{\left(uv^T\right)^2}{\left(uu^T\right)\left(vv^T\right)} = uv^T \left(vv^T\right)^{-1} vu^T \left(uu^T\right)^{-1} \qquad (2)$$

while the more general cross may be written as

$$c(u,v) = \frac{\left(uMv^T\right)^2}{\left(uMu^T\right)\left(vMv^T\right)} = uMv^T \left(vMv^T\right)^{-1} vMu^T \left(uMu^T\right)^{-1}. \qquad (3)$$

How do these rational trigonometric definitions relate to the more familiar notions of distance and angle? One may attempt to "introduce a square-root" of the quadrance $Q(v)$ and so define a length $|v|$, but this is problematic on at least two counts; if working algebraically it generally requires an extension field, but analytically, this is a computational process that does *not generally terminate*, and so the ostensible outputs cannot be said to be well-defined (hence the quotes). Furthermore for other bilinear forms, as in Einstein's special theory of relativity, the quadrance can be negative, in which case we need also to introduce complex extension fields.

One may attempt to introduce an "inverse sine of a square root" of the spread, or the "inverse cosine of a square root" of the cross, to get an "angle", but again the transcendental aspect of these operations and the functions involved means that in practice only an approximation to an "ideal angle" is obtained after terminating the program to get an output in a finite amount of time. And in other geometries, as in Einstein's relativistic geometry, the quantities that appear as crosses and spreads need not be in the familiar interval $[-1,1]$, so "applying inverse circular functions" is not directly appropriate.

When we move to rational trigonometry as a framework for metrical geometry, many new possibilities for precision, clarity and generality open up. The quantities and their relations become algebraic and rational; we are not forced to assume a "real number framework" involving an algebraic structure that is rarely, if ever, set out logically and correctly in its entirety. We may aspire to obtain complete and correct results to metrical questions without the need to invoke symbolic arithmetic involving un-evaluated symbols such as π, $\sqrt{2}$, and $\cos 5$, or resorting to approximate values such as 3.1415, 1.4142 or 0.2837 etc.

1.2 The affine laws of rational trigonometry

To enunciate the main laws of rational trigonometry, a first step is to extend the above notions from the vector space framework to the corresponding affine framework. We may consider the affine space A^n, whose points are n-tuples $A = [a_1, a_2, \cdots, a_n]$ with entries from some field, but now with a translational symmetry as well as the linear transformational symmetry. To a pair of such affine points A, B we may associate the displacement vector $v = \overrightarrow{AB} = (b_1 - a_1, b_2 - a_2, \cdots, b_n - a_n)$ in the usual fashion by taking differences of coordinates.

Suppose now that the associated vector space V^n of row vectors $v = (x_1, x_2, \cdots, x_n)$ is given a non-degenerate symmetric bilinear form $u \cdot v$ as above. The **quadrance** between the affine points A_1 and A_2 is then correspondingly defined to be

$$Q(A_1, A_2) \equiv \overrightarrow{A_1A_2} \cdot \overrightarrow{A_1A_2}.$$

The affine line A_1A_2 determined by two points A_1 and A_2 is a **null line** precisely when $Q(A_1, A_2) = 0$, that is when a direction vector for it is null.

The **cross** between non-null lines $l \equiv A_1A_2$ and $m \equiv B_1B_2$ is the number

$$c(l,m) \equiv \frac{\left(\overrightarrow{A_1A_2} \cdot \overrightarrow{B_1B_2}\right)^2}{Q(A_1, A_2)\, Q(B_1, B_2)}$$

while the **spread** between l and m is

$$s(l,m) \equiv 1 - c(l,m) = 1 - \frac{\left(\overrightarrow{A_1A_2} \cdot \overrightarrow{B_1B_2}\right)^2}{Q(A_1, A_2)\, Q(B_1, B_2)}.$$

These are just the cross and spread of the associated direction vectors, and are independent of the choice of points lying on the two lines. If one or both of the lines involved are null, then the cross and spread are undefined, and statements involving them will be considered empty. Note also that we do not require the two lines to be meeting in order for these quantities to be defined.

Two non-null lines are **perpendicular** precisely when the cross between them is 0, or equivalently when the spread between them is 1. These conditions are just a restatement of the orthogonality of corresponding direction vectors with respect to the underlying bilinear form.

Here then are the five main laws of rational trigonometry for this metrical affine situation, where we use the convention that a triangle $\overline{A_1A_2A_3}$ is a set $\{A_1, A_2, A_3\}$ of three distinct points with quadrances $Q_1 \equiv Q(A_2, A_3)$, $Q_2 \equiv Q(A_1, A_3)$ and $Q_3 \equiv Q(A_1, A_2)$, and spreads $s_1 \equiv s(A_1A_2, A_1A_3)$, $s_2 \equiv s(A_2A_1, A_2A_3)$ and $s_3 \equiv s(A_3A_1, A_3A_2)$.

Theorem 1 (Diagonal Rule or Pythagoras' theorem) *The lines A_1A_3 and A_2A_3 are perpendicular precisely when*

$$Q_1 + Q_2 = Q_3.$$

Theorem 2 (Triple quad formula) *The points A_1, A_2 and A_3 are collinear precisely when*

$$(Q_1 + Q_2 + Q_3)^2 = 2\left(Q_1^2 + Q_2^2 + Q_3^2\right).$$

Theorem 3 (Spread law)

$$\frac{s_1}{Q_1} = \frac{s_2}{Q_2} = \frac{s_3}{Q_3}.$$

Theorem 4 (Cross law)

$$(Q_1 + Q_2 - Q_3)^2 = 4Q_1Q_2(1 - s_3).$$

Note that the Cross law includes as special cases both the Triple quad formula and the Diagonal Rule when $s_3 = 0$ and $s_3 = 1$ respectively. The next result is the algebraic analog to the sum of the angles in a triangle formula.

Theorem 5 (Triple spread formula)

$$(s_1 + s_2 + s_3)^2 = 2\left(s_1^2 + s_2^2 + s_3^2\right) + 4s_1s_2s_3.$$

This last relation may be restated in terms of the corresponding crosses $c_1 \equiv c(A_1A_2, A_1A_3)$, $c_2 \equiv c(A_2A_1, A_2A_3)$ and $c_3 \equiv c(A_3A_1, A_3A_2)$ as follows.

Theorem 6 (Triple cross formula)

$$(c_1 + c_2 + c_3)^2 = 4c_1c_2c_3.$$

With these laws we need no longer be restricted to Euclidean geometry metrically, but can apply our computations for example to relativistic geometries, since the main laws of rational trigonometry are valid independent of the particular bilinear form chosen (provided it is non-degenerate). And the computations work over a general field, notably the rational numbers with finite field extensions introduced as needed. Rational trigonometry extends also to finite fields, and indeed current work of Michael Reynolds is developing powerful software for such investigations.

Another very important advantage is that the above notions of quadrance and spread, introduced over a vector space over a field, have projective analogs when we consider the projective space associated to such a space. In this way we may assign notions of *projective quadrance* and *projective spread* to hyperbolic geometry in the Cayley Klein sense, yielding a more algebraic and general form of *Universal hyperbolic geometry* in which many new phenomenon are visible, and which has closer connections to relativistic physics on account of the fact that we can work uniformly inside or outside the light cone, as described in [20]. The essential projective nature of this approach means that elliptic geometry is captured by the same laws as for hyperbolic geometry – not just analogs where circular transcendental functions are replaced by hyperbolic ones as in the classical situation.

So we have enlarged geometry many-fold by moving to rational trigonometry for our metrical computations: we can work over the rational numbers; or over a finite field; we can consider arbitrary bilinear forms, including relativistic geometries; and we can create projective analogs of both elliptic and hyperbolic geometries simultaneously in the same general arena.

But another vista still beckons by more explicitly adopting a linear algebraic point of view. How might we extend rational trigonometry to higher dimensions, to consider metrical relations in the spirit of Jordan's "canonical or principal angles", between higher dimensional objects in such spaces? For example how does a symmetric bilinear form allow us to define rational metrical relations between k-dimensional subspaces of an n-dimensional vector V^n or an associated affine space? And what theorems can we hope to find in these larger settings?

Cross matrices, cross and det-cross

Suppose that we have two $k \times n$ matrices P and R, both of rank k, representing k-subspaces of the vector space V^n over some field (with the rational numbers being the default choice), in the sense that the rows of each matrix are a basis of the corresponding k-subspace. Our aim is to introduce metrical invariants of the corresponding k-subspaces. The matrices PP^T and RR^T are both also of rank k, and so invertible $k \times k$ matrices. Then motivated by (2) and (3), we define the **cross matrix** of P and R to be

$$C = C(P,R) \equiv PR^T\left(RR^T\right)^{-1}RP^T\left(PP^T\right)^{-1}.$$

This is also a $k \times k$ matrix.

Now define the **cross** between P and R to be the normalized trace

$$c = c(P,R) \equiv \frac{1}{k}\operatorname{tr} C$$

and define the **spread** between P and R to be

$$s = s(P,R) \equiv 1 - c.$$

Define the **det-cross** between P and R to be the number

$$d(P,R) \equiv \det(C(P,R)).$$

The det-cross agrees with the square of the "cosine of the geometrical angle" of Risteski and Trenčevski as in (1), which we can see by considering the special case when P and R contain orthonormal vectors, so that $PP^T = RR^T = I$. But our introduction of the cross matrix yields a richer invariant that potentially gives us all the coefficients of the characteristic polynomial as invariants. These are some kinds of analogs of the canonical angles of Jordan.

The cross, spread and det-cross are numbers in the underlying field that depend on the matrices P and R. We now demonstrate that they really depend only on the subspaces determined by P and R. We first show that if we rearrange the rows of P by an invertible linear transformation, then the new cross matrix is similar to the original, where two matrices X and Y are **similar** precisely when there is an invertible matrix M with

$$X = MYM^{-1}.$$

Theorem 7 *If P,R are both $k \times n$ matrices of rank k, and M is an invertible $k \times k$ matrix, then $C(MP,R) = MC(P,R)M^{-1}$ so that $c(MP,R) = c(P,R)$ and $d(MP,R) = d(P,R)$.*

Proof. If M is an invertible $k \times k$ matrix then

$$\begin{aligned} C(MP,R) &= (MP)R^T\left(RR^T\right)^{-1}R(MP)^T\left((MP)(MP)^T\right)^{-1} \\ &= MPR^T\left(RR^T\right)^{-1}RP^TM^T\left(MPP^TM^T\right)^{-1} \\ &= MPR^T\left(RR^T\right)^{-1}RP^TM^T\left(M^T\right)^{-1}\left(PP^T\right)^{-1}M^{-1} \\ &= MPR^T\left(RR^T\right)^{-1}RP^T\left(PP^T\right)^{-1}M^{-1} \\ &= MC(P,R)M^{-1}. \end{aligned}$$

But since the trace and determinant of similar matrices are equal, we deduce that $c(MP,R) = c(P,R)$ and $d(MP,R) = d(P,R)$. □

Since the definition of the cross matrix is not quite symmetric in P and R, a separate calculation is required to establish the effect of changing the basis for the row space of R.

Theorem 8 *If P,R are both $k \times n$ matrices of rank k, and M is an invertible $k \times k$ matrix, then $C(P,MR) = C(P,R)$ so that $c(MP,R) = c(P,R)$ and $d(MP,R) = d(P,R)$.*

Proof. If M is an invertible $k \times k$ matrix then

$$\begin{aligned} C(P,MR) &= P(MR)^T\left((MR)(MR)^T\right)^{-1}(MR)P^T\left(PP^T\right)^{-1} \\ &= PR^TM^T\left(MRR^TM^T\right)^{-1}MRP^T\left(PP^T\right)^{-1} \\ &= PR^T\left(RR^T\right)^{-1}RP^T\left(PP^T\right)^{-1} \\ &= C(P,R). \end{aligned}$$

So clearly $c(P,MR) = c(P,R)$ and $d(P,MR) = d(P,R)$. □

There is one more important invariance with respect to these quantities: that they are unchanged under isometries of the Euclidean space with symmetric bilinear form $u \cdot v = uv^T$. Such an isometry is given by an $n \times n$ orthogonal matrix Q, with the property that $QQ^T = I$, acting on the right on row vectors and so also on $k \times n$ matrices.

Theorem 9 *If P,R are both $k \times n$ matrices of rank k, and Q is an orthogonal $n \times n$ matrix, then $C(PQ,RQ) = C(P,R)$ so that $c(MP,R) = c(P,R)$ and $d(MP,R) = d(P,R)$.*

Proof. If Q is an orthogonal $n \times n$ matrix then

$$\begin{aligned} &C(PQ,RQ) = \\ &= (PQ)(RQ)^T\left((RQ)(RQ)^T\right)^{-1}(RQ)(PQ)^T\left((PQ)(PQ)^T\right)^{-1} \\ &= PQQ^TR^T\left(RQQ^TR^T\right)^{-1}RQQ^TP^T\left(PQQ^TP^T\right)^{-1} \\ &= PR^T\left(RR^T\right)^{-1}RP^T\left(PP^T\right)^{-1} \\ &= C(P,R). \end{aligned}$$

As before it follows that $c(PQ,RQ) = c(P,R)$ and $d(PQ,RQ) = d(P,R)$. □

2 The case of 2-subspaces of V^4

Let us illustrate the above general notions in the specific case of 2-subspaces in V^4, the linear space of row vectors $v = \begin{pmatrix} x_1 & x_2 & x_3 & x_4 \end{pmatrix}$ whose elements belong to some field, which is typically the rational numbers. A two-dimensional subspace, or 2-subspace, is the span of two linearly independent vectors, and may be specified by the 2×4 matrix with these vectors as the rows. So for example

$$P = \begin{pmatrix} 2 & -1 & 5 & 2 \\ 1 & 1 & 1 & 7 \end{pmatrix}$$

represents the 2-subspace spanned by the two row vectors $\begin{pmatrix} 2 & -1 & 5 & 2 \end{pmatrix}$ and $\begin{pmatrix} 1 & 1 & 1 & 7 \end{pmatrix}$.

Clearly if we perform invertible elementary row operations on P, which is equivalent to multiplying on the left by an invertible matrix M, then we get another representative for the same subspace, for example

$$P' = \begin{pmatrix} 1 & 0 & 2 & 3 \\ 0 & 1 & -1 & 4 \end{pmatrix} = \begin{pmatrix} \frac{1}{3} & \frac{1}{3} \\ -\frac{1}{3} & \frac{2}{3} \end{pmatrix}\begin{pmatrix} 2 & -1 & 5 & 2 \\ 1 & 1 & 1 & 7 \end{pmatrix}$$

which is the span of $\begin{pmatrix} 1 & 0 & 2 & 3 \end{pmatrix}$ and $\begin{pmatrix} 0 & 1 & -1 & 4 \end{pmatrix}$. We may write this relationship as $P' = MP \sim P$ and observe that the two matrices represent the same subspace.

This generalizes the one-dimensional property of a one-dimensional subspace being unchanged if a representative vector is multiplied by a non-zero scalar (or 1×1 matrix). To simplify notation we will often associate both the subspace and a defining matrix for it by the same letter.

Example 1 *Generalizing the first example in the Introduction, suppose that* $P = \begin{pmatrix} 1 & 0 & 0 & 0 \\ 0 & 1 & 0 & 0 \end{pmatrix}$ *and* $R = \begin{pmatrix} 1 & 0 & x & y \\ 0 & 1 & z & w \end{pmatrix}$. *Then a computation shows that*

$$\begin{aligned} C = (P,R) &= PR^T \left(RR^T\right)^{-1} RP^T \left(PP^T\right)^{-1} \\ &= \left((xw-yz)^2 + x^2 + y^2 + z^2 + w^2 + 1\right)^{-1} \\ &\quad \begin{pmatrix} w^2+z^2+1 & -wy-xz \\ -wy-xz & x^2+y^2+1 \end{pmatrix} \end{aligned}$$

so that

$$c(P,R) = \frac{1}{2}\mathrm{tr}(C) = \frac{1}{2}\frac{x^2+y^2+z^2+w^2+2}{(xw-yz)^2+x^2+y^2+z^2+w^2+1}$$

$$s(P,R) = 1 - c(P,R) = \frac{1}{2}\frac{x^2+y^2+z^2+w^2+2(xw-yz)^2}{(xw-yz)^2+x^2+y^2+z^2+w^2+1}$$

and

$$d(P,R) = \det C = \frac{1}{(xw-yz)^2+x^2+y^2+z^2+w^2+1}.$$

3 Perpendicularity for 2-subspaces over the rational numbers

In the vector case, two vectors u and v are perpendicular precisely when $s(u,v) = 1$, or equivalently in terms of the cross $c(u,v) = 0$. We now show that the same holds true for 2-subspaces in V^4, assuming we are working over the rational numbers. Note that the general situation, over a different field, may be different! The computations in the proof of this theorem are useful independently.

Theorem 10 (Perpendicular 2-subspace) *Suppose that the underlying field is the rational numbers. If P is a 2-subspace of V^4, then the only 2-subspace T for which $c(P,T) = 0$ is the orthogonal subspace $T = P^\perp$.*

Proof. Since the cross is unchanged if we perform an orthogonal transformation or perform row reduction on representative vectors, the general case can be reduced to the case when $P = \begin{pmatrix} 1 & 0 & 0 & 0 \\ 0 & 1 & 0 & 0 \end{pmatrix}$. Then by row reduction, any other 2-subspace T has a representative matrix of one of the following kinds:

$$T_{12} = \begin{pmatrix} 1 & 0 & x & y \\ 0 & 1 & z & w \end{pmatrix}, \qquad T_{13} = \begin{pmatrix} 1 & 0 & 0 & y \\ 0 & 0 & 1 & w \end{pmatrix},$$

$$T_{14} = \begin{pmatrix} 1 & 0 & 0 & 0 \\ 0 & 0 & 0 & 1 \end{pmatrix}, \qquad T_{23} = \begin{pmatrix} 0 & 1 & 0 & y \\ 0 & 0 & 1 & w \end{pmatrix},$$

$$T_{24} = \begin{pmatrix} 0 & 1 & 0 & 0 \\ 0 & 0 & 0 & 1 \end{pmatrix}, \qquad T_{34} = \begin{pmatrix} 0 & 0 & 1 & 0 \\ 0 & 0 & 0 & 1 \end{pmatrix}.$$

We then compute that the various possibilities for the crosses with P are:

$$c(P,T_{12}) = \frac{1}{2}\frac{x^2+y^2+z^2+w^2+2}{(xw-yz)^2+x^2+y^2+z^2+w^2+1}$$

$$c(P,T_{13}) = \frac{1}{2}\frac{w^2+1}{w^2+y^2+1}$$

$$c(P,T_{14}) = \frac{1}{2}$$

$$c(P,T_{23}) = \frac{1}{2}\frac{w^2+1}{w^2+y^2+1}$$

$$c(P,T_{24}) = \frac{1}{2}$$

$$c(P,T_{34}) = 0.$$

Over the rational numbers, because squares are always positive, the only case when we can have $c(P,T) = 0$ is the case of

$$T = T_{34} = \begin{pmatrix} 0 & 0 & 1 & 0 \\ 0 & 0 & 0 & 1 \end{pmatrix}.$$

This is the orthogonal subspace of P. □

A Diagonal Rule for 2-subspaces

The Diagonal Rule, or Pythagoras' theorem, for vectors may be stated as follows.

Theorem 11 (One-dimensional Diagonal Rule) *If P and R are perpendicular 1-subspaces of a two-dimensional space, that is for which $c(P,R) = 0$, then for any 1-subspace T we have*

$$c(P,T) + c(R,T) = 1.$$

The reason why this somewhat unusual vector form for Pythagoras' theorem is equivalent to the usual affine one for triangles is as follows. Since the spread, or cross between two affine lines depends only on the direction vectors of those lines, they are unchanged if one or both of the lines are translated. So if we have a right triangle consisting of two 1-dimensional subspaces meeting perpendicularly at the origin, and another affine subspace lying in the same plane, the affine subspace may be translated to the origin where it becomes a 1-dimensional subspace, without any change to the respective spreads or crosses. Now we show that the one-dimensional result has a two-dimensional analog.

Theorem 12 (Two-dimensional Diagonal Rule) *If P and R are perpendicular 2-subspaces of a four-dimensional space, that is for which $c(P,R) = 0$, then for any 2-subspace T we have*

$$c(P,T) + c(R,T) = 1.$$

Proof. Without loss of generality, we can perform an orthogonal change of coordinates so that the first subspace P is represented by the matrix

$$P = \begin{pmatrix} 1 & 0 & 0 & 0 \\ 0 & 1 & 0 & 0 \end{pmatrix}.$$

The perpendicular subspace is then

$$R = \begin{pmatrix} 0 & 0 & 1 & 0 \\ 0 & 0 & 0 & 1 \end{pmatrix}$$

and we know that $c(P,R) = 0$. Over the rational numbers we know that R is the only 2-subspace with the property that $c(P,R) = 0$, but we do not require that here. Now any 2-dimensional subspace T, after row reduction, can be represented by one of the general matrices $T_{12}, T_{13}, T_{14}, T_{23}, T_{24}$ or T_{34} displayed in the proof of the Perpendicular 2-subspace theorem above. That proof already established the crosses between P and each of these matrices. We now similarly calculate the crosses between these matrices and the matrix R:

$$\begin{aligned}
c(R,T_{12}) &= \frac{1}{2}\frac{2w^2x^2 + w^2 - 4wxyz + x^2 + 2y^2z^2 + y^2 + z^2}{w^2x^2 + w^2 - 2wxyz + x^2 + y^2z^2 + y^2 + z^2 + 1} \\
c(R,T_{13}) &= \frac{1}{2}\frac{w^2 + 2y^2 + 1}{w^2 + y^2 + 1} \\
c(R,T_{14}) &= \frac{1}{2} \\
c(R,T_{23}) &= \frac{1}{2}\frac{w^2 + 2y^2 + 1}{w^2 + y^2 + 1} \\
c(R,T_{24}) &= \frac{1}{2} \\
c(R,T_{34}) &= 1.
\end{aligned}$$

Then using the preceding computations, we get

$$\begin{aligned}
&c(P,T_{12}) + c(R,T_{12}) = \\
&\quad \frac{1}{2}\frac{w^2 + x^2 + y^2 + z^2 + 2}{w^2x^2 + w^2 - 2wxyz + x^2 + y^2z^2 + y^2 + z^2 + 1} \\
&\quad + \frac{1}{2}\frac{2w^2x^2 + w^2 - 4wxyz + x^2 + 2y^2z^2 + y^2 + z^2}{w^2x^2 + w^2 - 2wxyz + x^2 + y^2z^2 + y^2 + z^2 + 1} = 1 \\
&c(P,T_{13}) + c(R,T_{13}) = \frac{1}{2}\frac{w^2 + 1}{w^2 + y^2 + 1} + \frac{1}{2}\frac{w^2 + 2y^2 + 1}{w^2 + y^2 + 1} = 1 \\
&c(P,T_{14}) + c(R,T_{14}) = \frac{1}{2} + \frac{1}{2} = 1 \\
&c(P,T_{13}) + c(R,T_{13}) = \frac{1}{2}\frac{w^2 + 1}{w^2 + y^2 + 1} + \frac{1}{2}\frac{w^2 + 2y^2 + 1}{w^2 + y^2 + 1} = 1 \\
&c(P,T_{13}) + c(R,T_{13}) = \frac{1}{2} + \frac{1}{2} = 1 \\
&c(P,T_{13}) + c(R,T_{13}) = 0 + 1 = 1
\end{aligned}$$

In all cases the sum of the two crosses is

$$c(P,T) + c(R,T) = 1. \qquad \square$$

4 Two-dimensional subspaces of V^3

Theorem 13 *The spread between two 2-subspaces of V^3 is one half of the spread between the direction vectors of the subspaces perpendicular to their common meet.*

Proof. Any two distinct 2-subspaces in V^3 meet in a one-dimensional subspace. Let us assume, by performing an orthogonal transformation, that this common 1-subspace is the span of the vector $(1,0,0)$. By row reduction, the two 2-subspaces may be taken to be

$$P = \begin{pmatrix} 1 & 0 & 0 \\ 0 & a & b \end{pmatrix} \quad \text{and} \quad R = \begin{pmatrix} 1 & 0 & 0 \\ 0 & c & d \end{pmatrix}.$$

Then

$$\begin{aligned}
C = C(P,R) &\equiv PR^T \left(RR^T\right)^{-1} RP^T \left(PP^T\right)^{-1} \\
&= \begin{pmatrix} 1 & 0 \\ 0 & \frac{(ac+bd)^2}{(a^2+b^2)(c^2+d^2)} \end{pmatrix}
\end{aligned}$$

with cross

$$c = c(P,R) = \frac{1}{2}\text{tr}C(P,R) = \frac{1}{2}\left(1 + \frac{(ac+bd)^2}{(a^2+b^2)(c^2+d^2)}\right)$$

and spread

$$\begin{aligned}
s = s(P,R) &= 1 - c(P,R) \\
&= \frac{1}{2}\frac{(ad-bc)^2}{(a^2+b^2)(c^2+d^2)}. \qquad \text{(Spread formula in } V^3\text{)}
\end{aligned}$$

This is one-half of the spread between the vectors $u = (0,a,b)$ and $v = (0,c,d)$. $\square$

As an immediate corollary we obtain the following:

Proposition 1 *For any 2-subspaces P and R of V^3 over the rational numbers the cross $c(P,R)$ and the spread $s(P,R)$ satisfy the inequalities*

$$\frac{1}{2} \le c(P,R) \le 1, \qquad 0 \le s(P,R) \le \frac{1}{2}.$$

Proof. Over the rational number field, squares are always positive. So the inequality for $c(P,R)$ follows immediately from the formula for it in the previous proof, while the inequality for $s(P,R)$ follows from that. □

Acknowledgements

The author would like to thank Hendra Gunawan for helpful discussions, and Michael Reynolds for his help in computing numerous examples of crosses and spreads in higher dimensional spaces, as well as the referee for useful suggestions.

References

[1] T.W. ANDERSON, *An Introduction to Multivariate Statistical Analysis*, John Wiley & Sons, Inc., New York, 1958.

[2] A. BJÖRCK, G.H. GOLUB, Numerical methods for computing angles between linear subspaces, *Math. Comp.* **27** (1973), 579–594.

[3] C. DAVIES, W. KAHAN, The rotation of eigenvectors by a perturbation. III, *SIAM J. Numer. Anal.* **7** (1970), 1–46.

[4] Z. DRMAČ, On principal angles between subspaces of Euclidean space, *SIAM J. Matrix Anal. Appl. (electronic)* **22** (2000), 173–194.

[5] A. GALÁNTAI, CS.J. HEGEDŨS, Jordan's principal angles in complex vector spaces, *Numer. Linear Algebra Appl.* **13** (2006), 589–598.

[6] H. GUNAWAN, O. NESWAN, W. SETYA-BUDHI, A formula for angles between two subspaces of inner product spaces, *Beitr. Algebra Geom.*, Contributions to Algebra and Geometry, **46**(**2**) (2005), 311–320.

[7] C. JORDAN, Essai sur la géométrie à n dimensions, *Bull. Soc. Math. France.* **3** (1875), 103–174.

[8] A.V. KNYAZEV, M.E. ARGENTATI, Principal angles between subspaces in an A-based scalar product: algorithms and perturbation estimates, *SIAM J. Sci. Comput.* **23** (2002), 2008–2040.

[9] N. LE, N.J. WILDBERGER, Incenter Circles, Chromogeometry, and the Omega Triangle, *KoG* **18** (2014), 5–18.

[10] N. LE, N.J. WILDBERGER, Universal Affine Triangle Geometry and Four-fold Incenter Symmetry, *KoG* **16** (2012), 63–80.

[11] D. MANSFIELD, N.J. WILDBERGER, Plimpton 322 is Babylonian Exact Sexagesimal Trigonometry, *Historia Math.* **44**(**4**) (2017), 395–419.

[12] J. MIAO, A. BEN-ISRAEL, Product cosines of angles between subspaces, *Linear Algebra Appl.* **237/238** (1996), 71–81.

[13] V. RAKOČEVIĆ, H.K. WIMMER, A variational characterization of canonical angles between subspaces, *J. Geometry* **78** (2003), 122–124.

[14] I.B. RISTESKI, K.G. TRENČEVSKI, Principal values and principal subspaces of two subspaces of vector spaces with inner product, *Beitr. Algebra Geom.,* Contributions to Algebra and Geometry **42**(**1**) (2001), 289–300.

[15] N.J. WILDBERGER, *Divine Proportions: Rational Trigonometry to Universal Geometry*, Wild Egg Books, Sydney, 2005, `http://wildegg.com`

[16] N.J. WILDBERGER, Affine and projective metrical geometry, 2007, `http://arxiv.org/abs/math/0701338`

[17] N.J. WILDBERGER, A Rational Approach to Trigonometry, *Math Horiz.* **15**(**2**)(2007), 16–20.

[18] N.J. WILDBERGER, One dimensional metrical geometry, *Geom. Dedicata* **128**(**1**) (2007), 145–166.

[19] N.J. WILDBERGER, Chromogeometry and relativistic conics, *KoG* **13** (2009), 43–50.

[20] N.J. WILDBERGER, Universal Hyperbolic Geometry I: Trigonometry, *Geom. Dedicata* **163**(**1**) (2013), 215–274.

[21] N.J. WILDBERGER, Universal Hyperbolic Geometry II: A pictorial overview, *KoG* **14** (2010), 3–24.

[22] N.J. WILDBERGER, Universal Hyperbolic Geometry III: First steps in projective triangle geometry, *KoG* **15**, (2011), 25–49.

[23] N.J. WILDBERGER, A. ALKHALDI, Universal Hyperbolic Geometry IV: Sydpoints and Twin Circumcircles, *KoG* **16** (2012), 43–62.

[24] H.K. WIMMER, Canonical angles of unitary spaces and perturbations of direct complements, *Linear Algebra Appl.* **287** (1999), 373–379.

N J Wildberger
orcid.org/0000-0003-3503-6495
e-mail: n.wildberger@unsw.edu.au
School of Mathematics and Statistics UNSW
Sydney 2052 Australia

Stručan rad
Prihvaćeno 5. 12. 2017.

BOJAN JANJANIN
JELENA BEBAN-BRKIĆ

Analiza izmjere Keopsove piramide

Survey Analysis of the Great Pyramid

ABSTRACT

The topic of this paper is an analysis of the survey of Cheops pyramid (also known as the Great pyramid), the most significant of the three pyramids of the Giza complex, the archeological site on the plateau of Giza, situated on the periphery of Cairo. It is assumed that Cheops as well as Khafre and Menkaure pyramids were built around 2686 – 2181 BC, known in the history as the Old Kingdom of Egypt. Our goal was to collect data about geodetic survey of Cheops pyramid and analyze it. Along with that, several hypotheses related to the construction method of the pyramid and possible purposes of the construction itself are described.

When analyzing the survey, two numbers, also called "two treasures of geometry", are constantly appearing, these are the number Pi (π) and the Golden ratio or golden number Fi (φ). One of the chapters is dedicated to these numbers.

Key words: geodetic survey, analysis of collected data, Ludolph's constant, Golden ratio

MSC2010: 00A99, 01A16, 86A30

Analiza izmjere Keopsove piramide

SAŽETAK

Tema ovog rada jest analiza izmjere Keopsove piramide, najznačajnije od triju većih piramida Giza kompleksa, arheološkog nalazišta na visoravni Giza, na periferiji Kaira. Pretpostavlja se da je Keopsova, kao i Kefrenova i Mikerinova piramida građena u periodu 2686. – 2181. pr. Kr., u povijesti poznatom kao Staro egipatsko Kraljevstvo. Cilj nam je bio prikupiti podatke o geodetskoj izmjeri Keopsove piramide te ih analizirati. Uz to je opisano i što je prethodilo izgradnji takve monumentalne građevine. Navedeno je nekoliko hipoteza koje su vezane za način gradnje piramide te su opisane i moguće svrhe same gradnje. Pri analizi izmjere neprestano se pojavljuju dva broja koja su nazivana i "dva blaga geometrije", a to su broj Pi (π) te Zlatni rez odnosno zlatni broj Fi (φ). Upravo tim brojevima posvećeno je jedno poglavlje ovog rada.

Ključne riječi: geodetska izmjera, analiza prikupljenih podataka, Ludolfova konstanta, zlatni rez

1 Uvod

Keopsova piramida, poznata i pod nazivom *Velika piramida*, najstarije je od sedam svjetskih čuda Starog svijeta i jedino koje je očuvano u potpunosti. To je najstarija i najveća piramida u Gizi, danas predgrađu Kaira.

Velika piramida podignuta je na umjetno poravnatoj kamenoj uzvisini. Prvotnom visinom od 146,7 metara bila je najviša građevina na svijetu sve do izgradnje Eiffelovog tornja (1889.). Baza piramide nije savršen kvadrat, ali najveće odstupanje između stranica koje su duge oko 230 metara iznosi nevjerojatnih 20 centimetara, odnosno 0,09 %.

Točnost orijentacije prema četiri strane svijeta također zapanjuje jer pomoću pronađenih podataka odstupanje iznosi 0,06 %. Današnji stručnjaci tvrde da je takvu točnost moguće ostvariti pomoću modernih laserskih uređaja i dobrog poznavanja astronomije.

Piramida se prostire na površini od 53 000 m^2, volumen joj se procjenjuje na 2,6 milijuna kubnih metara, a masa iznosi impresivnih 6,3 milijuna tona. Za izgradnju piramide upotrijebljeno je približno 2,3 milijuna kamenih blokova koje imaju prosječnu masu koja iznosi 2,6 tona. Prema vjerovanjima egiptologa za izgradnju piramide bilo je potrebno samo 20 godina.

Izgrađena je od različitog materijala koji je bio pribavljen iz raznih dijelova Egipta. Mnogi blokovi morali su biti dopremljeni do svog odredišta s više od tisuću kilometara udaljenosti.

U analizi izmjere često se pojavljuju brojevi 3,141 i 1,618. Navedeni brojevi se tamo ne nalaze slučajno, upravo ti brojevi su jedni od temelja na kojima leži geometrija Velike piramide.
Uvriježeno je mišljenje da su piramide izgrađene kao grobnice faraona te da su služile kako bi se preminuli faraoni povezali s duhovnim svijetom. Ljudi iz Drevnog Egipta vjerovali su da je smrt na Zemlji bila početak putovanja prema sljedećem "životu".
Pri pisanju ovog poglavlja služili smo se sljedećom literaturom: [4], [8], [18] i [20].

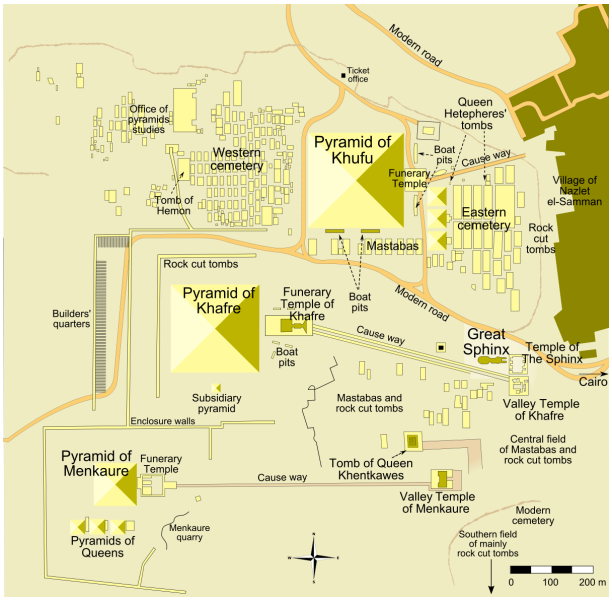

Slika 1: *Mapa kompleksa piramida u Gizi (Izvor: [28])*

Slika 2: *Fotografija kompleksa piramida u Gizi (Izvor: [28])*

Slika 3: *Fotografija Keopsove piramide (Izvor: autori)*

2 Značenje riječi piramida

Riječ piramida izvodi se iz grčke riječi *PYRAMIS* (što u prijevodu i znači piramida). U literaturi se nailazi na mišljenje da je riječ pyramis izvedenica egipatske riječi *PER-EM-US*, pronađene u matematičkom papirusu poznatom po nazivu *Rhind*[1]. Ta je riječ per-em-us opisana u egipatskoj matematičkoj raspravi kao naznaka visine piramide. Prevedena doslovce znači "ono što ide (ravno) gore" (od nečega označenog konačnim slogom US). Nažalost značenje tog sloga nije poznato i zato je riječ samo djelomično jasna. Egiptolozi ovo tumačenje smatraju neprihvatljivim te riječ pyramis prihvaćaju kao izvorno grčku riječ bez ikakve povezanosti s egipatskom terminologijom.

2.1 Sedam svjetskih čuda

Sedam svjetskih čuda jesu:

1. Velika piramida u Gizi (oko 2550. godina pr. Kr., Egipat)
2. Babilonski viseći vrtovi (oko 600. godina pr. Kr., današnje područje između Bagdada i Perzijskog zaljeva)
3. Fidijin kip Zeusa u Olimpiji (oko 440. godina pr. Kr., južna Grčka)
4. Artemidin hram u Efezu (oko 550. godina pr. Kr., današnja Turska)
5. Grobnica karijskog (Karija, maloazijska perzijska provincija) kralja Mauzola u Halikarnasu (oko 350. godina pr. Kr., današnji Bodrum, grad na obali Egejskog mora, Turska)

[1] Rhind – staroegipatski papirus kojeg je pronašao Aleksandar Henry Rhind, škotski krijumčar egipatskih relikvija, 1858. godine u ruševini manje građevine. Datiran je u vrijeme oko 1650. godine pr. Kr. iz XV. dinastije. Pismo kojim je pisano je hijeratičko. Od 1863. godine nalazi se u Britanskom muzeju.

6. Kolos s Rodosa (oko 280. godina pr. Kr., grčki otok Rodos)
7. Aleksandrijski svjetionik (oko 280. godina pr. Kr., Egipat).

3 Nastanak piramida i motivi gradnje

Premda se piramide nalaze na svim kontinentima svijeta, siguran razlog gradnji ostaje nejasan i nepoznat. Mnogi istraživači smatraju da postoji izgubljena povezanost između egipatskih piramida s piramidama u Južnoj Americi i Meksiku, s jakom asocijacijom da ih je gradio po značenju isti arhitekt [13].
Građene su uglavnom od kamena vapnenca dok su unutrašnje prostorije od granita. Blokovi na vrhovima su bili od granita ili bazalta obloženi zlatom, srebrom ili legurom zlata i srebra. Vanjske površine su bile polirane da bi bile vidljive iz daljine.
Nesuglasice o izvođenju riječi piramida/pyramis neznatne su u usporedbi s onima koje izaziva tumačenje svrhe postojanja samih piramida. Egiptolozi tvrde da su piramide grobnice. Peruolozi i drugi arheolozi koji istražuju u Srednjoj Americi, tvrde da su piramide bile *rezonatori* ili spremišta energije. Oni tvrde da se frekvencija zračenja zemlje, uključujući pravce magnetskih silnica i kozmičkih zračenja spajaju unutar piramidalne strukture stvarajući udarne frekvencije (na jednak način kao i što dvije tipke klavira, udarene skupa, stvaraju treću ili udarnu frekvenciju). Udarna frekvencija, smatraju, može stvoriti energetsko zračenje.

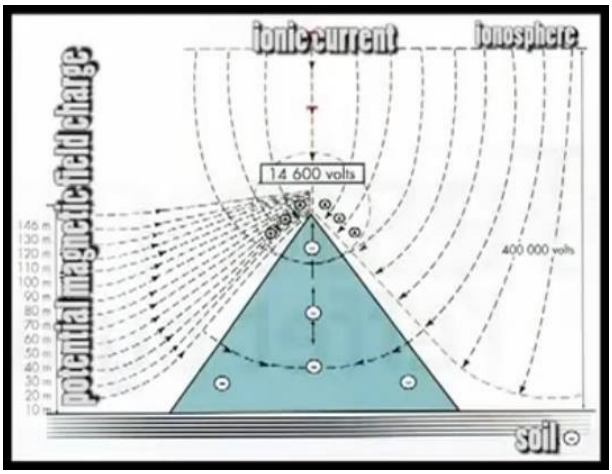

Slika 4: *Prikaz smjera djelovanja raznih sila na Veliku piramidu (Izvor: [15])*

Nameće se pitanje: za što je ta energija korištena i kako su arhitekti znali da se piramide mogu koristiti na takav način? Do danas na žalost ne postoje jednoznačni odgovori na gornja pitanja. U ovom članku ćemo se se bazirati na činjenicama koje se mogu povezati s matematikom i fizikom uz pomoć podataka koji su dobiveni geodetskom izmjerom.

3.1 Četvrta dinastija

Egipatska povijest dijeli se u dinastije. Od *Preddinastijskog* i *Ranodinastijskog perioda* (4. tisućljeće pr. Kr.) pa sve do perzijske vlasti i *Helenističko-rimskog perioda* (4. st. pr. Kr.), postojalo je ukupno trideset dinastija, kojima su vladali brojni vladari. Razdoblje u kojem su građene piramide se naziva *Staro egipatsko kraljevstvo* (2686. - 2181. pr. Kr). Drevni Egipat dostigao je civilizacijski vrh u tom razdoblju na području doline rijeke Nil. Ono obuhvaća vrijeme između treće i šeste dinastije. Period koji se odnosi na četvrtu dinastiju često je nazivan i *Zlatno doba*. Uobičajeno se smatra da je četvrta dinastija trajala od 2613. pr. Kr. do 2455. pr. Kr. Vladari/faraoni četvrte dinastije sastoje se od sedam generacija memfiskih kraljeva (Memphis – tadašnja prijestolnica, ruševine se nalaze 19 km južno od Kaira). O dinastijama Drevnog Egipta vidi u [7], [9] i [10].

Slika 5: *Na prikazu obiteljskog stabla plavim pravokutnicima su označeni faraoni, a imena kraljica crvenim. (Izvor: [29])*

Uz izgradnju triju piramida na platou Gize povezani su sljedeći vladari:
Kufu, **Sufis** ili punim imenom **Hnum-Kufu**; (2589. - 2566. pr. Kr.); najpoznatiji prema grčkoj inačici imena – **Keops**.
Iza navodnog vlasnika jednog od svjetskih čuda – Velike piramide u Gizi nije na žalost ostao nikakav prikaz. Tek se za jednu minijaturnu statuetu visine 5 cm smatra se da bi mogla prikazivati Keopsa. Za razliku od Keopsa, likovi nekih mnogo manje važnih vladara poznati su preko mnogih statua i slikarija. Tako je primjerice, Tutankhamona, faraona dječaka čije kraljevstvo nije ostavilo nikakva traga u povijesti, zbirka dragocjenosti iz njegove grobnice učinila simbolom faraonskog Egipta. Prema navodima jednog papirusa iz Novog kraljevstva Keops je sam izradio planove

za gradnju velike piramide u Gizi. Grčki povjesničar **Herodot** (484. - 424. pr. Kr.) govori o njemu kao tiraninu koji je s pomoću mnogobrojnih tisuća robova izgradio svoju piramidu.

Dždefra (Rađedef) (2566. - 2558. pr. Kr.)
Keopsov sin i nasljednik. Prvi faraon koji nosi titulu "sin Sunca" koja je od tada korištena u tradicionalnom faraonskom nazivlju do kraja egipatske povijesti. Smjestio je svoju kultnu *barku*[2] podno velike piramide. Njegova piramida ostala je nezavršena.

Kafra (Kefren) (2558. - 2532. pr. Kr.)
Pretpostavlja se da je on također bio Keopsov sin. Izgradio je drugu piramidu u Gizi, dok treća pripada kralju **Menkauri** (Mikerin) (2532. - 2503. pr. Kr.).

3.2 O lokaciji piramida

Velika piramida nalazi se na 30° sjeverne zemljopisne širine, na zapadnoj obali Nila na visoravni Giza, danas u predgrađu Kaira. Plato je dovoljno povišen kako kompleks ne bi poplavio nabujalim rijekama, a opet dovoljno blizu kako bi se prijevoz tereta mogao njima vršiti. Svako izlijevanje Nila "približilo" bi piramidu rijeci na udaljenost od nekoliko stotina metara. Drugi razlog izbora lijeve obale Nila jest čvrsti kameni fundament koji je mogao nositi čitav kompleks piramida. Ispitivanje tla i pronalazak čvrste kamene podloge zahtijevalo je nevjerojatno široko znanje iz mnogih područja vezanih s ispravnim geološkim procjenjivanjem.

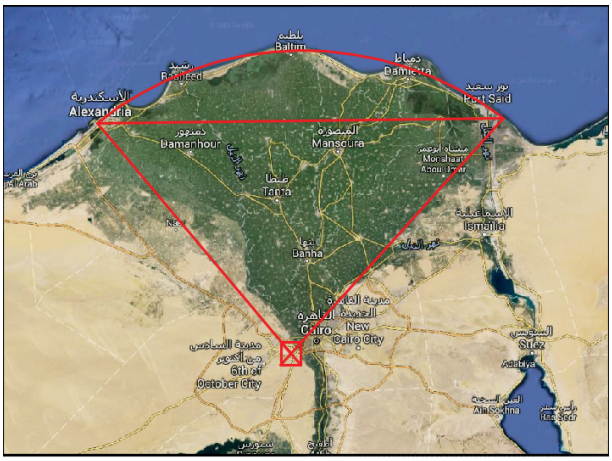

Slika 6: *Crvene linije prikazuju produljene dijagonale baze piramide; idealno zatvaraju deltu rijeke Nil (autori, u programu AutoCAD), (Izvor: [30])*

Osim toga egiptolozi, kartografi i ini istraživači uspostavili su niz odnosa, pravilnosti vezanih za njen geografski položaj. Navodimo neke od njih. Uzme li se vrh piramide za središte oko kojeg se opiše luk koji obuhvaća cijelo područje delte rijeke Nil, produžene dijagonale Piramide potpuno zatvaraju područje Delte (slika 6).
Kartografi navode: ako se pri određenoj projekciji piramida uzme kao središnja točka za iscrtavanje dviju međusobno okomitih linija na karti Zemlje, dobije se da su kopnena masa i oceani pravedno raspodijeljeni na četiri kvadrata (slika 7).

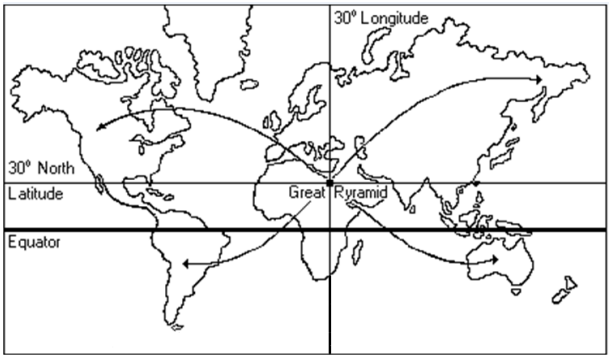

Slika 7: *Prikaz lokacije piramide s obzirom na ekvator (Izvor: [27])*

3.3 Plato - čišćenje i priprema za izgradnju

Nakon što je izabrano mjesto gdje će piramide biti izgrađene trebalo je očistiti velike količine pijeska i kamenja koji su pokrivali čvrsti kameni temelj, a zatim čitavo područje iznivelirati.
Poravnanje je toliko točno da Velika piramida odstupa od *savršene ravnine*[3], prema raznim autorima, u visinskom smislu oko 1,5 cm. U odnosu na dužinu do 230 m, pogreška od 1,5 cm zaista se može smatrati beznačajnom. Zaokruži li se 1,5 cm na 0,01 m dolazi se do izračuna da odstupanje iznosi 0,004 %. Ta se mala pogreška može vrlo lako mjeriti sa današnjim modernim tehnologijama i sofisticiranim uređajima.
Smatra se da je nivelacija izvršena urezivanjem brazdi u prirodnoj stijeni, nakon čega su punjene vodom. Tlo je tada brušeno sve dok nije postignuta jednaka razina s površinom vode.
Idući korak je bilo mjerenje područja kako bi se osigurala savršeno kvadratična baza i to duž osi sjever – jug odnosno istok – zapad. Napomenimo da je kompas u to doba bio nepoznat te da su graditelji na raspolaganju imali samo trokut i visak. Unatoč tome, Keopsova piramida bi rotacijom u

[2] Jedan od običaja pri pokopu faraona bilo je pohranjivanje barke u grobnicu. Taj je običaj bio povezan s vjerovanjem da će on nakon smrti putovati na barci nebeskim Nilom.

[3] Savršena ravnina u geodeziji bi predstavljala onu ravninu koja je paralelna s određenom nivo plohom. Nivo ploha je ploha koju možemo obići bez uspinjanja ili spuštanja i na kojoj je radnja sile teže za točkastu masu, koja se po njoj kreće, jednaka nuli. Ta ploha je u svim svojim točkama okomita na smjer vektora sile teže.

iznosu od svega 3 minute doživjela pomak koji bi joj osigurao idealan smještaj s obzirom na strane svijeta kao što se vidi na slici 8. Zbog toga se pretpostavlja da je egipatsko astronomsko znanje bilo izvan dosega znanstvenih ograničenja današnje civilizacije.

Slika 8: *Prikaz odstupanja piramide s obzirom na strane svijeta (nacrtali autori)*

4 Gradnja Velike piramide

4.1 Građevni materijal

Za potrebe izgradnje piramida dopremani su vapnenački blokovi iz kamenolomu u Turi, na istočnoj obali Nila, te blokovi granita iz blizine Asuana, dalje niz Nil.
Stručnjaci tvrde da su radnici u kamenolomu, radeći u malenim tunelima prokopanim duboko u ležište stijene, iskapali, klesali, cijepili, pričvršćivali klinovima i razbijali goleme kamene blokove. Nakon toga monolite su sjekli i glačali sve dok nisu dobili gotovo savršene kocke.
Međutim, ostaje otvoreno pitanje koji su alat pritom upotrebljavali. Vađenje tih golemih kamenih blokova, mase od dvije do sedamdeset tona, nije se moglo izvesti pomoću jednostavnog alata kojeg su arheolozi pronašli u kamenolomima. O tome postoji niz hipoteza, među kojima prevladava *teorija klina*.
Prema toj teoriji graditelji su dlijetom dubili rupe sve dok u njih ne bi mogli ugurati drveni klin. Drvo bi tada natopili vodom zbog čega se ono počelo širiti. Uslijed širenja nastala bi pukotina i taj kamen okružen klinovima bi se odvajao od stijene. Kao i sve ostale hipoteze, i ova ima svoje nedostatke i nedovoljno objašnjava način na koji su radnici u kamenolomu lomili kamen. Naime, svi alati su misteriozno nestali, ili su namjerno uklonjeni kada je sve bilo gotovo. To je tim čudnije s obzirom da je izgrađen velik broj piramida i upotrijebljeni su milijuni kamenih blokova (slika 9).

Slika 9: *Fotografija prikazuje kamene blokove pri osnovici Keopsove piramide (Izvor: autori)*

4.2 Transport kamenih blokova

Nakon odvajanja kamenih blokova slijedi problem transporta do odredišta. Stručnjaci tvrde da ih je bilo moguće transportirati jedino za vrijeme poplava Nila. Navodi se da su stotine, ako ne i tisuće ljudi na obali Nila vukli konopce koji su bili povezani s velikim brodovima te su tako usmjeravali brod na određeno mjesto.
Međutim, smatra se da je Egipćanima veći problem bio kopneni prijevoz. Pomicanje blokova po pijesku bio je zaista mukotrpna zadaća. Iako postoje nesuglasice o tome da li su u doba gradnje piramida Egipćani upotrebljavali kotač, odnosno vozila s kotačima, činjenica je da i ako su postojala, takva bi se vozila po pijesku prilično teško gibala. Jedini dokaz u tom smislu je slika u grobnici iz razdoblja pete dinastije u *Kemhesetu* u *Saqqari*, koja prikazuje *jurišne ljestve* na kotačima (slika 10).

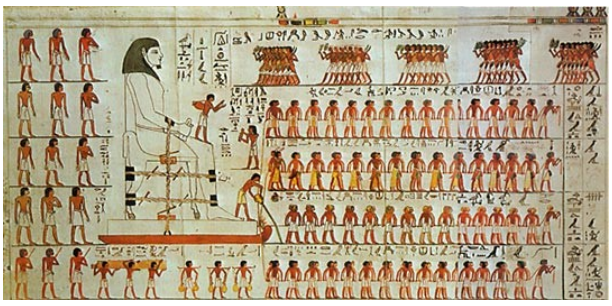

Slika 10: *Prikaz uporabe saonica ispred kojih se prolijevala voda ili ulje (Izvor: [25])*

Od raznih teorija koje se bave problemom transporta kamenih blokova našu je pažnju privukla ona koju je zastupao **Robert Nelson** (1794. - 1873.), znanstvenik iz New Jerseya. On je tvrdio da je na Nilu, negdje ispod kamenoloma, postojala brana zbog koje je u vrijeme poplava veliki dio zemlje pokrivala voda neznatne dubine od 90 do 120 cm. Takva je brana mogla ublažiti sve probleme plovidbe, dok je kontrolom njezine razine vodu bilo moguće dovesti

toliko blizu kamenoloma koliko je potrebno. Time bi se objasnilo postojanje školjki i drugih okamenjenih riječnih fosila pronađenih na različitim dubinama oko temelja Velike piramide. Nelson je nadalje tvrdio da je usporedno s rastom Piramide, područje bilo poplavljeno do visine potrebne za usklađivanje položaja brodova i Piramide. Kameni blok s broda bi jednostavno skliznuo na svoje mjesto. Može se uočiti sličnost između te tehnike i sistema kojim danas funkcioniraju brane. Ta teorija je toliko jednostavna da isključuje gradnju s pomoću kosih prilaza, potrebu za moćnim i složenim ručnim dizalima ali i teoriju saonica.
Zagovornik Roberta Nelsona u današnje vrijeme je inežnjer građevine **Chriss Massey**. Chriss Massey još pojednostavlja teoriju na način da iz funkcije izbacuje brodove te uvodi *plovke*. Plovak je napravljen od životinjskog tkiva koji je napunjen zrakom te pričvršćen za kamene blokove omogućuje plutanje bloka na površini vode (slika 11).

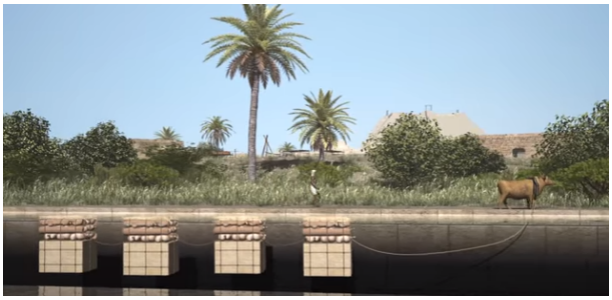

Slika 11: *Prikaz mogućeg prijevoza kamenih blokova rijekom Nil. Na kamenim blokovima se nalaze životinjska tkiva ispunjena zrakom. (Izvor: [31])*

4.3 Mogući načini gradnje

Način gradnje koji se primjenjivao u 4. dinastiji bio je složeniji, a time i neusporedivo zahtjevniji od onog prijašnjih piramida. Velika piramida zanimala je Herodota koji je Egipat posjetio u 5. stoljeću pr. Kr., vremenu koje bi približno odgovaralo 21. dinastiji, a to znači vremenu od barem 2000 godina nakon podizanja te fascinantne građevine. On u svom zapisu navodi jedan od mogućih načina gradnje piramide; pomoću sprava izrađenih od istesanih kratkih greda koje su služile za podizanje kamenih blokova sa stube na stubu te da je prvo bio dovršen vrh piramide pa ispod njega središnji dio koji leži na zemlji. Osim toga, u njegovom se zapisu prvi put spominje duljina gradnje. On je smatrao da je za dovršenje same piramide (bez ostatka kompleksa) bilo potrebno dvadeset godina (Hist. II. 125).
Gradnja piramida nastavlja se i u vrijeme pete i šeste dinastije, ali ona više veličinom i složenosti ni približno ne slijedi one piramide izgrađene za vrijeme ranijih dinastija. Za razliku od prijašnjih piramida novoizgrađene piramide ispisane su vjerskim tekstovima. Nakon toga, za vrijeme prijelaznog doba između starog i srednje kraljevstva gradnja piramida nestaje.

4.3.1 Poluga

Inženjer **Olaf Tellefsen** (1909. - 1990.) tvrdi kako Egipćani pri gradnji piramide nisu koristili rampe i saonice te da je za podizanje piramide bilo potrebno samo 3000 radnika. Tellefsen zasniva svoje argumente na promatranju trojice ljudi koji su pomicali veliki kamen prema obali Nila rabeći primitivan alat – polugu dugačku 6 metara. Uz pomoć poluge i valjaka podizali su blokove teške i to 2 tone. Tellefsen je zaključio da je posrijedi tehnička vještina koju su ljudi naslijedili iz prošlosti. Shodno tomu čitav je piramidalni kompleks mogao biti izgrađen uporabom poluge.

Kent Weeks i **I.E.S. Edwards**, poznati i priznati suvremeni egiptolozi, odbacuju Tellefsenovu hipotezu ostajući pri onoj nasipa, rampi i saonica. Svoje spoznaje baziraju na pronalasku rampi u blizini piramida, koje imaju zakošenje od 150°, što smatraju "iznimno pogodnim kutom za povlačenje blokova".

Važno je napomenuti kako mnoga arheološka nalazišta sadrže ostatke stare i nekoliko tisuća godina te da će u svjetlu otkrića *ugljika 14* (^{14}C)[4] određivanje njihove starosti biti podvrgnuto daljnjim ispitivanjima. Ipak, kako u [24] ističu Ines Krajcar Bronić et al., "*Treba naglasiti da se metodom ^{14}C određuje starost materijala, a ne predmeta koji je od tog materijala izrađen, Na primjer, ako se određuje starost drvenog kipa, ^{14}C metodom odredit ćemo vrijeme kad je drvo prestalo rasti, a ne kad je neki umjetnik izradio kip. Ovom bi se metodom uspješno mogli datirati različiti organski materijali,kao što su drvo, drveni ugljen, treset, bilje, žito, tkanine, kosti, stari do 60 000 godina. Tako se mogu odrediti i starosti sekundarnih karbonata (sige, sedra, jezerski i morski sedimenti), školjaka, koralja, itd.*"

4.3.2 Gradnja iznutra

Zanimljivu ideju o gradnji piramide prezentirao je francuski arhitekt **Jean-Pierre Houdin** (rođen 1951. godine), koji je pomoću 3D softvera razvijenog u *Dassault Systemes* (tvrtka koja se bavi razvojem 3D tehnologije) zaključio da je piramida građena pomoću spiralne rampe koja se nalazila unutar piramide, i još uvijek bi trebala biti tamo. Prema njemu, prva trećina piramide napravljena je vanjskom velikom rampom. U isto se vrijeme gradila i unutrašnja rampa, otprilike 3 metra široka i s nagibom od 7 %. Kako je piramida rasla i počela se raditi iznutra, korišteno je kamenje od kojeg je napravljena vanjska rampa.

[4] Ugljik 14 je radioaktivni izotop ugljika s jezgrom koja sadrži 6 protona i 8 neutrona. Prisutan je u ogranskim materijalima i osnova je za određivanje starosti organskog uzorka u arheologiji i geologiji.

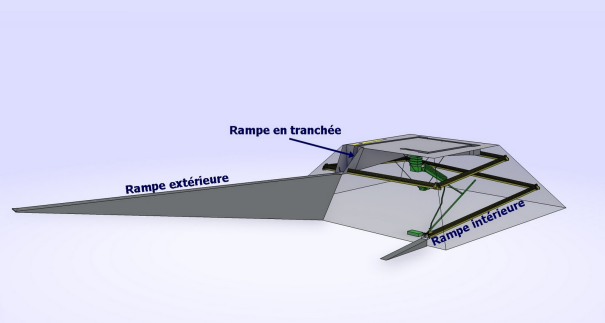

Slika 12: *Prikaz vanjske rampe koja je služila u izradi donjeg dijela piramide te unutarnje rampe koja je služila pri izradi piramide nakon što je vanjska rampa dosegnula nagib od 7° (Izvor: [16], [17])*

Prema Houdiniju, od samog su početka planirane tri komore u piramidi, na različitim razinama, pretpostavlja iz razloga kako bi Keops mogao biti dostojno pokopan u slučaju da umre tijekom gradnje. Prva je uklesana u samo postolje piramide, ispod razine tla, prije nego što je gradnja i počela. Zatim se počela raditi tzv. Kraljičina odaja, a deset godina iza nje i Kraljeva odaja, u samom srcu piramide. Tu je, na kraju, i položen Keopsov sarkofag.

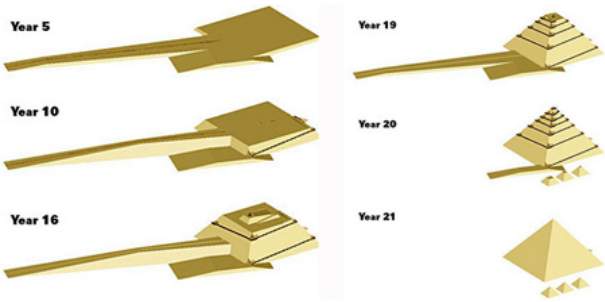

Slika 13: *Prikaz napredovanja gradnje piramide kroz godine (Izvor: [16])*

4.4 Broj ljudi i vrijeme koje je bilo potrebno za izgradnju piramide

Veliku piramidu je prema Herodotu gradilo 400 000 radnika. On pretpostavlja da su ljudi bili podijeljeni u četiri skupine a svaka je imala 100 000 ljudi i provodila je na gradilištu 4 mjeseca. Ako se ovaj broj prihvati kao točan treba imati na umu da tih 400 000 ljudi mora negdje biti smješteno, mora biti opskrbljeno hranom i pićem te imati sve potrebno za održavanje zdravstvene higijene. Međutim, nedostaje nalaz o ikakvoj strukturi ili građevini koja se koristila za smještaj tako velikog broja radnika. Postoji i mogućnost da radnici nisu živjeli na gradilištu nego da su tamo svakodnevno dolazili s drugog mjesta, što otvara pitanje načina prijevoza i dužine putovanja. Herodotov navod o 400 000 ljudi zaposlenih na izgradnji piramide osporavaju mnogi, jer bi, kako se smatra da je broj žitelja u Starom kraljevstvu bio između 1,5 i 2 milijuna značilo da je zdanje gradila 1/4 do 1/5 cjelokupne populacije. Stoga je 100 000 ljudi puno realniji broj.

Nekolicina autora smatra da su nakon gradnje piramide radnici pogubljeni kako ne bi otkrili tajne prolaze koji su vodili do grobne komore. To je pak većini arheologa neprihvatljivo jer bi se takvim skupnim pogubljenjima izbrisao velik broj žitelja.

Drugi slučaj u kojem su arheolozi demonstrirali svoju voljnost prihvaćanja Herodotovih tvrdnji je vezan za dvadesetogodišnje vremensko razdoblje gradnje piramide.

4.5 Provjera teorija gradnje

Japanci su se 1978. godine odlučili na sljedeći pothvat: podići piramidu visoku 18 metara pomoću metoda kojima su se navodno služili prvobitni graditelji piramida. U stvari su napravili ono što je trebalo učiniti puno ranije.

Tvrtka *Nippon Corporation* dobila je dozvolu egipatske vlade da na platou u Gizi, jugoistočno od Mikerinove piramide, sagradi mini-piramidu. Nisu smjeli upotrebljavati kamenje iz kompleksa u Gizi, a mini-piramida mogla je tamo ostati samo nekoliko dana nakon završetka gradnje. Nakon toga su je trebali potpuno srušiti i okolnom području vratiti prvobitan izgled.

Složivši se s postavljenim uvjetima, Japanci su se prihvatili vađenja kamenih blokova iz kamenoloma udaljenog oko 14 km i njihovog transporta do gradilišta. Blokove teške oko jedne tone nisu međutim uspjeli prevesti brodom preko Nila, to su učinili parobrodom; nisu ih mogli preko pješčane pustinje otpremiti do gradilišta, to su učinili helikopterom; grupe radnika pojedini blok nisu mogle podići više od pola metra, za to su se služili dizalicom.

Cijeli je projekt sniman, nakon čega je mini-piramida srušena. Pothvat što su ga poduzeli Japanci, pokazao je da su pretpostavke tradicionalnih istraživača o načinu gradnje vrlo upitne.

5 Prve geodetske izmjere piramide

5.1 Talesova izmjera

Vjeruje se da je grčki filozof, matematičar i astronom, **Tales iz Mileta** (624. - 547. pr. Kr.), bio prvi koji je točno izmjerio visinu piramide. Napravio je to pomoću užeta i njegove sjene, te je uveo i upotrijebio pojam omjera dužina.

Problem koji se javlja kod ovakvog mjerenja visine piramide je taj što dužinu sjene treba mjeriti od središta baze piramide. Tales daje rješenje i za taj problem (slika 14). S pomicanjem sjene piramide pomiče se i linija koja povezuje vrh sjene sa središtem baze piramide. Kada ta linija

bude paralelna sa osnovicom baze (na slici plave linije) dio sjene koji se nalazi unutar piramide bit će dug kao pola osnovice baze (stranica a). Vanjski dio se izmjeri i na taj način se izračuna koliko je visoka piramida (vidi [2]).

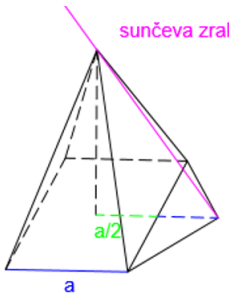

Slika 14: *Prikaz Talesovog načina izmjere visine piramide (nacrtali autori)*

5.2 Rezultati izmjera triju velikih piramida

Prve sustavne geodetske izmjere triju velikih gizaških piramida načinio je u drugoj polovici 19. stoljeća **Sir Flinders Petrie** (1853. - 1941.), glasoviti britanski arheolog i egiptolog te neumorni istraživač egipatskih starina, kojeg se drži "ocem egipatske arheologije". Njegove izmjere, dane tablicom 1, upućuju da su im osnovice strogo kvadratna oblika te da su precizno orijentirane prema glavnim stranama svijeta. Premda se piramide razlikuju po osnovnim dimenzijama one imaju bliske proporcije koje, za svaku od njih, najbolje karakteriziraju veoma ujednačeni prikloni kutovi njihovih trokutnih bočnih ploha i prikloni kutovi bridova plašta prema osnovici (α_0 i β_0) (vidi sliku 15).

Tablica 1: *Podaci prve izmjere provedene u drugoj polovici 19. stoljeća (Petrie)*

Strana	Duljina (m)	Kut otklona
Sjeverna	230.363	-3' 20"
Istočna	230.320	-3' 57"
Južna	230.365	-3' 41"
Zapadna	230.342	-3' 54"
Prosjek	230.348	-3' 43"

Britanski topograf **J. H. Cole** (1891. - 1963.), utemeljitelj modernog sustava triangulacije, je početkom 20. stoljeća sa svojim geodetskim timom izvodio višegodišnja opsežna mjerenja kompleksa u Gizi i proveo račun izjednačenja pogrešaka rezultata mjerenja.
U radu *Survey of Egypt*, Paper No. 39 objavljenom 1925. godine u Kairu, iznijeo je podatke o:

- prvobitnoj duljini stranice osnovice a_0,
- prvobitnoj visini h_0,
- pripadnom priklonom kutu α_0 bridova plašta prema osnovici, s pripadnim srednjim kvadratnim pogreškama za tri velike piramide.

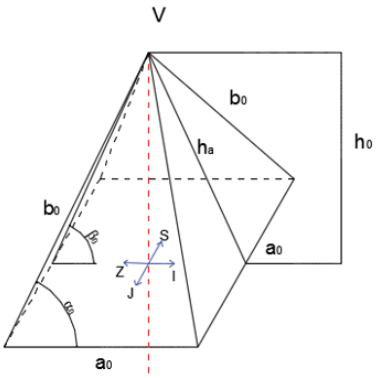

Slika 15: *Prikaz svih stranica i kutova piramide koji su mjereni u geodetskim izmjerama (nacrtali autori)*

S kojom zadivljujućom preciznošću je bila sagrađena Velika piramida na prethodno pomno poravnatom kamenitom platou najrječitije govore Coleovi podaci o izmjerenim vršnim kutovima njezine osnovice i njihovim malenim odstupanjima od pravoga kuta (tablica 3).
Podjednako su fascinantni i njegovi podaci o mjerenjima određenim prvobitnim duljinama, kutu otklona i ukupnom linearnom otklonu pojedinih stranica osnovice Velike piramide u odnosu na referentne geografske pravce sjever-jug i istok-zapad prema geografskim polovima određenim Zemljinom osi vrtnje (slika 8 i tablica 4).

Tablica 2: *Procijenjene prvobitne dimenzije i pripadni prikloni kutovi bridova plašta triju velikih gizaških piramida (Cole)*

Naziv piramide	Prva ili Velika	Druga	Treća
Kralj graditelj	Keops	Kefren	Menkaura
a_0 - stranica osnovice	230,36 ± 0,02 m	215,26 ± 0,04 m	105,50 ± 0,08 m
h_0 - visina piramide	146,72 ± 0,18 m	143,87 ± 0,33 m	65,55 ± 0,05 m
h - današnja visina	138,8 m	136,4 m	62,0 m
α_0 - prikloni kut plašta	51° 52' 00" ± 2"	53° 12' 00" ± 4"	51° 10' 30" ± 1' 20"
h_0/α_0	0,63692	0,66836	0,62133
$h_0/\alpha_0 = 1/2\tan a_0$	0,63691	0,66836	0,62131

Tablica 3: *Podaci izmjere vršnih kutova osnovice Velike piramide*

Kut osnovice	Izmjereni kut	Odstupanje od 90°
Sjeverozapadni	89° 59’ 58”	- 0’ 02”
Jugozapadni	90° 00’ 33”	+ 0’ 33”
Jugoistočni	89° 56’ 27”	- 3’ 33”
Sjeveroistočni	90° 03’ 02”	+ 3’ 02”

Ovi rezultati pokazuju da je osnovica Velike piramide, promatrana kao cjelina, neznatno zakrenuta u smjeru zapada, suprotno kazaljci na satu, za oko + 3’ 06” (aritmetička sredina kuta otklona).

1984. godine bazu Velike piramide mjere američki arheolozi **Mark Lehner** (rođen 1950.) i **David Goodman** (rođen 1947.). Uz samu izmjeru napravljena je i *geodetska mreža* (mreža koja se određuje tako da se odrede fiksne točke s poznatim koordinatama te se sva mjerenja vrše pomoću tih točaka) koja je služila za izmjeru cijelog Gizaškog kompleksa. Za ishodište mreže odabrano je središte baze piramide kojemu su dodijeljene koordinate (N 100 000, E 500 000). Tim postupkom je onemogućen prikaz koordinata u negativnom iznosu. Kako bi izmjera bila olakšana Lehner i Goodman su tražili karakteristične točke na bazi piramide na koje će se njihova izmjera vezati te tako olakšati potrebna prekobrojna mjerenja da bi se dobila ocjena točnosti mjerenja. Primjer je karakteristična točka koja se nalazi u SI uglu, 115,802 metara sjeverno od središta Velike piramide i 115,607 metara istočno od istog. S obzirom na njihovu notaciju, koordinate navedene točke bi imale vrijednosti *Northing* 100 115,802 i *Easting* 500 115,607. Mreža se može koristiti za područje koje se pruža u krugu od 100 kilometara oko Velike piramide.

Nakon što se izvrši pretvorba u koordinate geodetske mreže sa ishodištem u središtu Velike piramide može se upotrijebiti metoda *linearne regresije*[5] na podatke dobivene Lehner/Goodman izmjerom. To je zbog oštećenja nekih rubnih dijelova baze Velike piramide a naročito njene sjeverne strane pogodno za određivanje koordinata vrhova baze. Koristeći uz to i geometriju četverokuta i s obzirom na točnost mjerenja, pogreška koje se može javiti pri određivanju koordinata SI ugla iznosi 16×9 centimetara. Ako se ova pogreška želi svesti na minimum onda se treba pretpostaviti, kao što su raniji učinili Petrie i Cole, da je sjeverna strana paralelna južnoj te da je mjesto sjecišta dijagonale sa osnovicom pravo mjesto gdje se nalazio vrh baze. Rezultati Lehner/Goodman izmjere nakon primjene opisanog postupka na sve rubove baze Velike piramide prikazani su u tablici 5.

Tablica 5: *Prikaz rubova baze Velike piramide uz pomoć koordinate izvedenih iz mreže čije je ishodište smješteno u središte baze s koordinatama (N 100 000, E 500 000)*

Ugao	Northing	Easting	Pogreška (m)
SI	100115.288	500115.034	±.054
JI	99885.006	500115.262	±.093
JZ	99884.759	499884.954	±.060
SZ	100115.095	499884.645	±.050

Pomoću ovih podataka mogu se izračunati duljine stranice i pripadajući kutovi.

U tablicama 6 i 7 dana je usporedba Petrie-ove, Cole-ove i Lehner/Goodman-ove izmjere stranica i pripadnih kutova.

Tablica 4: *Podaci izmjere stranica osnovice Velike piramide i njihova otklona (znak “+” ispred kuta otklona ističe da se radi o pozitivnim smjeru vrtnje)*

Stranica osnovice	Duljina a_0	Najveća pogreška na krajevima	Kut otklona Δf	Otklon stranice $a_0 \times \Delta f$
S - sjeverna	230,253 m	6 mm na oba kraja	+ 2’ 30”	0,168 m
I - istočna	230,391 m	6 mm na oba kraja	+ 1’ 57”	0,131 m
J - južna	230,454 m	10 mm Z i 30 mm I	+ 5’ 30”	0,369 m
Z - zapadna	230,357 m	30 mm na oba kraja	+ 2’ 28”	0,165 m

[5]Postupak uklapanja funkcije (pravca, kojeg nazivamo *pravcem regresije*) u skup točaka koje predstavljaju određene podatke. Ta funkcija može služiti kao matematički model tih podataka i možda neće prolaziti ni kroz jednu točku, ali modelira podatke tako da u izvjesnom smislu njihova međusobna udaljenost bude sto manja. Ovakva metoda obrade eksperimentalnih podataka poznata je pod nazivom *metoda najmanjih kvadrata*.

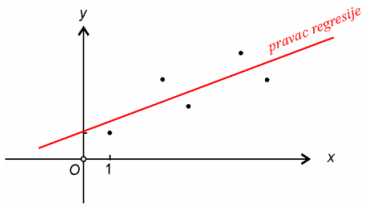

Tablica 6: *Prikaz rezultata svih izmjera stranica:*

Strana	←	**Lehner/Goodman**	→	**Petrie**	**Cole**	**Dorner**
	Min	Mean	Max			
Sjever	230.286	230.389	230.493	230.363	230.253	230.328
Istok	230.135	230.282	230.429	230.320	230.391	230.369
Jug	230.155	230.309	230.462	230.365	230.454	230.372
Zapad	230.227	230.337	230.447	230.342	230.357	230.372
Prosjek		230.329		230.348	230.364	230.360

Tablica 7: *Prikaz rezultata izmjere odstupanja kutova od 90°:*

Strana	←	**Lehner/Goodman**	→	**Petrie**	**Cole**	**Dorner**
	Min	Mean	Max			
Sjever	-1’ 19”	-2’ 52”	-4’ 25”	-3’ 20”	-2’ 28”	-2’ 28”
Istok	-1’ 12”	-3’ 24”	-5’ 36”	-3’ 57”	-5’ 30”	-3’ 26”
Jug	-1’ 24”	-3’ 41”	-5’ 58”	-3’ 41”	-1’ 57”	-2’ 31”
Zapad	-2’ 58”	-4’ 37”	-6’ 14”	-3’ 54”	-2’ 30”	-2’ 47”
Prosjek		-3’ 38”		-3’ 43”	-3’ 06”	-2’ 48”

6 Pokazuju li piramide kontinentalni pomak?

Provedene geodetske izmjere potrebno je povezati sa geologijom, znanošću koja se bavi proučavanjem Zemlje, koja pokušava objasniti kako je Zemlja oblikovana i kako se mijenja. Geolozi stoga mogu dati odgovor na pitanje može li kontinentalni pomak i tektonika ploča uzrokovati promjene na Platou u Gizi te jesu li oni uzroci odstupanja u orijentaciji Piramide?
Sa instrumentima i oruđem koje su imali na raspolaganju, stari su astronomi, geodeti i graditelji Velike piramide postigli točnost od 3.4 lučnih minuta prema sjeveru. Nakon 4000 godina astronomi s akademije *Academie Royale* su uspjeli odrediti način na koji će orijentirati opservatorij u Parizu 1667. godine, te su ga i prenijeli u prirodu tako da je taj opservatorij orijentiran s točnošću od 6 lučnih minuta, što je skoro dvostruko odstupanje od onog koje su postigli stari Egipaćani. Smatra se da je Velika piramida orijentirana savršeno točno te da je danas njezina minorno narušena orijentacija uzrokovana kontinentalnim pomakom i tektonikom ploča.
U nastavku će biti navedeni geološki procesi koji se zbivaju u prirodi i koji su mogli doprinijeti narušavanju orijentacije i promjene nagiba platoa na kojem se nalaze Egipatske piramide:

1. Tektonika ploča
2. Podizanje razine Sredozemnog mora
3. Potresi
4. Plimni valovi
5. Vulkanske erupcije
6. Gibanje Zemaljskog pola

Međutim, zbog položaja Platoa prema Sredozemnom moru, zapisa o posljedicama potresa, ne postojanju vulkana na području Egipta, pomaka geografskih koordinata uzrokovanih gibanjem Zemaljskog pola koji iznosi 31,1 lučnu sekundu kroz 4500 godina što je premalo da bi se uzelo u obzir, znanstvenici odbacuju pojave (2), (3), (4), (5) i (6).
Kontinentalni pomaci i praćenje tektonike ploče je vrlo kompliciran i zahtjevan zadatak. Objašnjenje tih procesa i razne teorije preopširne su da budu objašnjene u ovom radu. S tim u vezi navest ćemo samo neke rezultate vezane za mogući pomak sjeveroistočnog dijela Afričke ploče na mjestu gdje se dotiče sa Euroazijskom i Arapskom pločom, područja na kojem se nalazi Velika piramida.
Pomak tektonskih ploča za određenu točku na zemljinoj površini određuje se uz pomoć raznih metoda geodetskih mjerenja. Najčešće se upotrebljavaju: Satelite Laser Rangig (SLR), Very Long Basiline Interferometry (VLBI) i Global Position System (GPS), tj. globalni navigacijski satelitski sustavi (GNSS). Pretpostavlja se da je kretanje tektonskih ploča pravilno i predvidivo, osim na području gdje se javljaju česti potresi i vulkanske erupcije koje uzrokuju neravnomjeran pomak ploča u određenom periodu, što ovdje nije slučaj.
Razna mjerenja su obavljana od strane američkih istraživača koji su uz pomoć GPS tehnologije promatrali pomake na području Egipta u razdoblju od 1994. do 1997. S obzirom na brzinu gibanja Afričke ploče od $5-6\pm2$ mm/god., došli su do zaključka da pomak Platoa

tijekom 4500 godina nema skoro nikakav značaj na horizontalni i vertikalni pomak piramide.

Rotacija Afričke ploče bi mogla imati puno veći utjecaj na orijentaciju piramide. Ako se računa rotacija ploče pomoću HS2 - NUVEL 1 modela za traženo područje dobiva se rotacija od 58.32" odnosno 0.0162° u smjeru istok-zapad u periodu od 4500 godina. Ako se ovi rezultati primijene na sadašnji položaj Velike piramide oni skoro pa neće imati nikakav utjecaj. To znači da je Velika piramide izgrađena sa malim odmakom od idealne orijentacije u prostoru ili da je izgrađena puno ranije nego što mnogo raznih egiptologa i istraživača tvrdi.

Ako se pretpostavi da se Afrička ploča rotira jednolikom brzinom i ako se pretpostavi da je Velika piramida bila savršeno točno orijentirana u prostoru kada je izgrađena, onda se pomoću ovih podataka dolazi do zaključka da je piramida sagrađena prije 24700 godina.

7 Analiza unutrašnje strukture

Ulaz u Piramidu nalazi se na sjevernoj strani, nešto više od 17 metara iznad površine zemlje i 7 metara od sredine osnovice baze. Smješten je u devetnaestom od ukupno 203 reda, koliko ih Piramida danas ima. Ulaz prelazi u silazni hodnik pod kutom od 26° 28' 24". Silazni hodnik visok je oko 1,20 metara i širok metar, a njime se prelazi udaljenost nešto veća od 104 metra. Otprilike prva njegova četvrtina prolazi kroz Piramidu, dok je ostatak oko 78 m probijen kroz čvrstu stijenu po kojoj Piramida počiva. Silazni hodnik nakon toga ide vodoravno nekih 9 m, te na kraju ulazi u podzemnu dvoranu. Podzemna dvorana nalazi se otprilike 30 m ispod površine zemlje, odnosno osnovice Piramide, a po površini je veća od svih ostalih. Dugačka je oko 8 m, široka 14 m, a visoka nešto više od 4 m. Ulaz u dvoranu je u donjem istočnom uglu sjevernog zida.

Najpopularnija hipoteza o namjeni podzemne dvorane kaže da je ona prvobitno trebala poslužiti kao pogrebna komora. Međutim, izgleda da su arhitekti od toga odustali, primjerice zbog neizdrživih fizičkih uvjeta i nedostatka zraka na mjestu na kojemu je trebalo iskopati potreban niz dvorana, kao i zbog moguće opasnosti od poplave. Dvorane i hodnici napravljeni su u samom tijelu Piramide, na različitim razinama. To bi moglo objasniti nedovršeni izgled podzemnog kompleksa kao i namjera da se moguće pljačkaše navede na krivi zaključak da unutrašnjost piramide nikada nije dovršena i da ih se odvrati o potrage za blagom.

Smatra se da je s istom svrhom ulaz u uzlazni hodnik skriven u stropu silaznog hodnika, tridesetak metara od ulaza u Piramidu. Kut nagiba uzlaznog hodnika identičan je kutu silaznog i iznosi 26° 28' 24". Uzlazni hodnik sastoji se od dva dijela, jedan dužine 18 m a drugi, širine oko 1 m i visine 1.1 m, 33.5 m i završava raskrižjem.

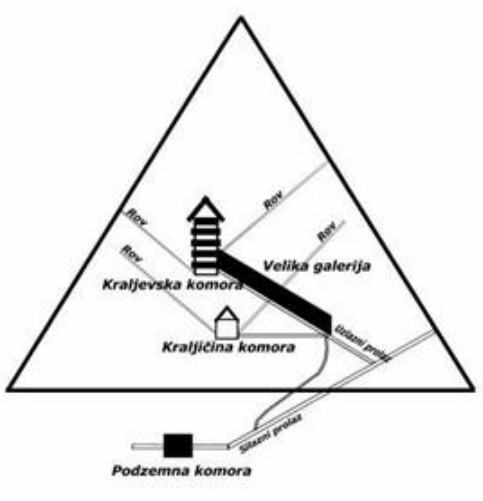

Slika 16: *Prikaz presjeka Velike piramide (Izvor: [26])*

Na raskrižju započinje vodoravni hodnik dugačak 40 m i širok oko 1 m, koji završava na dnu istočnog kuta sjevernog zida Kraljičine dvorane, dugačke gotovo 6 m i malo šire od 5 m. Ta se dvorana nalazi točno ispod vrha Piramide, u ravnini s dvadeset i petim redom. Strop dvorane napravljen je od kosih blokova, čiji kut nagiba iznosi oko 30° 30'. Ukupna visina od poda do vrha krovnog zabata Kraljičine dvorane je nešto više od 6 m.

Jedna od zanimljivosti Kraljičine dvorane su dva kanala, pretpostavlja se za zrak, jedan u sjevernom i drugi u južnom zidu. Isklesani su u kamenim blokovima i naglo završavaju, ostavljajući još 12 cm zida. Kanali su pravokutnog oblika sa stranicama dugačkim 21.5 cm × 20 cm.

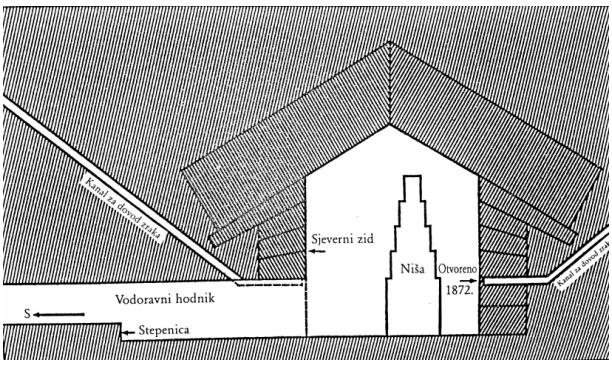

Slika 17: *Prikaz presjeka Kraljičine dvorane (Izvor: [14])*

Na izlazu iz vodoravnog hodnika počinje se protezati velika galerija koja je za razliku od drugih hodnika visoka 8.6 metara te 46.68 metara duga. Ona vodi do kraljeve odaje. Kraljeva odaja, kao najviša od postojećih triju, s visinom od 5.85 m, proteže se 10.47 m od istoka prema zapadu te 5.23 m u smjeru sjever-jug. Na visini od jednog metra nalaze se dva okna koja vode prema vanjskim stranama piramide, njihova svrha je prema vjerovanjima Starih Egipćana

je putokaz prema zvijezdama koji olakšava odlazak u drugi svijet. Strop u kraljevoj odaji posebno je ojačan koso postavljenim kamenim pločama radi velike težine piramide. Tako ojačan strop daje sigurnost Kraljevoj odaji i smanjuje mogućnost savijanja. U kraljevoj odaji pronađen je sarkofag koji po vjerovanjima pripada vladaru Keopsu.

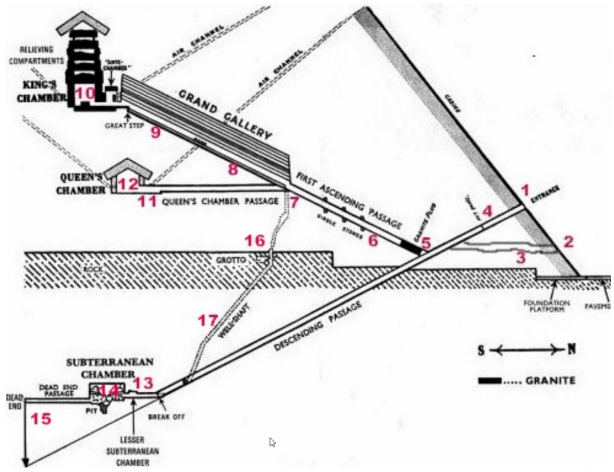

Slika 18: *Prikaz otvora Kraljičine dvorane (odaje) koje je otkrio Rudolf Gantenbrik (Izvor: [23])*

8 Svrha gradnje piramide; od enciklopedije izgubljenog znanja do elektrane

Proučavajući literaturu o starom Egiptu ([1], [4], [11]), nailazi se na mnogo različitih tumačenja svrhe gradnje piramida. Svoje su ideje branili stručnjaci raznih područja, pisci, ali i mistici i vidovnjaci. Oni ovdje neće biti ponaimenice navedeni, već će biti iznesene neke od njihovih ideja.

Osim uobičajenog stava egiptologa, prema nekim autora piramide su podignute prije više od 10 000 godina te nisu izgrađene kao grobnice nego kao spremišta povijesti čovječanstva od samog početka pa sve do danas; povijest je zapisana jezikom matematike, geometrije i astronomije, a Velika piramida predstavlja kroniku prošlosti, sadašnjosti i budućnosti.

Zagovornici hipoteze da Egipćani nisu podigli Veliku piramidu to pak potkrepljuju činjenicom da su unutarnji zidovi bez natpisa, slika i drugog simbolizma obično povezanog s fino izrađenom kraljevskom dekoracijom.

Zamisao da su drevni Egipćani imali nekakvu vrstu električne rasvjete, povezana je sa zagonetkom kako su ljudi duboko u podzemlju mogli oslikavati zidove bez baklji, bez da je ostalo tragova čađe. Objašnjenje da su koristili komplicirani sustav ogledala mnogi uzimaju za neostvarljivo. Više o pretpostavci da je Kraljeva odaja bila srce elektrane u Gizi i razna objašnjenja s tim u vezi mogu se naći na primjer u knjizi Christofera Dunna: *The Giza Power Plant* [21].

9 Konstante povezane s piramidom

9.1 Veza s astronomijom

Do kraja 19. stoljeća sakupila se velika i zanimljiva zbirka povezanosti raznih izmjera piramida s astronomijom. Smatramo da te poveznice mogu biti prilično subjektivne jer svaka veličina u prirodi može biti prikazana na puno raznih načina iz kojih se mogu izvući fascinantni zaključci. Bez obzira na našu sumnju u objektivnost pri takvom zaključivanju mišljenja smo da se u radu o Velikoj piramidi uspostavljene veze ne smije zaobići.

Slijedi prikaz dijela podataka koji se mogu pronaći u literaturi ([1], [14], [22]):

1. Dužina stranice osnovice koja iznosi 9131 palac (palac – 2,54 cm) podijeljena s jednim laktom (25 palaca) iznosi 365.24, što je broj dana u solarnoj godini.

2. Opseg kruga čiji je promjer dužina predvorja kraljeve odaje (116.25 palaca) iznosi 365.24 palca.

3. Širina Kraljeve dvorane (206.066 palaca) pomnožena s kvadratnim korijenom broja π iznosi 365.24 palca.

4. Dvostruka dužina Kraljeve dvorane (412.12 palaca) izmjerena na podu Velike galerije od te se udaljenosti vertikalno uzdiže 365.24 palca.

5. Zbroj svih stranica osnovice jednak je broju dana u stoljeću.

6. Ukupan broj palaca svih stranica trideset i petog reda jednak je broju dana u 80 solarnih godina.

7. Dvostruka dužina osnovice (2×9131.26 palaca) jednaka je broju godina u precesiji ekvinocija i, osim toga, ukupnom broju palaca svih stranica pedesetog reda;

8. Zbroj dužine i visine Kraljeve dvorane podijeljen s njezinom dužinom jednak je broju π.

9. Zbroj dužine i širine sarkofaga pronađenog u Kraljevoj odaji, podijeljen s njegovom visinom jednak je broju π.

10. Velika piramida je savršeni kalendar koji pokazuje godišnja doba i funkcionira poput ogromnog Sunčevog sata čija sjena, između ostalog, označava solsticije i trajanje godine.

11. Ako označimo da je osnovica baze piramide ekvivalentna ekvatoru tada se u vrhu piramide nalazi središte mjeseca koji je smješten na površini Zemlje (slika 19).

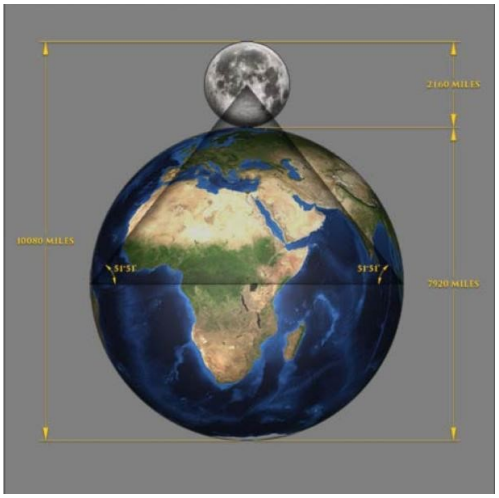

Slika 19: *Prikaz piramide kao spojnice Zemlje i Mjeseca (Izvor: [19])*

9.2 Zlatni broj Fi (φ) i broj Pi (π)

9.2.1 O zlatnom rezu i Fibonaccijevim brojevima

Zlatni rez, koji se još naziva zlatna sredina, božanski ili zlatni omjer je matematičko-strukturalna konstanta koja se najčešće veže za umjetnost. Smatra se jednom od temeljnih konstanta matematike, čiju nam važnost opisuje i citat slavnog njemačkog znanstvenika Johannesa Keplera: "Geometrija posjeduje dva blaga: jedno je Pitagorin teorem, a drugo zlatni rez. Prvo se može usporediti s čistim zlatom, a drugo s draguljem neprocjenjive vrijednosti."
Geometrijski, *Zlatni rez je način podjele neke mjerljive veličine, na primjer odsječka AC, tako da omjer između većeg i manjeg dijela bude jednak omjeru između njihova zbroja i većeg* (slika 20).

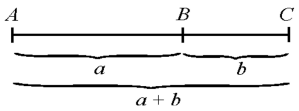

Slika 20: *Prikaz Zlatnog reza*

Ako je B točka koja u omjeru zlatnog reza dijeli AC i ako je $AB = a$, $BC = b$ onda je po definiciji

$$\frac{a}{b} = \frac{a+b}{a}. \tag{1}$$

Sređujući (1) dobivamo $a^2 = ab + b^2$, odakle dijeljenjem s b^2 slijedi

$$\left(\frac{a}{b}\right)^2 - \frac{a}{b} - 1 = 0, \tag{2}$$

tj.

$$x^2 - x - 1 = 0.$$

Nepoznanica $x = \frac{a}{b}$ iznosi $\frac{1+\sqrt{5}}{2} = 1,6180...$ za pozitivan, odnosno $\frac{1-\sqrt{5}}{2} = -0,6180...$ za negativan korijen. Osim toga, rješenja su do na predznak recipročna: $0,6180... = \frac{1}{1,6180...}$.
Omjer zlatnog reza obično se simbolički označava grčkim slovom φ. Tako je

$$\varphi^2 - \varphi - 1 = 0 \quad \text{ili} \quad \varphi^2 = \varphi + 1.$$

Množenjem obje strane proizvoljan broj puta s φ dobije se

$$\varphi^n = \varphi^{n-1} + \varphi^{n-2}, \tag{3}$$

što zlatni rez povezuje s nizom ***Fibonaccijevih brojeva***.
U matematici, Fibonaccijevi brojevi oblikuju niz definiran *rekurzivnom funkcijom* (funkcija kojoj se definirajuća funkcija primjenjuje unutar definicije):

$$F(n) := \begin{cases} 0 & \text{ako je } n = 0 \\ 1 & \text{ako je } n = 1 \\ F(n-1) + F(n-2) & \text{ako je } n > 1. \end{cases} \tag{4}$$

Dakle, nakon prve početne vrijednosti, svaki sljedeći broj je zbroj dvaju prethodnika. Dobivamo tako redom

$$0, 1, 1, 2, 3, 5, 8, 13, 21, 34, 55, 89, 144, ... \tag{5}$$

Lako je sada uočiti da se svojstvo (3) koje generira geometrijski niz

$$1, \varphi, \varphi^2, ..., \varphi^n, ... \tag{6}$$

nalazi i u Fibonaccijevom nizu (5), za $n > 0$. Naime, količnik svakog člana niza (5) i njemu prethodnog člana teži veoma brzo ka φ. Vrijednosti osciliraju oko idealne veličine:

$$\frac{3}{2} < \frac{8}{5} < \frac{21}{13} < ... < \varphi < ... < \frac{34}{21} < \frac{13}{8} < \frac{5}{3}.$$

Koliko je brzo asimptotski dostižu najbolje se vidi iz

$$\frac{55}{34} = 1,6176... < \varphi < \frac{89}{55} = 1,6181...$$

9.2.2 Ludolfova konstanta π

Arhimedova[6] ili **Ludolfova**[7] **konstanta** π (pi) najčešća je konstanta koja se javlja u matematici i prirodnim znanostima. Od njenih mnogobrojnih definicija izdvajamo sljedeću: π *je omjer opsega kruga i njegovog promjera*.
Broj π je *iracionalan* broj, što znači da se ne može prikazati u obliku razlomka čiji je brojnik cijeli, a nazivnik prirodni broj. Njegov decimalni prikaz je stoga beskonačan i neperiodičan:

$$\pi = 3,14159265358979... \tag{7}$$

Danas, uz pomoć računala, broj točno izračunatih decimala vrtoglavo raste. Na primjer, 2013. godine je broj točnih znamenaka iznosio dvanaest tisuća milijardi. Ipak, sve do pojave računala su pokušaji izračuna broja π davali aproksimacije koje su relativno sporo konvergirale prema točnom decimalnom prikazu.
Tako se prvi pokušaji javljaju u starom Egiptu; zabilježeno je da se u 17. st. pr. Kr. za spomenuti omjer rabio broj 3,16049. Njegova pogreška točnosti je unutar 1 % i vrlo je mala za dostupne alate računa tog doba. Sljedeću bolju aproksimaciju osmislio je Arhimed oko 280. godine pr. Kr. Upisivao je i opisivao poligone unutar i izvan jedinične kružnice, čime je dobio, iako grubu, donju i gornju granicu za površinu kruga. Iz toga je zaključio sljedeće:

$$\frac{223}{71} < \pi < \frac{22}{7}, \quad \text{tj.} \quad 3,1408 < \pi < 3,1429.$$

Točnost na 2 decimale postiže se tek za $n = 96$, dok je $n = 1000$ potrebno za 3. Veći skok u izračunu broja decimala zabilježen je krajem šesnaestog stoljeća: **Ludolph van Ceulen** je izračunao π na 35 decimala, a potom u osamnaestom stoljeću: **William Hanks**, 707 decimala. Kao zanimljivost navedimo da je samo prvih 528 od 707 znamenaka točno.
Od 1988. broj π ima i svoj dan, 14. ožujka (3.14 u engleskoj notaciji).
Više o zlatnom rezu i općenito o matematičkim konstantama može ne naći npr. u [3], [6], [12].

9.3 Pi i Fi u izmjerama

John Taylor (1781. - 1864.) je bio engleski izdavač, esejist i pisac. U knjizi *The great pyramid; why was it built & who built it?* (1859.), Taylor tvrdi da su broj π i zlatni rez namjerno uključeni u dizajn Velike piramide u Gizi. On je do svojih zaključaka došao temeljem analize jednog Herodotovog knjiškog zapisa.
Njegove teorije je zatim proširio **Charles Piazzi Smyth** (1819. - 1900.), talijansko-škotski astronom poznat po mnogim inovacijama u astronomiji i po svojim mjeriteljskim studijama.
Prva teorija Johna Taylora vezana uz mjere Velike piramide glasila je da je njezina ukupna visina jednaka dvostrukoj dužini osnovice, pa je nagađao da se to nalazi u izravnoj vezi s odnosom dijametra prema obujmu kruga. U oba slučaja dobiva se broj 3,141592... Ta se vrijednost može objasniti i na drugi način – da se visina piramide prema dvostrukoj dužini osnovice odnosi kao 1 naprama 3,14159...
Na temelju ove pretpostavke Taylor je dobio kut nagiba od 51° 51' 14.3" koji se obično naziva π *kutom* ili *idealnim kutom*. Usporedbom idealnog priklonog kuta plašta Velike piramide sa srednjom vrijednošću određenom Coleovim izmjerama (Tablica 1) očita je gotovo savršena podudarnost. Razlika među njima je u tehničkom smislu beznačajna i iznosi neznatne 2' 22", što uvjerljivo govori koliko su tijekom njezine gradnje bili pedantno vođeni prikloni kutovi ploha i bridova prema zadanoj geometrijskoj proporciji. Pokazalo se da vrijednost broja π postoji samo kod Velike piramide i nije pronađena niti kod jedna druge piramide u Egiptu.
Niz pitanja javlja se oko značenja spomenute vrijednosti broja π. Pojavljuje li se ona slučajno ili ne? Je li on ili ona izrazio/la svoju mudrost i poznavanje broja π uključivši ga u geometriju Piramide? Ako se broj π pojavljuje tek slučajno ili kao izračunata konstanta tada ne bi trebali očekivati da će se on ponovno pojaviti kod bilo koje druge dimenzije Velike piramide. Međutim, to je uistinu potvrđeno, ne jednom već mnogo puta.
Jedan od takvih slučajeva odnosi se na izračunavanje volumena granitnog vratnog krila koje se nalazi u predvorju Kraljeve dvorane. Visina od 48.57 palaca (1.23 m) puta debljina od 15.7 palaca (0.40 m) puta širina od 41.2 palca (1.05 m) podjeljeno s 10 000 daje broj od 3.1417 što je približno jednako broju π. U ovom slučaju su ostavljeni palci budući da se kod prenošenja u metrični sustav ne dobivaju iste vrijednosti, a mjerne jedinice starih Egipćana nisu bile izvedene iz metričnog nego iz "prirodnog" sustava (lakat, palac, stopa itd...).
Za drugu potvrdu pojave broja π zaslužan je Piazzi Smyth. On ga je izveo iz visine trideset i petog reda Piramide podijeljene s desetinom vodoravne udaljenosti od te točke do vertikalne osi. Do tog je proračuna došao promatranjem debljine građevnog kamenja. Piramida je građena vodoravnim nizovima kvadratnih kamenih blokova čija debljina kod osnovice iznosi oko 1.27 m. Kako se Piramida, niz po niz, uzdiže u visinu, debljina kamenih blokova smanjuje se do 0.68 m u trideset petom redu. Tada, u trideset i šestom redu, dolazi do iznenadnog povratka na debljinu od 1.27 m, koja uglavnom ostaje takva u preostalim redovima. Zbog

[6] Arhimed (3 st. pr. Kr.), grčki matematičar, fizičar i astrolog
[7] Ludolph van Ceulen (1540. - 1610.), njemački matematičar

toga je Smyth procijenio da je tridest i peti red vrlo znakovit te je, izmjerivši vodoravnu udaljenost od njega do središnje osi Piramide, otkrio da ona iznosi 3652.42 stope ili broj dana u godini pomnožen s deset.
Osim broja π u Veliku piramidu je uključen i broj Fi (φ), tj. zlatni broj. Zabilježeno je da su svećenici iz Egipatkog hrama Herodotu rekli da je Velika piramida oblikovana tako da površina bilo koje strane bude jednaka kvadratu visine. Matematičari su pojednostavili odnose u Velikoj piramidi jednostavno ju povezavši s pravokutnim trokutom čija osnovica ima jediničnu dužinu jedan, visina kvadratni korijen od φ, a hipotenuza φ (slika 21).

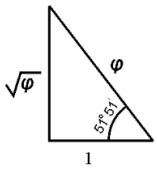

Slika 21: *Prikaz pravokutnog trokuta s π kutom čija osnovica ima jediničnu dužinu (nacrtali autori)*

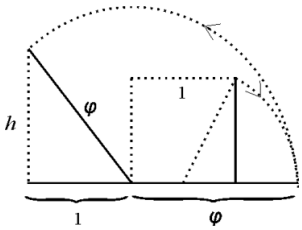

Slika 22: *Geometrijska konstrukcija zlatnog reza i veza s visinom h velike piramide (nacrtali autori)*

Većina egiptologa je složna oko tvrdnje da su Egipćani u potpunosti razumjeli trigonometrijska svojstva Pitagorinog trokuta, te da su proporcije Velike piramide određene vrijednostima brojeva π i φ. Oni isto tako tvrde da su brojni umjetnički prikazi oblikovani i izvedeni uz namjerno uključivanje tih brojeva, te i dalje aktivno tragaju za drugim mogućim odnosima.
Na primjer, da je visina Velike piramide pomnožena s 10^9 jednaka točnoj udaljenosti Zemlje od Sunca, često je ponavljana i pisana tvrdnja. Međutim, iz samog izričaja ove tvrdnje jasno je da ona ne vrijedi. Dokaz tome je što Zemlja oko Sunca putuje po eliptičnoj putanji tako da ova vrijednost može biti prosječna ili srednja udaljenost. Zato bi, da bude točna, spomenuta tvrdnja trebala glasiti ovako: Visina Velike piramide pomnožena s 10^9 i pretovrena u milje jednaka je prosječnoj srednjoj udaljenosti Zemlje od Sunca. Ova zanimljiva veza također je potvrđena i kod drugih izmjera Velike piramide. Neki autori navode da se ta udaljenost točnije dobiva iz nacrta osnovice prije nego iz visine Velike piramide. Smyth kaže da se spomenuta vrijednost također može dobiti ili tako da se visina trdeset i petog reda kamenih blokova pomnoži s 10 ili tako da se dužina predvorja pomnoži s 100.
Kamen smutnje pri određivanju mjera Velike piramide su i *piramidni* (sveti) *lakat* i *piramidni palac*. Profesor Smyth potaknuo je uvođenje piramidnog lakta i piramidnog palca kao standardne jednice u mjernom sustavu Velike piramide. Ustanovio je da je 999 piramidnih palaca jednako 1000 standrardnih palaca. Na isti je način izračunao da je mjerna jedinica upotrijebljena pri oblikovanju i izgradnji Velike piramide bila lakat koji ima 25 piramidnih palaca. Kod navođenja mjera iz praktičnih je razloga najbolje uzeti da Piramidni palac odgovara standardnom.

10 Izrada 3D modela piramide

U sklopu izrade diplomskog rada [5], autor je izradio 3D model piramide koji je poslužio kao stvarno predočenje građevine u mjerilu kako bi se dobio dojam o odnosu duljine stranica i visine piramide.
Model piramide je u mjerilu 1 : 1150 zbog nemogućnosti printanja stranice veće od 20 cm (slika 23).

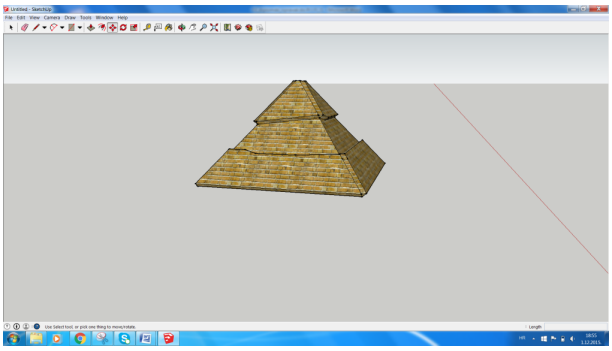

Slika 23: *Prikaz konačnog oblika piramide (Modelirano upotrebom programa SketchUp 2015)*

11 Zaključak

Keopsova piramida jedna je od najvećih misterija svijeta koju znanstvenici pokušavaju riješiti već više od 2000 godina. Mnogi tvrde da znaju što predstavlja ta monumentalna građevina te na koji je način građena. Fascinantna je činjenica koja govori kako je Velika piramida preživjela sve svjetske katastrofe i da dan danas još ponosno stoji na svom mjestu bez nekih značajnih oštećenja.
Provedena je jedna studija za potrebu koje je napravljena replika piramide od kartona i u koji je postavljen žilet za brijanje. Svaki dan nakon upotrebe žileta istraživač je preko noći ostavljao isti u maketi piramide, a ujutro je taj isti žilet izgledao kao da nije niti korišten. Pokušavao je to objasniti pomoću magnetnog polja koje djeluje na piramidu, ali nikada nije uspio znanstveno to i dokazati. Takvih i sličnih pokušaja je bilo mnogo, ali niti jedan nije dao

rezultate koji mogu potvrditi pravi razlog građenja piramide i opisati sve sile koje na nju djeluju.
Međutim, nema nejasnoća kada su u pitanju brojevi koji se pojavljuju u analizi. Oni su dobiveni na bezbroj različitih načina i omjera i uvijek su isti, a to su broj π i Zlatni broj φ. Broj π je u prvotnim izmjerama prikazan kao 3,16 te varira u svom iznosu zbog mjernih jedinica koje su korištene pri gradnji piramide. Vjeruje se da su Egipćani za izradu piramide imali nešto malo drugačije mjerne jedinice nego danas i postoji puno hipoteza koje vuku poveznicu između tadašnje jedinice palac i današnjeg shvaćanja istog. Uspije li se odgonetnuti kojim mjernim jedinica su se služili graditelji i koliko one iznose, taj bi korak zasigurno pomogao u razotkrivanju tajni koje se kriju u dimenzijama Velike piramide.

Dozvolit ćemo si ovdje spomenuti staru tvrdnju koja kaže: "Iako se piramide nalaze u Egiptu, to ne znači da su i egipatske." Može li to ukazivati na činjenicu da je u Egiptu postojao utjecaj neke naprednije civilizacije, zaslužne za izgradnju Velike piramide? Radi se o često postavljanom pitanju, na koje treba pronaći odgovor. Taj je odgovor iznimno značajan, budući da može dovesti do konačnog rješenja brojnih tajni vezanih uz njeno postojanje.

Literatura

[1] R. BUVAL, A. GILLBERT, *Zemlja Ozirisova; Razotkrivanje zagonetke piramida*, Mozaik knjiga, Zagreb, 2003.

[2] B. ČEKRLIJA, *Vremeplovom kroz matematiku*, Laktaši, Grafomark, 2000, http://www.antonija-horvatek.from.hr/povijest-matematike/Vremeplovom-kroz-matematiku-Boris-Cekrlija.pdf (pristupljeno 23. 10. 2016.)

[3] M. GHYKA, *Filozofija i mistika broja*, Književna zajednica Novog Sada, 1987.

[4] H.W. JANSON, A.F. JANSON, *Povijest Umjetnosti*, Stanek, Varaždin, 2013.

[5] B. JANJANIN, *Analiza izmjere Keopsove piramide*, diplomski rad, Geodetski fakultet, Sveučilište u Zagrebu, 2015.

[6] D. KUŠAR, The Golden Section and the Origin of this Name, *Journal for Geometry and Graphics* **11**(**1**) (2007), 83–92.

[7] MANETHO, *Od Sincela prema Eusebiju (fr.7, 12) i Afrikanu (fr.8 11)*, London, 1971, (prijevod: W.G. Waddell), http://penelope.uchicago.edu/Thayer/E/Roman/Texts/Manetho/History_of_Egypt/1*.html (pristupljeno 23. 10. 2016.)

[8] S. MEHLER, *Zemlja Ozirisova*, Teledisk, Zagreb, 2003.

[9] G. NOVAK, I. URANIĆ, *Povijest starog Egipta*, Školska knjiga, Zagreb, 2002.

[10] C. NUGUE, *Velike civilizacije svijeta*, Extrade, Rijeka, 2000.

[11] D. POŠTIĆ, *Misterij piramida*, Nova arka, Zagreb, 1996.

[12] T. STRMEČKI, B. KOVAČIĆ, Matematičke konstante (1), *Poučak* **58** (2014).

[13] M. TOTH, G. NIELSEN, *Moć piramida*, CID-NOVA, Zagreb, 2000.

[14] M. TOTH, *Proročanstva piramida*, CID-NOVA, Zagreb, 2001.

[15] http://alizul2.blogspot.hr/2012/01/secrets-hidden-in-pyramids-of-egypt.html (pristupljeno 12. 3. 2015.)

[16] http://metro-portal.hr/kako-je-izgradjena-keopsova-piramida/13124 (pristupljeno 27. 3. 2015.)

[17] http://pyramidales.blogspot.hr/2011/03/la-rampe-interieure-deux-niveaux-de-la.html (pristupljeno 20. 5. 2015.)

[18] http://venia-mag.net/tuska-metal-festival-2005-helsinki-park-15-17-07-2005/civilisations/egypt/ (pristupljeno 29. 5. 2015.)

[19] http://www.ancient-origins.net/ancient-places-africa-opinion-guest-authors/mathematical-encoding-great-pyramid-002323 (pristupljeno 16. 3. 2015.)

[20] http://www.casopis-gradjevinar.hr/assets/Uploads/JCE-53-2001-02-06.pdf (pristupljeno 15. 3. 2015.)

[21] http://www.gizapower.com/ (pristupljeno 10. 3. 2015.)

[22] http://www.gizapyramid.com/ (pristupljeno 10. 3. 2015.)

[23] http://www.gizapyramid.com/newtour5.htm (pristupljeno 10. 5. 2015.)

[24] http://www.irb.hr/Istrazivanja/Zavodi/Zavod-za-eksperimentalnu-fiziku/Laboratorij-za-mjerenje-niskih-radioaktivnosti/Odredivanje-starosti-metodom-14C (pristupljeno 21. 9. 2015.)

[25] http://www.jutarnji.hr/life/znanost/napokon-razotkriven-veliki-misterij-znamo-kako-su-drevni-egipcani-gradili--piramide/796414 (pristupljeno 5. 6. 2016.)

[26] http://www.soulsofdistortion.nl/croatian/SODA_chapter8.html (pristupljeno 23. 6. 2017.)

[27] http://www.studyofoahspe.com/id49.html (pristupljeno 11. 3. 2015.)

[28] https://hr.wikipedia.org/wiki/Piramide_u_Gizi (pristupljeno 10. 3. 2015.)

[29] https://hr.wikipedia.org/wiki/Popis_faraona (pristupljeno 17. 6. 2015.)

[30] https://www.google.hr/maps/@30.5427367,30.486107,287968m/data=!3m1!1e3 (pristupljeno 10. 5. 2016.)

[31] https://www.youtube.com/watch?v=dGH93mt81BA) (pristupljeno 28. 10. 2015.)

Bojan Janjanin
e-mail: janjanin.bojan@gmail.com

Jelena Beban-Brkić
e-mail: jbeban@geof.hr

Faculty of Geodesy, University of Zagreb
Kačićeva 26, HR-10000 Zagreb, Croatia

How to get KoG?

The easiest way to get your copy of KoG is by contacting the editor's office:

Marija Šimić Horvath
msimic@arhitekt.hr
Faculty of Architecture
Kačićeva 26, 10 000 Zagreb, Croatia
Tel: (+385 1) 4639 176
Fax: (+385 1) 4639 465

The price of the issue is €15 + mailing expenses €5 for European countries and €10 for other parts of the world.

The amount is payable to:

ACCOUNT NAME:	Hrvatsko društvo za geometriju i grafiku Kačićeva 26, 10000 Zagreb, Croatia
IBAN:	HR8623600001101517436

Kako nabaviti KoG?

KoG je najbolje nabaviti u uredništvu časopisa:

Marija Šimić Horvath
msimic@arhitekt.hr
Arhitektonski fakultet
Kačićeva 26, 10 000 Zagreb
Tel: (01) 4639 176
Fax: (01) 4639 465

Za Hrvatsku je cijena primjerka 100 KN + 10 KN za poštarinu.

Nakon uplate za:

HDGG (za KoG), Kačićeva 26, 10000 Zagreb
IBAN: HR8623600001101517436

poslat ćemo časopis na Vašu adresu.

Ako Vas zanima tematika časopisa i rad našeg društva, preporučamo Vam da postanete članom HDGG-a (godišnja članarina iznosi 150 KN). Za članove društva časopis je besplatan.